AD NUMBER

ADB222599

NEW LIMITATION CHANGE

TO

Approved for public release, distribution unlimited

FROM

Distribution authorized to DoD only. Other requests shall be referred to Embassy of Australia, Attn: Joan Bliss, Head. Pub. Sec. -Def/Sci., 1601 Massachusetts Ave., NW, Washington, DC 20036.

AUTHORITY

DSTO ltr, 17 May 2001

S-70A-9 Black Hawk Helicopter: Internal Panel Cracking Investigation

D.C. Lombardo, C.G. Knight,
L. Krake, S.A. Dutton
and P.W. Smith

DEPARTMENT OF DEFENCE
DEFENCE SCIENCE AND TECHNOLOGY ORGANISATION

S-70A-9 Black Hawk Helicopter: Internal Panel Cracking Investigation

D.C. Lombardo, C.G. Knight, L. Krake, S.A. Dutton, and P.W. Smith

Airframes and Engines Division
Aeronautical and Maritime Research Laboratory

DSTO-TR-0457

ABSTRACT

The Australian Army S-70A-9 Black Hawk fleet is experiencing numerous occurrences of cracking in an internal fuselage panel. The panel is not primary structure (i.e. it is not flight-critical), but it is essential. Cracking has occurred only on the right-hand side panel, and the standard repair scheme is inadequate. In October 1994, the Australian Army approached DSTO and the Royal Australian Air Force (RAAF) Aircraft Research and Development Unit (ARDU) for assistance in determining the cause of the cracking. To try to minimise the panel cracking, the Army had suspended use of the External Stores Support System (ESSS) which is used to carry external fuel tanks. Since this suspension was causing operational hardships, the Army wanted to know what was causing the cracking to determine whether less severe restrictions might be imposed until a proper repair could be devised for the panel.

In February 1995, DSTO and ARDU personnel conducted a flight investigation, at RAAF Base Edinburgh, South Australia, with Black Hawk A25-206. The data gathered were analysed and the results indicated that the ESSS was not responsible for the cracking. The panel strains are largely insensitive to the presence of the ESSS.

The cause of the cracking is a structural deficiency in the panel. Beads, pressed into the panel to provide stiffening, are creating a stress concentration factor of approximately 3.0 which couples with the large Ground-Air-Ground loading cycle to cause the cracking. Once initiated, the high frequency in-flight loading to which the panel is subjected causes the cracks to propagate rapidly.

There are no operational restrictions which the Army might apply to reduce the frequency or severity of the cracking. The only relief will come when a redesigned panel is installed.

RELEASE LIMITATION

Australian Department of Defence and the Defence Force Personnel and their equivalent in the USA may have access to this document. Others inquiring should be referred to Chief, Airframes and Engines Division AMRL.

DEPARTMENT OF DEFENCE

DEFENCE SCIENCE AND TECHNOLOGY ORGANISATION

Published by

DSTO Aeronautical and Maritime Research Laboratory
PO Box 4331
Melbourne Victoria 3001

Telephone: (03) 9626 8111
Fax: (03) 9626 8999

AR No. AR-009-947
January 1997

Conditions of Release and Disposal

S-70A-9 Black Hawk Helicopter: Internal Panel Cracking Investigation

Executive Summary

- Due to the urgent nature of the investigation detailed in this report, most of the results of the investigation were previously provided to the Australian Defence Force in a preliminary report. This report, while furthering some of the work contained in the preliminary report, aims mainly to provide a permanent record of the investigation and the subsequent data analysis.

- In February 1995, the Aeronautical and Maritime Research Laboratory (in conjunction with the Royal Australian Air Force's Aircraft Research and Development Unit, conducted a flight investigation on Black Hawk A25-206.

- The flight investigation was performed at the request of the Australian Regular Army because their Black Hawk fleet is experiencing numerous occurrences of cracking in an internal fuselage panel. The panel is not primary structure (i.e. it is not flight-critical), but it is essential. Cracking has occurred only on the right-hand side panel, and the standard repair scheme is inadequate.

- To try to minimise the panel cracking, the Army had suspended use of the External Stores Support System (ESSS), which is used to carry external fuel tanks. Since this suspension was causing operational hardships, the Army wanted to know what was causing the cracking to determine whether less severe restrictions might be imposed until a proper repair could be devised for the panel.

- The main conclusion of the flight investigation is that the ESSS is not responsible for the cracking. The panel strains are largely insensitive to the presence of the ESSS.

- The cause of the cracking is a structural deficiency in the panel. Beads, pressed into the panel to provide stiffening, are creating a stress concentration factor of approximately 3.0 and it is this increase in stress around the beads that is responsible for the cracking. Once initiated, the high frequency loading to which the panel is subjected causes the cracks to propagate rapidly.

- There are no operational restrictions which the Army might apply to reduce the frequency or severity of the cracking. The only relief will come when a redesigned panel is installed.

- Another requirement of the flight investigation was to determine if the change in the rigging procedure for the ESSS fuel tank ejector racks had produced a detrimental effect on the panel cracking. The data acquired in the flight investigation did not show any such effect.

Authors

D. C. Lombardo

Airframes and Engines Division

Mr Domenico Lombardo is an engineer in the Helicopter Life Assessment area in the Airframes and Engines Division at AMRL. He joined AMRL in 1987 after graduating from the Royal Melbourne Institute of Technology with a Bachelor of Engineering (Aeronautical) degree with honours.

His initial work at AMRL was in support of F/A-18 and F-111 structural fatigue investigations, but since 1990, he has been working in helicopter structural integrity. During 1992, he was assigned to the U.S. Army Vehicle Structures Directorate, NASA Langley Research Centre, Virginia, U.S.A., working on a low-cost usage monitoring system for the Black Hawk helicopter.

His main role is to provide advice to the Australian Defence Force on structural integrity matters affecting the operation of their helicopters. He is also involved in research into helicopter usage monitoring and is involved with a sub-committee of TTCP HTP 8 looking at issues related to helicopter usage monitoring.

He is currently studying for a Master of Applied Science degree, majoring in Artificial Intelligence.

C. G. Knight

Airframes and Engines Division

Mr Chris Knight is a Professional Officer in the Airframes and Engines Division at AMRL. He joined AMRL in 1994 after graduating from the University of New South Wales with an honours degree in Aerospace Engineering. He has worked in helicopter life assessment in the areas of life substantiation and finite element investigation of structural designs.

L. Krake

Airframes and Engines Division

Mr Luther Krake graduated from the University of Melbourne in 1994, having obtained a Mechanical Engineering degree with honours. Since commencing employment at AMRL at the start of 1995, he has been involved with helicopter life assessment for platforms including the Iroquois, Black Hawk, and Seahawk. He has also contributed to

research into early detection and diagnosis of fatigue cracks in spur gears using vibration analysis methods. More recently he has been involved in the helicopter flight dynamics area, where he has contributed to the validation and modification of the GenHel helicopter aerodynamic and dynamic simulation computer model. He has also acted as system administrator for a networked Silicon Graphics Indigo2 workstation.

S. A. Dutton

Airframes and Engines Division

Mr Scott Dutton graduated from the University of Queensland in 1985 with a Bachelor of Engineering (Electrical) degree with second class honours. He commenced employment with AMRL in 1986.

Since that time he has been working in the field of test cell and aircraft flight trials instrumentation. He has provided instrumentation for various engine test cells including the RAAF F-111 cell at Amberley. He has participated in numerous flight investigations primarily of rotary wing aircraft. These investigations have included first-of-class flight trials with the Royal Australian Navy, rotor track and balance trials, gearbox vibration trials, and most recently the panel cracking investigation described in this report.

P. W. Smith

Airframes and Engines Division

Mr Peter Smith is a Technical Officer with the Airframes and Engines Division and he joined AMRL in December 1989. He received a Certificate of Technology in Aircraft Engineering (Avionics) from the Royal Melbourne Institute of Technology in 1984.

He has been involved with instrumentation and control systems on fatigue tests such as the F/A-18 centre bulkhead test in 1989/90 and the F/A-18 International Follow-On Structural Testing Program during its initial commissioning phase (1990 - 1994). He assisted in the installation of the data acquisition hardware for the Black Hawk flight trial described in this report. He is currently assigned to the Pilatus PC-9 training aircraft fatigue test, and is responsible for maintaining the CYBER Systems control and data acquisition system.

Contents

Abbreviations

AMRL	Aeronautical and Maritime Research Laboratory (DSTO Laboratory in Melbourne)
ARDU	Aircraft Research and Development Unit (RAAF Base in Edinburgh)
CG	Centre of Gravity
DARTH	Data Acquisition and Real Time Hardware
DSTO	Defence Science and Technology Organisation
ESSS	External Stores Support System
FFT	Fast Fourier Transform
ksi	1 ksi = 1000 pound/in^2
PC	Personal Computer
RAAF	Royal Australian Air Force
RP	Range-Pair
STI	Special Technical Instruction
TP	Turning Point
VMES	Von Mises Equivalent Strain

1. Introduction

The Australian Regular Army, via the Army Aircraft Logistics Management Squadron, requested assistance (Ref. 1) from DSTO and ARDU to solve a cracking problem in the Black Hawk fleet. This report contains the results of the flight investigation that arose from that request. Due to the urgent nature of the task, the results of the analysis of the data obtained from the flight investigation were previously provided to the Army and the RAAF in a preliminary report (Ref. 2). This report, while furthering some of the work contained in Ref. 2, aims mainly to provide a permanent record of the flight investigation and the subsequent data analysis.

The background to the flight investigation is given in Ref. 3, but is repeated briefly below.

- The cracking in question is occurring in an internal fuselage panel which lies between frames FS295 and FS308 (Figs 1 and 2) and which is made of 7075-T6 aluminium alloy. For simplicity, this internal panel will be referred to in this report as the "panel". To provide stiffness, the panel has several beads pressed into it.

- The cracking is widespread across the fleet, but has so far occurred only in the right-hand panel.

- The Army suspected that the carriage of external fuel tanks on the External Stores Support System (ESSS) was responsible for the cracking and so suspended their use pending the results of the DSTO/ARDU task.

- One item that the Army believed could have had a bearing on the crack growth is the method for rigging (installing) the fuel tank racks onto the ESSS.

- Due to the perception that the ESSS was responsible for, or at least a major contributor to, the panel cracking, the flight investigation was based on assessing the impact that the ESSS had on the panel strains.

The aim of the flight investigation was not to determine whether fatigue-damaging strains were being applied to the panel as the numerous cracked panels are proof that such strains exist. The aim was to determine what aircraft configuration and/or flight conditions caused the strains to reach levels where fatigue damage would occur. If these configurations and/or flight conditions could be identified, the Army might then be in a position to minimise the frequency or severity of the cracking.

2. Instrumentation

The Black Hawk operated by ARDU (serial no. A25-206) was selected as the flight investigation aircraft because (i) it was a dedicated flight test aircraft and (ii) it had no cracks in its panels. The aircraft was flown to AMRL on 30 November 1995 where it was subsequently fitted with 26 strain gauges (46 channels), 9 accelerometers and the DARTH data acquisition system (Ref. 4). The instrumentation system is described in Ref. 3.

During the fitting of the instrumentation system, problems were discovered with the ESSS support struts. The struts were discovered to have damage to their composite tube which was outside the permitted level specified in the Black Hawk Structural Repair Manual. It was subsequently discovered that a majority of the ESSS struts in service had the same damage and this raised an airworthiness issue. Fitment of the instrumentation to the struts was delayed until four undamaged struts were sent to AMRL from 5 Aviation Regiment, Townsville. See Appendix 1 for more detail.

Both uniaxial and planar-rosette strain gauges were used. The strain gauges were arranged in two groups; one for gauges on the left side of the aircraft and one for gauges on the right side of the aircraft. Only one group of strains was recorded at a time because of limitations in the data acquisition system.

The accelerometer and strain gauge locations are shown in Figs 3 and 4, and described in Table 1.

3. Flight Investigation

After completion of its instrumentation fitment, the aircraft returned to ARDU on 18 January 1996. The flight investigation was conducted from Edinburgh RAAF Base over the period 6 February to 22 February 1995. DSTO personnel went to ARDU to participate in the flight investigation. The aircraft was flown in 12 configurations and in up to 21 flight conditions per configuration (Tables 2 and 3). The complete list of the flight conditions flown for each aircraft configuration and the system for naming the files under which the data are saved is shown in Tables 4 and 5.

The aircraft configurations and flight conditions were slightly altered from those given in Ref. 3. These changes were introduced as a result of the daily post-flight analyses of the flight data and discussions with ARDU engineers and pilots.

The flight investigation proceeded smoothly with only two minor problems being discovered. The first involved a non-functioning signal amplifier in the signal conditioning unit. This particular amplifier was connected to the ESSS strain gauges and the problem was discovered before any of the ESSS aircraft configurations was flown. The amplifier was replaced with a spare and the problem did not recur. The

second problem involved the filters on the DARTH unit's input circuitry. When aircraft power was switched over from main engine generators to the APU generator, voltage surges caused the volatile memory circuits controlling the filters to reset to their minimum values rather than the programmed values. This problem was resolved by switching the unit off and then on after the aircraft was switched to APU power. The integrity of the flight data was not compromised by this problem as it only manifested itself during the main engine-to-APU switchover (i.e. after landing) and not APU-to-main engine switchover (i.e. before take-off).

In the course of the flight investigation, a total of 900 Mb of flight data was obtained. These data currently reside on MS DOS-compatible CD-ROM discs and Sony QD2120 QIC-80 format mini-data tapes. The data on the mini-data tapes are in compressed form using PKZIP[1].

4. Results

4.1 Maximum and Minimum Strains

A summary of the maximum and minimum strains recorded during the various flight conditions is shown in Figs 5 - 7 (Fig. 8 shows what the maximum and minimum strains represent). These figures show the strains for three "typical" configurations: non-ESSS, ESSS with two full tanks, and ESSS with two half-full tanks. Most of the panel strain gauges were rosette gauges. In order to provide an easy comparison of the rosette strains with standard tensile test data, these strains were converted to their Von Mises equivalent strains (Ref. 5). Von Mises strains are shown for gauges SLP1 to SLP5 and SRP1 to SRP5. All other strain gauges were uniaxial and so their strain readings did not require further conversion.

4.1.1 Strain Concentration Effects

Gauges SLP1 and SRP1 measured the strain in the flat parts of the panel while gauges SLP2 - SLP5 and SRP2 - SRP5 measured the strain near the beads. For the left-hand panel, the strains recorded by SLP2 - SLP5 are higher than those recorded by SLP1 by factors averaging between 2.5 and 3.1. The result is the same for the right-hand panel.

This result tallies with a finite element investigation (Ref. 6) of the installation-induced stress in the panel. It is also in agreement with the theoretical results obtained during investigations into the accident to RAAF P3-C Orion A9-754 at Cocos Island on 26 April 1991. These theoretical results (Refs 7 and 8) show that, under the type of loading experienced by the panel, the beads will induce a stress (strain) concentration factor of three.

---

[1] PKZIP 2.01, PKWARE, Brown Deer, Wisconsin, U.S.A., U.S. Patent 5 051 745

However, the actual strain concentration factor present at the edges of the beads may be higher because:

(i) Strain gauges are finite in size and hence the strains that they measure are not the peak strains, but an average of the strains over the area of the strain gauge. The smaller the gauge, the smaller will be this averaging effect. In areas of uniform strain, the averaging effect is unimportant, but in areas of high strain gradient the effect can become important (Ref. 9). Gauges SLP1 and SRP1 are in a region where a low strain gradient exists so their readings can be considered to be typical of the strains existing in that part of the panel. However, gauges SLP2 - SLP5 and SRP2 - SRP5 are probably in regions of high strain gradient where the strain averaging would cause the gauge output to under-read the peak strain existing at the centre of the rosette. Note that using planar rosette strain gauges, rather than stacked rosette gauges (Fig. 9), means that the rosette is averaging the strain over a larger area. However, stacked gauges were unavailable in-country and the time required for their purchase would have delayed the flight investigation by months.

(ii) In attempting to measure peak strains, it is more important to know the location of the peak than it is to have the correct type of strain gauge. Having a microscopic strain gauge is not much use if it is installed away from the strain peak. Normally, the approximate location of the peak is known and several gauges are installed in the vicinity with the hope that one will be in the right position. However, this option was not available as there were only a limited number of data acquisition channels available. With the limited choices available, the perceived most reasonable positions were chosen for gauges SLP2 - SLP5 and SRP2 - SRP5. It is possible that shifting the gauges a few millimetres fore or aft may have produced higher strain readings.

4.1.2 Left-hand Panel and Right-hand Panel Strains

Figures 5 - 7 show that the right-hand panel almost always has higher strains than the left-hand panel. This is consistent with Army fleet experience in that cracking has so far occurred only on the right-hand side. It does not imply that the left-hand panel will not crack, just that, all else being equal, the right-hand panel should crack before the left.

4.2 Range-Pair Analysis

Maximum and minimum flight strains show only part of the fatigue loading environment. Consider Fig. 10 in which two different load histories are shown. Both the load histories will appear to be the same if only the maximum and minimum strains are examined. However, the load history shown in Fig. 10(b) is more fatigue-damaging than that in Fig. 10(a) because it would subject a component to several load cycles instead of one. Hence, a range-pair analysis was undertaken as detailed in Appendix 2 to determine if this effect was indeed occurring. The possibility that landings with the ESSS might be more fatigue-damaging to the panel than landings

without the ESSS (Ref. 2, para. 21 of attachment) was the main focus of the range-pair analysis.

Table 6 shows the results of applying the results of the range-pair analysis to a fatigue damage analysis for the strain data obtained from gauges SLP2, SRP2, SLP5, and SRP5. Two aircraft configurations are considered: Non-ESSS, and ESSS with two full external tanks; both configurations were at a gross weight of 20000 lb. The analysis was only aimed at determining which aircraft configuration was more fatigue-damaging under the various flight conditions. Hence, an appropriate material SN curve from Mil Handbook 5F (Ref. 10, Fig. 3.7.4.1.8(d)) was chosen for use in the fatigue calculations. The use of this curve meant that the strains had to be converted to Von Mises equivalent strains and the range-pair analysis was performed on the Von Mises strains.

Since only a relative result was required (i.e. ESSS or Non-ESSS is more damaging), Table 6 does not show any actual values for the fatigue damage.

The conclusion that can be drawn from Table 6 is that the presence of the ESSS does not have a detrimental effect on the panel. The only flight condition where the ESSS produces more fatigue damage is that for level flight at 0.9VH. This situation was indicated in the preliminary report (Ref. 2, para. 22 of attachment).

However, the reverse conclusion cannot be drawn. That is, the conclusion cannot be made that the panel is definitely damaged more when the ESSS is not installed. A more extensive analysis would need to be performed to determine the magnitude of the difference in fatigue damage between the Non-ESSS and ESSS conditions, for each flight condition.

4.3 Significance of ESSS and Non-ESSS Configurations for the Panel Strains

For almost all flight conditions the use of ESSS is not more detrimental to the fatigue life of the panel than not having the ESSS. What is evident is that the right-hand panel is almost always more highly loaded than the left-hand panel.

The only flight condition to show noteworthy differences between the ESSS and non-ESSS conditions was level flight at 0.9VH (120 knots). Level flight at 0.9VH produced higher panel strains when the ESSS was installed. This behaviour was reasonably consistent across the different aircraft configurations. However, the range of maximum-minimum strains for this flight condition is small enough to conclude that this condition is not particularly fatigue-damaging.

4.4 The Old versus New Rigging Procedure

One of the issues that the Army thought might be significant in the panel cracking problem was the method of rigging (installing) the fuel tanks onto the ESSS. The

procedure was changed when Special Technical Instruction STI-Black Hawk-62 (Ref. 11) was issued in August 1992. An analysis of the strains measured from the two different rigging procedures was performed and is included at Appendix 3. The analysis shows that there is no significant difference in the panel strains produced by the two rigging procedures.

4.5 Frequency Analysis

A Fast-Fourier Transform (FFT) of selected strain gauge signals was performed. A sample of these is shown in Figs 11 and 12. The FFTs show the various driving frequencies which make up the overall recorded signal. For example, Fig. 11 shows that the main drivers behind the strains at gauge SRP2b (i.e. arm B of the rosette) during Hover are the Main Rotor passing frequency (17.2 Hz) and the Tail Rotor rotational frequency (19.8 Hz). Figure 12 also shows the FFT for the SRP2b gauge signal, but this time for Autorotation at zero forward airspeed. In this case, the significant contributors are again the Main Rotor passing frequency and the Tail Rotor rotational frequency.

Since an FFT analysis was not of immediate use, further investigation of the data via the FFT approach was not performed.

4.6 Left-hand Panel Strains Versus Right-hand Panel Strains

As indicated in Section 4.1.2, the strains in the right side panel were almost always higher than the strains in the left side panel. One possible source of the difference is the tail rotor thrust. Due to its configuration and location on the aircraft, the Black Hawk's tail rotor produces both sidewards thrust (to provide the anti-torque force) and lift. The tail fin also provides sidewards thrust under some flight conditions. These thrust and lift loads will induce bending in the tailboom in two planes (left-right and up-down) as well as torsion and these tailboom bending and torsion loads are transmitted to the main cabin structure.

To provide some data to check this hypothesis, a decision was reached between DSTO and ARDU personnel to modify the flight investigation to include some autorotations. During autorotation the main rotor is disengaged and allowed to overspeed by up to 5%. As the main rotor is disengaged no anti-torque reaction force is required and so the resultant thrust from the tail rotor and fin should be almost zero.

Since the left-to-right panel strain difference was not the focus of the flight investigation, the autorotations were flown on the last day of the flight investigation. Hence only one aircraft configuration was used (ESSS with no tanks, approx. 16000 lb gross weight), and only a few flight conditions were flown (Table 4(k)).

Analysis of the strain data showed that the strains in both panels became approximately equal for most of the flight conditions (Fig. 13). This behaviour

suggests that the tail rotor thrust is the cause of the left-to-right strain differences. In some cases, a strain reversal occurred; that is the left-hand panel had slightly higher strains than the right-hand panel. The strain reversal could have several causes such as a gust encountered during the descent, or a force from the tail fin[2].

Ideally, an analytical analysis would be required to confirm that the tail rotor thrust is the cause of the differences in the left-to-right panel strains. However, because the strain differences were not the focus of the flight investigation, and because of the lack of detailed information available on the Black Hawk structure, this analysis was not done.

4.7 Data Reliability

The reliability of the data is good since:

(i) The right-hand panel has higher strains than the left-hand panel
This is consistent with Army fleet experience in that cracking has so far occurred only on the right-hand side.

(ii) The high strains seen at the locations of gauges SLP2 - SLP5 and SRP2 - SRP5

The locations of these gauges were chosen after examining the incidence of cracking in the 5 Aviation Regiment Black Hawks in Townsville. A crack indicates that the surrounding material is under high strains. Without exception, the gauges indicated that such high strains did exist.

(iii) The behaviour of the strain and accelerometer readings
The time histories of the strain and accelerometer readings were as expected.

(iv) Correlation with theoretical results
The strains at the edges of the beads were measured to be approximately three times those recorded away from the edges and this correlates with finite element models of the panel (Ref. 6) and theoretical analyses undertaken for the P3-C Orion (Refs 7 and 8).

[2] During autorotation, the main rotor will still be turning the gears in the main rotor gearbox. The friction in the gearbox may be enough to induce a small rotation in the fuselage such that the fuselage will tend to spin in the same direction as the main rotor (i.e. the opposite of what happens in normal flight). As the fuselage rotates slightly, the resulting airflow over the fin would then set up a counteracting force to port rather than starboard as in normal flight.

5. Conclusions

The conclusion of the flight investigation is that the ESSS is not responsible for the cracking in the panel. The panel is overloaded (from a fatigue point of view) whether or not the ESSS is present. This implies that the Army-imposed restriction on the use of the ESSS is not achieving any worthwhile benefits in terms of preventing panel cracking.

The source of the cracking is the presence of the beads in the panel which raise the local strains by a factor of at least three. These beads represent an inherent structural deficiency in the airframe. If this conclusion is correct then other operators of the Black Hawk should experience, or be experiencing, the same problem whether or not they use the ESSS.

Given that the ESSS imposes significant loads on the airframe then, since the panel strains are not affected by the ESSS, some other part of the airframe must be carrying these stresses. The most likely elements of the airframe would be the overhead sections of frames FS295 and FS308 (which support the transmission) as well as parts of the underfloor structure.

The cracking problem is not of concern to the RAN. The Army S-70A-9 Black Hawk and the RAN S-70B-2 are structurally dissimilar in the forward fuselage area. Whilst the panel in the Black Hawk extends from cabin floor to roof, the equivalent Seahawk panel extends only halfway up the cabin. That is, the Seahawk is missing the top half of the panel, and since almost all the cracking in the Black Hawk panels is occurring in the top half, then the cracking does not occur in the RAN aircraft.

6. Comments on Panel Redesign

Any proposed redesign of the panel should consider removing the beads. This one change will provide the greatest benefit in reducing the panel strains to non-damaging levels. However, the beads are there to provide necessary stiffening to the panel and so this stiffening must be provided by other means.

Any modification or redesign that is proposed to solve the problem should be justified by both theoretical analyses and structural tests. The data acquired during the flight investigation should be used in both the analyses and the tests.

Acknowledgments

The authors would like to thank the following people for their help during the flight investigation:

- Mr Ken Fraser of AMRL for all his behind-the-scenes assistance, especially with all the paper work, which helped ensure that the flight investigation proceeded as smoothly as possible.

- MAJs Dave Fawcett and Cameron Ross who piloted the aircraft and made useful contributions regarding the selection of aircraft configurations and flight conditions to investigate. As well, we would like to thank MAJ Fawcett for his assistance in procuring office accommodation and computing facilities for the DSTO staff.

- SGTs Moule and Barnett, and CPLs Slattery, Weston, and Gauge who acted well above the call of duty in altering the aircraft configuration almost daily to suit DSTO requirements.

- Mr Geoff Swanton of AMRL for his contribution of computer code, which was incorporated into the range-pair program presented in this report.

References

1. Army LM Squadron Minute to AMRL, Army LMS/4080/A25/109 Pt 1 (10), **Development Test and Evaluation Task Request,** 11 November 1994.

2. **Cause of Black Hawk Inner Fuselage Panel Cracking,** AMRL Minute to Commanding Officer, Army Aircraft Logistics Management Squadron, AMRL Reference M2/998, dated 12 May 1995.

3. Lombardo, D.C., Patterson, A.K., Ferrarotto, P., Dutton, S.A., Powlesland, I.G., Fraser, K.F, **Preparation of S-70A-9 Black Hawk for Flight Tests to Investigate Cause of Cracking of Inner Fuselage Panel,** DSTO Technical Note, DSTO-TN-0004, February 1995.

4. Harvey, J.F., Kent, S.A., **A Computer Controlled Data Acquisition System,** DSTO Technical Note, ARL-TN-12, August 1993.

5. Lardner, T.J. (ed.), 1978, **An Introduction to the Mechanics of Solids,** 2 ed. McGraw-Hill International, Tokyo, Japan, pp. 337 - 342.

6. Knight, C.G., **Installation-Induced Stress in a Black Hawk Inner Fuselage Panel,** DSTO Technical Report, DSTO-TR-0329, May 1996.

7. Molent, L., **Structural Investigations into the Collapse of the Wing Leading Edges of Orion P3-C,** Proceedings of the PICAST 2 - AAC 6 Conference, Melbourne, Australia, 20-23 March 1995, pp. 787-794.

8. Wong, A.K., Ryall, T.G., Richmond, M.J., **Structural Assessment of the Orion P3 Wing Leading Edge Using a State-of-the-Art Thermal Imaging System,** Proceedings of the PICAST 2 - AAC 6 Conference, Melbourne, Australia, 20-23 March 1995, pp. 795-800.

9. Lombardo, D.C., **Stress Concentration Factors in the Design of Loading Forks,** DSTO Technical Memorandum, ARL-STRUC-TM-508, May 1989.

10. United States Department of Defense, Military Handbook, MIL-HDBK-5F, **Metallic Materials and Elements for Aerospace Vehicle Structures,** 1 November 1990.

11. **Inspect ESSS Ejector Rack,** Royal Australian Air Force (RAAF), Special Technical Instruction, STI-Black Hawk-62, 21 August 1995, RAAF file reference: AIR2/4080/A25/9-1/4 (12).

12. Bertucio, W., Toni, D., Schmitz, B., **Structural Analysis of UH-60A Mid-Fuselage,** Sikorsky Engineering Report, SER-70742, 15 June 1983.

13. Sharp, P.K., Lamb, S., and Goldsmith, N.T., **S-70A-9 Black Hawk External Stores Support System (ESSS) Support Struts,** AMRL Defect Assessment and Failure Analysis Investigation No. M1/95, 5 January 1995.

14. **Black Hawk Structural Repair Manual,** Royal Australian Air Force Publication, DI(AF) AAP7210.015-3, 12 May 1994.

15. Fraser, R.C., **A One-Pass Method For Counting Range Mean Pair Cycles For Fatigue Analysis,** Aeronautical and Maritime Research Laboratory, ARL-STRUC-NOTE-454, 1979.

16. Kreyszig, Erwin, **Advanced Engineering Mathematics, Sixth Edition,** John Wiley and Sons, Brisbane, 1988.

17. Lombardo, D.C., Graham, A.D. and Harris, F.G., **Stress Reduction in F-111 Wing Fuel Vent Holes by Using Neat-Fit Plugs - A Thermoelastic Analysis,** Aeronautical and Maritime Research Laboratory, Aircraft Structures Technical Memorandum, STR-TECH-MEMO 509, August 1989.

Table 1: Description of sensors used in the flight investigation

Channel	Analogue or Digital	Location	Sensor Type[a]	Code[b]
01	A	Rear strut ESSS	Su	SLE6, SRE6
02	A	Front strut ESSS	Su	SLE5, SRE5
03	A	Upper surface ESSS (FS295) Fwd	Su	SLE1, SRE1
04	A	Upper surface ESSS (FS308) Aft	Su	SLE2, SRE2
05	A	Lower surface ESSS (FS295) Fwd	Su	SLE3, SRE3
06	A	Lower surface ESSS (FS308) Aft	Su	SLE4, SRE4
07	A	Internal panel	Sr	SLP1a, SRP1a
08	A	Internal panel	Sr	SLP1b, SRP1b
09	A	Internal panel	Sr	SLP1c, SRP2c
10	A	Internal panel	Sr	SLP2a, SRP2a
11	A	Internal panel	Sr	SLP2b, SRP2b
12	A	Internal panel	Sr	SLP2c, SRP2c
13	A	Internal panel	Sr	SLP3a, SRP3a
14	A	Internal panel	Sr	SLP3b, SRP3b
15	A	Internal panel	Sr	SLP3c, SRP3c
16	A	Internal panel	Sr	SLP4a, SRP4a
17	A	Internal panel	Sr	SLP4b, SRP4b
18	A	Internal panel	Sr	SLP4c, SRP4c
19	A	Internal panel	Sr	SLP5a, SRP5a
20	A	Internal panel	Sr	SLP5b, SRP5b
21	A	Internal panel	Sr	SLP5c, SRP5c
22	A	Internal panel	Su	SLP6, SRP6
23	A	Internal panel	Su	SLP7, SRP7
24	A	ESSS wing tip (forward)	A	ALE1
25	A	ESSS wing tip (mid-point)	A	ALE2
26	A	ESSS wing tip (aft)	A	ALE3
27	A	ESSS wing tip (forward)	A	ARE1
28	A	ESSS wing tip (mid-point)	A	ARE2
29	A	ESSS wing tip (aft)	A	ARE3
30	A	C.G. lateral	A	CGY
31	A	C.G. vertical	A	CGZ
32	A	C.G. longitudinal	A	CGX
33[c]	D	Left/Right indicator	Dsw	-
34[c]	D	Left/Right Indicator	Dsw	-

Notes: (a) Sensor types: Su = Strain Gauge (uniaxial), Sr = Strain Gauge (rosette), A = Accelerometer, Dsw = Digital Switch

(b) An 'L' in the code indicates that the sensor was on the left-hand side of the aircraft, while an 'R' indicates that it was on the right-hand side. An 'a', 'b', or 'c' in the code indicates arm A, B, or C, respectively (Fig. 4) of the rosette gauge.

(c) These switches acted as a follows:

	Output Signal	
	Ch 33	Ch 34
Right side being recorded	1	0
Left side being recorded	0	1
Fault	0	0
No connection	1	1

Table 2: Summary of aircraft configurations

No.	Take-off Gross Weight (lb) (nominal)	ESSS	ESSS Outboard Tanks	ESSS Fuel State	Hook Load (lb)	Rigging Procedure (Appendix 3)
1	16000	No				Current
2	20000	No				Current
3	20000	Yes	No			Current
4	20000	Yes	Yes	Empty		Current
5	20000	Yes	Yes	Full		Current
6	20000	Yes	Yes	Half Full		Current
7	20000	Yes	Yes	Full		Pre-STI
8	16000	Yes	No			Current
9	16600	Yes	No		3500 (bombs)	Current
10	16600	Yes	No		4500 (bombs)	Current
11	16600	Yes	No		6000 (bombs)	Current
12	16600	Yes	No		3500 (Land Rover)	Current

Table 3: Flight conditions

Flight Condition	Description
Landing - NML	Normal Landing
Landing - OPL	Operational Landing: Simulated by hovering a short distance above the ground and then dropping the collective to achieve a 2g average deceleration during touch-down. Readings indicated that very short transient levels of up to 5g were experienced.
Landing - ADL	Aerodynamically-Braked Landing: Touch down, with the tail wheel, at 60 KIAS, then apply aft cyclic to reduce forward speed to zero, and then allow the main wheels to touch down.
BRK Turn Left	Break Turn to the Left: Fly straight and level at 100 KIAS and then rapidly apply left cyclic to achieve 80° - 90° angle of bank.
Mod Pull-Out	Moderate Symmetric Pull-Out (2g): Enter 30° dive at 120 KIAS and then apply sufficient aft cyclic to achieve 2g. At end of pull-up, aircraft is approx. 60° nose-up. Recover via roll to the right.
LT 30°, 0.5VH	Left Turn at 30° angle of bank at 0.5VH (70 KIAS)
LT 30°, 0.7VH	Left Turn at 30° angle of bank at 0.7VH (100 KIAS)
LT 45°, 0.5VH	Left Turn at 45° angle of bank at 0.5VH (70 KIAS)
LT 45°, 0.7VH	Left Turn at 45° angle of bank at 0.7VH (100 KIAS)
RT 30°, 0.5VH	Right Turn at 30° angle of bank at 0.5VH (70 KIAS)
RT 30°, 0.7VH	Right Turn at 30° angle of bank at 0.7VH (100 KIAS)
RT 45°, 0.5VH	Right Turn at 45° angle of bank at 0.5VH (70 KIAS)
RT 45°, 0.7VH	Right Turn at 45° angle of bank at 0.7VH (100 KIAS)
Hover	
LF 0.3VH	Level flight at 0.3VH (40 KIAS)
LF 0.5VH	Level flight at 0.5VH (70 KIAS)
LF 0.7VH	Level flight at 0.7VH (100 KIAS)
LF 0.9VH	Level flight at 0.9VH (120 KIAS)
Step Input Aft Step Input Left Step Input Right	One and a half inch step inputs (aft, left, and right) to the cyclic control stick.

Table 4(a) - Flight conditions flown for each aircraft configuration

Aircraft Configuration Shake-down flight for internal sensors	ESSS: No Take-off Weight: 16200 lb			Day 1 7 Feb 1995		
Flight Condition		Filename Left Side Gauges	Filename Right Side Gauges	Recording Start Time: Left/Right	Recording Duration Left/Right (sec)	Note
On ground, rotors turning, flat pitch		PORT	STBD	1400/1401		0
On ground, rotors turning, 30% collective			COLLECT	-/1403		0
Calibration - Pre-flight		PORT01	STBD01	1049/1050		
Level Flight	Hover	HOVERP	HOVERS	1105/1106		1
Level Flight	70 KIAS	70KP	70KS	1111/1112		2
Level Flight	120 KIAS	120KP	120KS	1116/1115		
Left Turn at 30 AOB	70 KIAS	30DEGLP	30DEGLS	1118/1120		3
Right Turn at 30 AOB	70 KIAS	30DEGRP	30DEG2S	1121/1123		
Left Turn at 45 AOB	100 KIAS	45DEGLP	45DEGLS	1125/1127		
Right Turn at 45 AOB	100 KIAS	45DEGRP	45DEGRS	1126/1128		
Moderate Pull-out	120 KIAS	PULLUPP	PULLUPS	1133/1131		
Step Input - 1 inch - Left Cyclic	80 KIAS	80LATLP		1135/-		
Step Input - 2 inch - Left Cyclic	80 KIAS	80LAT2P		1136/-		
Step Input - 1 inch - Aft Cyclic	80 KIAS	AFTSTPP	AFTSTPS	1150/1153		
Step Input - 2 inch - Aft Cyclic	80 KIAS	AFTSTP2P	AFTSTP2S	1152/1154		
Normal Landing		LND1P	LND1S	1145/1155		
Aerodynamically-braked Landing		RUN1P	RUN1S	1148/1156		
Calibration - Post-flight		PORT01A	STBD01A	1203/1204		

Notes: All notes are listed on the page following Table 4(k)

Table 4(b) - Flight conditions flown for each aircraft configuration

Aircraft Configuration	ESSS: No Take-off Weight: 16000 lb			Day 2 8 Feb 1995		
Flight Condition		Filename Left Side Gauges	Filename Right Side Gauges	Recording Start Time: Left/Right	Recording Duration Left/Right (sec)	Note
Calibration - Pre-flight		PORT02	STBD02	1223/1221		
Level Flight	Hover	N100LF0L	N100LF0R	1232/1259	31/30	4
Level Flight	40 KIAS	N100LF3L	N100LF3R	1237/1302	30/30	
Level Flight	70 KIAS	N100LF5L	N100LF5R	1239/1303	32/39	
Left Turn at 30 AOB	70 KIAS	N100L35L	N100L35R	1240/1304	31/31	
Right Turn at 30 AOB	70 KIAS	N100R35L	N100R35R	1242/1305	32/30	
Left Turn at 45 AOB	70 KIAS	N100L45L	N100L45R	1243/1307	30/31	
Right Turn at 45 AOB	70 KIAS	N100R45L	N100R45R	1245/1308	30/31	
Level Flight	100 KIAS	N100LF7L	N100LF7R	1246/1309	32/32	
Left Turn at 30 AOB	100 KIAS	N100L3ML	N100L3MR	1248/1310	40/30	
Right Turn at 30 AOB	100 KIAS	N100R3ML	N100R3MR	1249/1312	32/31	
Left Turn at 45 AOB	100 KIAS	N100L4ML	N100L4MR	1249/1312	30/30	
Right Turn at 45 AOB	100 KIAS	N100R4ML	N100R4MR	1251/1313	34/35	
Level Flight	120 KIAS	N100LF9L	N100LF9R	1252/1315	30/31	
Moderate Pull-out	120 KIAS	N100MPOL	N100MPOR	1254/1317	34/30	
Step Input - 1.5 inch - Left Cyclic	80 KIAS	N100STLL	N100STLR	1256/1318	18/17	
Step Input - 1.5 inch - Right Cyclic	80 KIAS	N100STRL	N100STRR	1253/1319	20/21	
Step Input - 1.5 inch - Aft Cyclic	80 KIAS	N100STAL	N100STAR	1258/1320	18/18	
Break Turn Left	100 KIAS	N100BRKL	N100BRKR	1323/1322	18/17	
Normal Landing		N100NMLL	N100NMLR	1330/1336	22/18	
Aerodynamically-braked Landing		N100ADLL	N100ADLR	1332/1337	20/18	
Operational Landing		N100OPLL		1334/-	20/-	5
Calibration - Post-flight		PORT02A	STBD02A	1344/1343		

Notes: All notes are listed on the page following Table 4(k)

Table 4(c) - Flight conditions flown for each aircraft configuration

Aircraft Configuration	ESSS: No Take-off Weight: 20000 lb		Internal Fuel (pre-flight) 2100 lb Internal Fuel (post-flight) 1390 lb	Day 3 9 Feb 1995		
Flight Condition		Filename Left Side Gauges	Filename Right Side Gauges	Recording Start Time: Left/Right	Recording Duration Left/Right (sec)	Note
Calibration - Pre-flight		PORT03	STBD03	1023/1022		
Level Flight	Hover	N200LF0L	N200LF0R	1034/1059	33/34	
Level Flight	40 KIAS	N200LF3L	N200LF3R	1036/1101	34/35	
Level Flight	70 KIAS	N200LF5L	N200LF5R	1037/1102	34/35	
Left Turn at 30 AOB	70 KIAS	N200L35L	N200L35R	1038/1103	33/31	
Right Turn at 30 AOB	70 KIAS	N200R35L	N200R35R	1039/1104	34/34	
Left Turn at 45 AOB	70 KIAS	N200L45L	N200L45R	1040/1105	34/34	
Right Turn at 45 AOB	70 KIAS	N200R45L	N200R45R	1042/1106	37/35	
Level Flight	100 KIAS	N200LF7L	N200LF7R	1044/1107	34/34	
Left Turn at 30 AOB	100 KIAS	N200L3ML	N200L3MR	1045/1108	33/44	
Right Turn at 30 AOB	100 KIAS	N200R3ML	N200R3MR	1045/1109	35/37	
Left Turn at 45 AOB	100 KIAS	N200L4ML	N200L4MR	1048/1110	35/35	
Right Turn at 45 AOB	100 KIAS	N200R4ML	N200R4MR	1049/1111	32/35	
Level Flight	120 KIAS	N200LF9L	N200LF9R	1050/1112	35/34	
Moderate Pull-out	120 KIAS	N200MPOL	N200MPOR	1051/1113	21/19	
Step Input - 1.5 inch - Left Cyclic	80 KIAS	N200STLL	N200STLR	1053/1115	19/18	
Step Input - 1.5 inch - Right Cyclic	80 KIAS	N200STRL	N200STRR	1054/1116	19/20	
Step Input - 1.5 inch - Aft Cyclic	80 KIAS	N200STAL	N200STAR	1055/1117	18/19	
Break Turn Left	100 KIAS	N200BRKL	N200BRKR	1056/1118	18/22	
Normal Landing		N200NMLL	N200NMLR	1126/1122	18/19	
Aerodynamically braked landing		N200ADLL	N200ADLR	1127/1123	23/22	
Operational Landing		N200OPLL	N200OPLR	1127/1124	17/19	
Calibration - Post-flight		PORT03A	STBD04A	1133/1134		

Table 4(d) - Flight conditions flown for each aircraft configuration

Aircraft Configuration	ESSS:	Yes			Day 4	13 Feb 1995
	Take-off Weight:	19500 lb				
Shake-down flight for ESSS sensors	ESSS Tanks:	No				
and calibration recordings	Fuel/Tank:	-				
Flight Condition		Filename Left Side Gauges	Filename Right Side Gauges	Recording Start Time: Left/Right	Recording Duration Left/Right (sec)	Note
Sensor calibration with known load		PORT500	STBD500	1240/1242		6
Sensor calibration with known load		PORT1000	STBD1000	1252/1250		6
Calibration - Pre-flight		PORT04	STBD04	1357/1356		
Level Flight	100 KIAS	100KL	100KR	1410/1417	30/30	
Moderate Pull-out	120 KIAS	2GL	2GR	1413/1418	19/16	
Break Turn Left	100 KIAS	BRKL	BRKR	1412/1417	15/	
Aerodynamically braked landing		ACCL	ACCR	1414/1419	20/20	
Operational Landing		DROPL	DROPR	1415/1420	15/8	
Test recording after landing			GENAPU	-/1438		7
Calibration - Post-flight		PORT04A	STBD04A	1441/1440		

Notes: All notes are listed on the page following Table 4(k)

Table 4(e) - Flight conditions flown for each aircraft configuration

Aircraft Configuration	ESSS: Yes Take-off Weight: 20000 lb ESSS Tanks: No	Internal Fuel (pre-flight) 2150 lb Internal Fuel (post-flight) 1490 lb		Day 5 14 Feb 1995	
Flight Condition	Filename Left Side Gauges	Filename Right Side Gauges	Recording Start Time: Left/Right	Recording Duration Left/Right (sec)	Note
Calibration - Pre-flight	PORT05	STBD05	0900/0901		
Level Flight Hover	E200LF0L	E200LF0R	0915/0941	30/30	8
Level Flight 40 KIAS	E200LF3L	E200LF3R	0920/0943	30/30	
Level Flight 70 KIAS	E200LF5L	E200LF5R	0923/0945	30/30	
Left Turn at 30 AOB 70 KIAS	E200L35L	E200L35R	0924/0946	36/32	
Right Turn at 30 AOB 70 KIAS	E200R35L	E200R35R	0925/0946	35/33	
Left Turn at 45 AOB 70 KIAS	E200L45L	E200L45R	0926/0947	33/33	
Right Turn at 45 AOB 70 KIAS	E200R45L	E200R45R	0926/0948	34/32	
Level Flight 100 KIAS	E200LF7L	E200LF7R	0927/0949	30/30	
Left Turn at 30 AOB 100 KIAS	E200L3ML	E200L3MR	0928/0950	32/34	
Right Turn at 30 AOB 100 KIAS	E200R3ML	E200R3MR	0929/0951	32/37	
Left Turn at 45 AOB 100 KIAS	E200L4ML	E200L4MR	0930/0952	32/35	
Right Turn at 45 AOB 100 KIAS	E200R4ML	E200R4MR	0932/0953	32/33	
Level Flight 120 KIAS	E200LF9L	E200LF9R	0933/0955	30/30	
Moderate Pull-out 120 KIAS	E200MPOL	E200MPOR	0934/0956	19/18	
Step Input - 1.5 inch - Left Cyclic 80 KIAS	E200STLL	E200STLR	0935/0958	16/22	
Step Input - 1.5 inch - Right Cyclic 80 KIAS	E200STRL	E200STRR	0936/0959	16/17	9
Step Input - 1.5 inch - Aft Cyclic 80 KIAS	E200STAL	E200STAR	0937/1000	16/16	
Break Turn Left 100 KIAS	E200BRKL	E200BRKR	09381000	15/16	
Normal Landing	E200NMLL	E200NMLR	1009/1006	9/16	
Aerodynamically braked landing	E200ADLL	E200ADLR	1010/1007	17/20	
Operational Landing	E200OPLL	E200OPLR	1011/1007	9/15	
Test recording after landing	GENAPU		1013/-		7
Calibration - Post-flight	PORT05A	STBD05A	1017/1017		

Notes: All notes are listed on the page following Table 4(k)

Table 4(f) - Flight conditions flown for each aircraft configuration

Aircraft Configuration	ESSS: Yes Take-off Weight: 20000 lb ESSS Tanks: Yes Fuel/Tank: Zero	Internal Fuel (pre-flight) 2320 lb Internal Fuel (post-flight) 1250 lb		Day 6 15 Feb 1995	
Flight Condition		Filename Left Side Gauges	Filename Right Side Gauges	Recording Start Time: Left/Right	Recording Duration Left/Right (sec)	Note
Calibration - Pre-flight		PORT06	STBD06	0853/0851	15/15	
Level Flight	Hover	E220LF0L	E220LF0R	0903/0932	30/30	
Level Flight	40 KIAS	E220LF3L	E220LF3R	0907/0934	303/0	
Level Flight	70 KIAS	E220LF5L	E220LF5R	0908/0935	30/30	
Left Turn at 30 AOB	70 KIAS	E220L35L	E220L35R	0909/0938	30/30	
Right Turn at 30 AOB	70 KIAS	E220R35L	E220R35R	0910/0939	30/30	
Left Turn at 45 AOB	70 KIAS	E220L45L	E220L45R	0913/0939	30/30	
Right Turn at 45 AOB	70 KIAS	E220R45L	E220R45R	0916/0941	30/30	
Level Flight	100 KIAS	E220LF7L	E220LF7R	0919/0942	45/30	
Left Turn at 30 AOB	100 KIAS	E220L3ML	E220L3MR	0920/0943	30/30	
Right Turn at 30 AOB	100 KIAS	E220R3ML	E220R3MR	0926/0944	30/30	
Left Turn at 45 AOB	100 KIAS	E220L4ML	E220L4MR	0921/0945	30/30	
Right Turn at 45 AOB	100 KIAS	E220R4ML	E220R4MR	0922/0946	30/30	
Level Flight	120 KIAS	E220LF9L	E220LF9R	0924/0948	30/30	
Moderate Pull-out	120 KIAS	E220MPOL	E220MPOR	0925/0949	16/16	
Step Input - 1.5 inch - Left Cyclic	80 KIAS	E220STLL	E220STLR	0926/0950	16/16	
Step Input - 1.5 inch - Right Cyclic	80 KIAS	E220STRL	E220STRR	0927/0950	16/16	
Step Input - 1.5 inch - Aft Cyclic	80 KIAS	E220STAL	E220STAR	0927/0950	16/16	
Break Turn Left	100 KIAS	E220BRKL	E220BRKR	0929/0951	16/16	
Normal Landing		E220NMLL	E220NMLR	1001/0957	16/16	
Aerodynamically braked landing		E220ADLL	E220ADLR	1003/0958	16/16	
Operational Landing		E220OPLL	E220OPLR	1004/1000	16/16	
Calibration - Post-flight		PORT06A	STBD06A	1009/1011	12/12	

Table 4(g) - Flight conditions flown for each aircraft configuration

Aircraft Configuration	ESSS: Yes Take-off Weight: 20400 lb ESSS Tanks: Yes Fuel/Tank: 100%	Internal Fuel (pre-flight) 1600 lb Internal Fuel (post-flight) 710 lb		Day 7 16 Feb 1995	
Flight Condition	Filename Left Side Gauges	Filename Right Side Gauges	Recording Start Time: Left/Right	Recording Duration Left/Right (sec)	Note
Calibration - Pre-flight	PORT07	STBD07	0918/0919		
Ground Taxi Hover	-	E22FTAXR	-/0933		
Level Flight Hover	E22FLF0L	E22FLF0R	0958/0937	30/30	
Level Flight 40 KIAS	E22FLF3L	E22FLF3R	0959/0940	30/30	
Level Flight 70 KIAS	E22FLF5L	E22FLF5R	1000/0941	32/30	
Left Turn at 30 AOB 70 KIAS	E22FL35L	E22FL35R	1001/0942	34/33	
Right Turn at 30 AOB 70 KIAS	E22FR35L	E22FR35R	1002/0943	30/32	
Left Turn at 45 AOB 70 KIAS	E22FL45L	E22FL45R	1003/0944	32/35	
Right Turn at 45 AOB 70 KIAS	E22FR45L	E22FR45R	1004/0946	32/36	
Level Flight 100 KIAS	E22FLF7L	E22FLF7R	1005/0947	31/30	
Left Turn at 30 AOB 100 KIAS	E22FL3ML	E22FL3MR	1006/0948	33/36	
Right Turn at 30 AOB 100 KIAS	E22FR3ML	E22FR3MR	1007/0949	33/29	
Left Turn at 45 AOB 100 KIAS	E22FL4ML	E22FL4MR	1008/0950	33/35	
Right Turn at 45 AOB 100 KIAS	E22FR4ML	E22FR4MR	1008/0951	33/32	
Level Flight 120 KIAS	E22FLF9L	E22FLF9R	1010/0952	30/30	
Moderate Pull-out 120 KIAS	E22FMPOL	E22FMPOR	1011/0953	16/18	
Step Input - 1.5 inch - Left Cyclic 80 KIAS	E22FSTLL	E22FSTLR	1012/0954	16/17	
Step Input - 1.5 inch - Right Cyclic 80 KIAS	E22FSTRL	E22FSTRR	1012/0954	16/16	
Step Input - 1.5 inch - Aft Cyclic 80 KIAS	E22FSTAL	E22FSTAR	1013/0955	16/18	
Break Turn Left 100 KIAS	E22FBRKL	E22FBRKR	1012/0957	18/17	
Normal Landing	E22FNMLL	E22FNMLR	1021/1024	17/12	
Aerodynamically braked landing	E22FADLL	E22FADLR	1022/1025	24/18	
Operational Landing	E22FOPLL	E22FOPLR	1023/1026	12/10	
Calibration - Post-flight	PORT07A	STBD07A	1033/1032		

Table 4(h) - Flight conditions flown for each aircraft configuration

Aircraft Configuration	ESSS: Yes Take-off Weight: 19900 lb ESSS Tanks: 2 Fuel/Tank: 100%	Internal Fuel (pre-flight) 1200 lb Internal Fuel (post-flight) 440 lb		Day 7 16 Feb 1995	
Flight Condition	Filename Left Side Gauges	Filename Right Side Gauges	Recording Start Time: Left/Right	Recording Duration Left/Right (sec)	Note
Level Flight 70 KIAS	P22FLF5L	P22FLF5R	1151/1218	30/30	10
Level Flight 100 KIAS	P22FLF7L	P22FLF7R	1158/1225	30/54	11
Level Flight 120 KIAS	P22FLF9L	P22FLF9R	1203/1231	31/30	
Left Turn at 30 AOB 100 KIAS	P22FL3ML	P22FL3MR	1209/1237	35/34	
Right Turn at 30 AOB 100 KIAS	P22FR3ML	P22FR3MR	1214/1242	33/32	
Low-level flight	LOWL	LOWR	1007/1305	60/60	12

Notes: All notes are listed on the page following Table 4(k)

Table 4(i) - Flight conditions flown for each aircraft configuration

Aircraft Configuration	ESSS: Yes Take-off Weight: 20000 lb ESSS Tanks: Yes Fuel/Tank: 50%	Internal Fuel (pre-flight) 2310 lb Internal Fuel (post-flight) 960 lb		Day 8 17 Feb 1995	
Flight Condition	Filename Left Side Gauges	Filename Right Side Gauges	Recording Start Time: Left/Right	Recording Duration Left/Right (sec)	Note
Calibration - Pre-flight	PORT08	STBD08	0915/0915		
Level Flight Hover	E22HLF0L	E22HLF0R	0922/0943	32/33	
Level Flight 40 KIAS	E22HLF3L	E22HLF3R	0926/0945	32/33	
Level Flight 70 KIAS	E22HLF5L	E22HLF5R	0927/0946	32/34	
Left Turn at 30 AOB 70 KIAS	E22HL35L	E22HL35R	0928/0947	32/32	
Right Turn at 30 AOB 70 KIAS	E22HR35L	E22HR35R	0929/0948	32/36	
Left Turn at 45 AOB 70 KIAS	E22HL45L	E22HL45R	0930/0949	34/33	
Right Turn at 45 AOB 70 KIAS	E22HR45L	E22HR45R	0931/0950	34/32	
Level Flight 100 KIAS	E22HLF7L	E22HLF7R	0932/0951	32/33	
Left Turn at 30 AOB 100 KIAS	E22HL3ML	E22HL3MR	0933/0952	33/32	
Right Turn at 30 AOB 100 KIAS	E22HR3ML	E22HR3MR	0934/0953	32/33	
Left Turn at 45 AOB 100 KIAS	E22HL4ML	E22HL4MR	0935/0954	33/33	
Right Turn at 45 AOB 100 KIAS	E22HR4ML	E22HR4MR	0936/0955	33/32	
Level Flight 120 KIAS	E22HLF9L	E22HLF9R	09370956	34/33	
Moderate Pull-out 120 KIAS	E22HMPOL	E22HMPOR	0938/0957	17/17	
Step Input - 1.5 inch - Left Cyclic 80 KIAS	E22HSTLL	E22HSTLR	0939/0958	18/17	
Step Input - 1.5 inch - Right Cyclic 80 KIAS	E22HSTRL	E22HSTRR	0940/0959	17/17	
Step Input - 1.5 inch - Aft Cyclic 80 KIAS	E22HSTAL	E22HSTAR	0941/0959	17/17	
Break Turn Left 100 KIAS	E22HBRKL	E22HBRKR	0941/1000	17/20	
Normal Landing	E22HNMLL	E22HNMLR	1007/1004	19/30	
Aerodynamically braked landing	E22HADLL	E22HADLR	1008/1005	22/25	
Operational Landing	E22HOPLL	E22HOPLR	1009/1006	16/16	
Calibration - Post-flight	PORT08A	STBD08A	1026/1027		

Table 4(j) - Flight conditions flown for each aircraft configuration

Aircraft Configuration ESSS Tanks with Old Rigging	ESSS: Take-off Weight: ESSS Tanks: Fuel/Tank:	Yes 20000 lb Yes 100%	Internal Fuel (pre-flight) 2310 lb Internal Fuel (post-flight) 960 lb		Day 9 20 Feb 1995	
Flight Condition		Filename Left Side Gauges	Filename Right Side Gauges	Recording Start Time: Left/Right	Recording Duration Left/Right (sec)	Note
Calibration - Pre-flight		PORT09	STBD09	0949/0948		
Level Flight	70 KIAS	R22FLF5L	R22FLF5R	1003/1033	30/30	
Level Flight	100 KIAS	R22FLF7L	R22FLF7R	1009/1040	30/30	13,14
Left Turn at 30 AOB	100 KIAS	R22FL3ML	R22FL3MR	1020/1046	30/35	
Right Turn at 30 AOB	100 KIAS	R22FR3ML	R22FR3MR	1025/1047	32/30	
Level Flight	120 KIAS	R22FLF9L	R22FLF9R	1030/1048	30/30	
Low-level flying		R22FLOWL	R22FLOWR	1052/1054	60/75	15
Rotor brake application - at shutdown			R22FRBKR	-/1102		16
Calibration - Post-flight		PORT09A	STBD09A	1104/1103		

Notes: All notes are listed on the page following Table 4(k)

Table 4(k) - Flight conditions flown for each aircraft configuration

Aircraft Configuration Hook loads and Autorotations	ESSS: Yes Take-off Weight: 16600 lb ESSS Tanks: No			Day 10 21 Feb 1995	
Flight Condition	Filename Left Side Gauges	Filename Right Side Gauges	Recording Start Time: Left/Right	Recording Duration Left/Right (sec)	Note
Calibration - Pre-flight	PORT10	STBD10	1411/1412		
Level Flight Hover	E100LF0L	E100LF0R	1443/1436	30/30	17,18
Level Flight 70 KIAS	E100LF5L	E100LF5R	1445/1437	30/31	
Level Flight 100 KIAS	E100LF7L	E100LF7R	1447/1439	31/31	
Left Turn at 30 AOB 100 KIAS	E100L3ML	E100L3MR	1448/1441	30/33	
Right Turn at 30 AOB 100 KIAS	E100R3ML	E100R3MR	1449/1442	32/33	
Level Flight Hover	B200LF0L	B200LF0R	1457/1507	30/30	19,20
Level Flight 70 KIAS	B200LF5L	B200LF5R	1459/1505	30/32	21
Level Flight 100 KIAS	B200LF7L	B200LF7R	1501/1503	30/49	22
Level Flight Hover	L200LF0L	L200LF0R	1523/1514	30/31	23, 24
Level Flight 70 KIAS	L200LF5L	L200LF5R	1519/1516	31/30	25
Level Flight 100 KIAS	L200LF7L	L200LF7R	1520/1518	30/30	26
Level Flight Hover	B300LF0L	B300LF0R	1601/1617	30/30	27, 28
Level Flight 70 KIAS	B300LF5L	B300LF5R	1602/1609	31/31	
Level Flight 100 KIAS	B300LF7L	B300LF7R	1604/1610	31/31	29
Left Turn at 30 AOB 100 KIAS	B300L3ML	B300L3MR	1605/1611	40/48	
Right Turn at 30 AOB 100 KIAS	B300R3ML	B300R3MR	1607/1614	45/43	30
Level Flight Hover	B400LF0L	B400LF0R	1652/1658	31/30	31, 32
Level Flight 70 KIAS	B400LF5L	B400LF5R	1654/1656	30/30	33
Autorotation: Zero forward airspeed 0	A100LF0L	A100LF0R	1627/1640	30/30	34
Autorotation: Forward flight 70 KIAS	A100LF5L	A100LF5R	1628/1641	3030	
Autorotation: Forward flight 100 KIAS	A100LF7L	A100LF7R	1633/1645	30/30	
Autorotation: Left Turn at 30 AOB 100 KIAS	A100L3ML	A100L3MR	1634/1646	30/31	
Autorotation: Right Turn at 30 AOB 100 KIAS	A100R3ML	A100R3MR	1635/1647	39/33	
Calibration - Post-flight	PORT10A	STBD10A	1701/1700		

Notes for Table 4

0. These two recordings were made on the previous day (6/2/1995) for test purposes.
1. For recording of left gauges: 3 knot headwind, at approx 500 ft above sea level Similar conditions for recording of right gauges
2. All steady state flight conditions except hover were at approximately 1000 ft pressure altitude
3. Recording started 3 seconds before turn was commenced; after commencement of turn, time to achieve bank angle was 2 seconds; this was the procedure followed throughout the flight investigation for all turns
4. For recording of left gauges: 2 knot headwind, at approx 500 ft above sea level Similar conditions for recording of right gauges except vibration levels appeared to be higher
5. Not enough fuel left to record operational landing for right-hand gauges
6. For PORT500 and STB500, a 500 lb practice bomb was installed on the outboard pylon of the port ESSS wing and another on the outboard pylon of the starboard ESSS wing. Total bomb load for each ESSS wing was 500 lb.
   For PORT1000 and STBD1000, additional 500 lb practice bombs were installed on the inboard pylons of each ESSS wing. Total bomb load for each ESSS wing was 1000 lb.
7. Data recorded after landing to capture the period just prior to, and just after, switchover from the main engine generators to the APU. The calibration switch was moved from the full positive to the full negative position several times during the recording period.
8. Headwind of 13 knots
9. Roll-rate achieved during recording of file E200STRL and was less than the typical roll rate for the left and right cyclic inputs. Usually, an angle of bank of approximately 60° was reached during a typical lateral step input, but for E200STRL and E200STRR, only 45° angle of bank was reached.
10. All filenames beginning with P indicate that cine cameras were mounted on the forward section of the aircraft, just below the pilot's and co-pilot's doors, facing backwards to record the motion of the ESSS tanks.
11. Just prior to recording of P22FLF7R at 1225 hours, started transferring fuel from the ESSS tanks to the internal tank. By 1230 ESSS fuel tanks had 1400 lb of fuel each (i.e. 100 lb of fuel had been transferred from each tank).
12. These runs recorded a low-level flight profile which included some terrain following flight, pull-ups, and banked turns. The data recorded in LOWL were not usable because the power to the amplifiers had not been switched back on after the left-to-right sensor leads had been swapped.
13. During recording of R22FLF7L, speed varied between 100 and 105 KIAS.
14. One of the cine cameras jammed. No more films were taken.
15. Flight condition as per note 12
16. Rotor-brake applied with main rotor speed at approximately 40% of flight speed.

17 Initial runs with no hook load

18 Headwind of 10 knots

19 Picked up 3500 lb of practice bombs

20 Headwind of 17 knots during recording of B200LF0L and 14 knots for B200LF0R

21 Aircraft was 5° nose down, with 60% matched torque from both engines.

22. Aircraft was 11° nose down, with 94% matched torque from both engines. Load was trailing approximately 10 feet behind the cabin floor hook point.

23. Picked up 3500 lb Land Rover. Fuel state now 690lb.

24. Headwind of 15 knots

25. Aircraft was 3° nose down.

26. Aircraft was 11° nose down, with 97% matched torque from both engines.

27. Landed to pick up fuel (now 1200 lb) and then picked up 4500 lb of practice bombs.

28. Headwind of 18 knots during recording of B300LF0L and 14 knots for B300LF0R

29. Aircraft was 9° nose down.

30. Couldn't get speed constant. Speed varied by up to 15 knots.

31. Picked up 6000 lb of practice bombs.

32. Headwind of 12 knots during recording of B400LF0L and 14 knots for B400LF0R

33. At approximately the 15 second mark during the recording, the bombs moved in the sling.

34. Autorotations began at 9000 feet and reached sink speeds of 5000 feet/minute. This allowed two to three flight conditions to be recorded during each autorotation.

Table 5 Explanation of file naming system

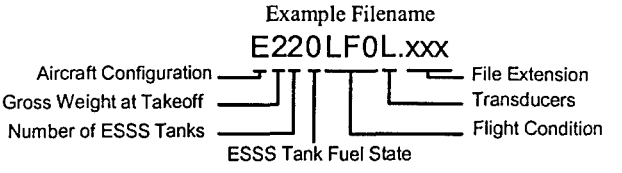

Item	Codes or Values
Aircraft Configuration	N No ESSS fitted E ESSS fitted A ESSS fitted - Autorotation flights B ESSS fitted - Hook loads - bombs L ESSS fitted - Hook loads - Land Rover R ESSS fitted - Old rigging method (Appendix 3)
Gross Weight at Take-off (nominal)	1: 16000 2: 20000 3: 21000 4: 22500
Number of ESSS tanks (outboard)	0 or 2
ESSS Tank Fuel State	0: Zero Fuel H: Half Full F: Full
Flight Condition	LF*n* Level flight at 0.*n* VH, $0 \le n \le 9$ L*nv* Left turn with: *n* = 3 for 30° angle of bank = 4 for 45° angle of bank *v* = 5 for speed at 0.5VH = M for max allowed speed (0.7VH) R*nv* Right turn with *n*, *v* as above for L*nv* MPO Moderate pullout NML Normal landing ADL Aerodynamically-braked landing OPL Operational landing STL Step input - 1.5 inches of left cyclic STR Step input - 1.5 inches of right cyclic STA Step input - 1.5 inches of aft cyclic BRK Break turn left LOW Low-level flying RBK Rotor brake application during rotor shutdown TAX Ground taxiing
Transducers	L Left-hand side transducers being read R Right-hand side transducers being read
File extension	DAT The raw data files (binary format) 0*nn* Data in the DAT file for channel *nn* (ASCII format) R*nn* Used by the FFT viewer A*nn* Range-paired data (from 0*nn* files) B*nn* Range-paired data (from P*nn* files) C*nn* Range-paired data (from Q*nn* files) E*nn* Range-paired data (from V*nn* files) P*nn* Principal strain, ε_P (from 0*nn* files) Q*nn* Principal strain, ε_Q (from 0*nn* files) T*nn* Principal strain angle, θ (from 0*nn* files) V*nn* Von Mises equivalent strain (from 0*nn* files) Y*nn* Range-paired data (from Z*nn* files) Z*nn* Offset-corrected data (from 0*nn* files)

Table 6(a) Panel fatigue damage comparison between ESSS and Non-ESSS configurations (strain gauges SLP2 and SRP2)

Flight Condition			Left or Right Panel	Configuration Causing More Fatigue Damage	
				Non-ESSS	ESSS
Level Flight:		Hover	L	●	
			R	●	
Level Flight:		40 KIAS	L	●	
			R	●	
Level Flight:		70 KIAS	L	●	
			R	●	
Level Flight		100 KIAS	L	●	
			R	●	
Level Flight		120 KIAS	L		●
			R		●
Left Turn	30 AOB:	70 KIAS	L	●	
			R	●	
Right Turn	30 AOB	70 KIAS	L	●	
			R	●	
Left Turn	30 AOB	100 KIAS	L	●	
			R	●	
Right Turn	30 AOB	100 KIAS	L	●	
			R	●	
Left Turn	45 AOB	70 KIAS	L	●	
			R	●	
Right Turn	45 AOB	70 KIAS	L	●	
			R	●	
Left Turn	45 AOB	100 KIAS	L	●	
			R	●	
Right Turn	45 AOB	100 KIAS	L	●	
			R	●	
Moderate Pull-out		120 KIAS	L	●	
			R	●	
Break Turn Left		100 KIAS	L	●	
			R	●	
Normal Landing			L	●	
			R	●	
Aerodynamically-braked Landing			L	●	
			R	●	
Operational Landing			L	●	
			R	●	

Table 6(b) Panel fatigue damage comparison between ESSS and Non-ESSS configurations (strain gauges SLP5 and SRP5)

Flight Condition			Left or Right Panel	Configuration Causing More Fatigue Damage	
				Non-ESSS	ESSS
Level Flight:		Hover	L	●	
			R	●	
Level Flight:		40 KIAS	L	●	
			R	●	
Level Flight:		70 KIAS	L	●	
			R	●	
Level Flight		100 KIAS	L		●
			R	●	
Level Flight		120 KIAS	L		●
			R		●
Left Turn	30 AOB:	70 KIAS	L		●
			R	●	
Right Turn	30 AOB	70 KIAS	L	●	
			R	●	
Left Turn	30 AOB	100 KIAS	L		●
			R	●	
Right Turn	30 AOB	100 KIAS	L		●
			R	●	
Left Turn	45 AOB	70 KIAS	L	●	
			R	●	
Right Turn	45 AOB	70 KIAS	L	●	
			R	●	
Left Turn	45 AOB	100 KIAS	L	●	
			R	●	
Right Turn	45 AOB	100 KIAS	L	●	
			R	●	
Moderate Pull-out		120 KIAS	L	●	
			R	●	
Break Turn Left		100 KIAS	L	●	
			R	●	
Normal Landing			L		●
			R	●	
Aerodynamically braked landing			L		●
			R	●	
Operational Landing			L	●	
			R	●	

Table 7 Typical Range-Mean-Pair table

RANGE MEAN PAIR TABLE with 8 levels.
Range: -300 to 500
The increment between levels is 100.00 uE

PEAKS (uE)								
LEVEL 1 (-300.00 to -200.01)	65							
LEVEL 2 (-200.00 to -100.01)	55	20						
LEVEL 3 (-100.00 to -0.01)	0	5	4					
LEVEL 4 (0.00 to 99.99)	0	0	4	16				
LEVEL 5 (100.00 to 199.99)	0	0	0	8	67			
LEVEL 6 (200.00 to 299.99)	0	0	0	3	124	153		
LEVEL 7 (300.00 to 399.99)	0	0	0	1	3	16	15	
LEVEL 8 (400.00 to 499.99)	0	0	0	1	0	1	45	42
	1	2	3	4	5	6	7	8
	TROUGHS							

Unpaired turning points: 1 0 0 0 0 0 0 1

A total of 648 range-pairs were derived from 1297 data points.

However the nominal value was used to pair 532 pts.

Table 8 Indicative fatigue damage calculations (see Appendix 3.2.1).

Flight Condition		Gauge	Indicative Fatigue Damage		
Code	Description		Old Rigging	New Rigging	Old - New
L3M	Left Turn 30° Angle of Bank 100 KIAS	SLP1	2.04E-09	1.91E-09	1.39E-10
		SLP2	9.69E-08	1.05E-07	-7.58E-09
		SLP3	4.75E-08	4.49E-08	2.54E-09
		SLP4	5.34E-08	5.41E-08	-6.75E-10
		SLP5	1.01E-07	9.40E-08	6.58E-09
		SRP1	7.48E-09	5.86E-09	1.62E-09
		SRP2	1.23E-07	1.11E-07	1.19E-08
		SRP3	1.27E-07	1.11E-07	1.54E-08
		SRP4	1.02E-07	9.07E-08	1.15E-08
		SRP5	2.44E-07	2.28E-07	1.62E-08
LF5	Level Flight 0.5VH (40 KIAS)	SLP1	3.02E-09	2.86E-09	1.64E-10
		SLP2	7.24E-08	8.07E-08	-8.31E-09
		SLP3	3.29E-08	3.69E-08	-4.01E-09
		SLP4	3.95E-08	4.85E-08	-9.04E-09
		SLP5	7.83E-08	8.41E-08	-5.80E-09
		SRP1	6.52E-09	3.49E-09	3.03E-09
		SRP2	8.49E-08	1.05E-07	-1.96E-08
		SRP3	7.71E-08	7.57E-08	1.44E-09
		SRP4	6.73E-08	7.08E-08	-3.48E-09
		SRP5	1.71E-07	1.75E-07	-4.54E-09
LF7	Level Flight 0.7VH (100 KIAS)	SLP1	1.60E-09	2.41E-09	-8.09E-10
		SLP2	9.24E-08	9.07E-08	1.68E-09
		SLP3	3.98E-08	3.90E-08	7.71E-10
		SLP4	4.65E-08	4.93E-08	-2.78E-09
		SLP5	9.15E-08	8.61E-08	5.45E-09
		SRP1	8.61E-09	3.77E-09	4.84E-09
		SRP2	1.05E-07	1.03E-07	2.90E-09
		SRP3	1.03E-07	1.02E-07	1.90E-09
		SRP4	8.20E-08	8.76E-08	-5.64E-09
		SRP5	2.06E-07	2.22E-07	-1.60E-08
LF9	Level Flight 0.9VH (120 KIAS)	SLP1	4.27E-09	1.79E-09	2.48E-09
		SLP2	1.44E-07	1.21E-07	2.31E-08
		SLP3	6.65E-08	5.17E-08	1.48E-08
		SLP4	7.33E-08	6.21E-08	1.12E-08
		SLP5	1.40E-07	1.10E-07	3.06E-08
		SRP1	8.88E-09	7.86E-09	1.02E-09
		SRP2	2.02E-07	1.78E-07	2.34E-08
		SRP3	2.15E-07	2.03E-07	1.19E-08
		SRP4	1.59E-07	1.54E-07	4.46E-09
		SRP5	3.85E-07	3.85E-07	3.95E-10
R3M	Right Turn 30° Angle of Bank 100 KIAS	SLP1	2.46E-09	1.92E-09	5.32E-10
		SLP2	1.09E-07	9.98E-08	8.91E-09
		SLP3	4.89E-08	3.89E-08	1.01E-08
		SLP4	5.93E-08	5.06E-08	8.77E-09
		SLP5	1.08E-07	8.73E-08	2.07E-08
		SRP1	7.29E-09	3.78E-09	3.51E-09
		SRP2	1.14E-07	1.11E-07	3.83E-09
		SRP3	1.05E-07	1.10E-07	-5.34E-09
		SRP4	8.98E-08	9.66E-08	-6.80E-09
		SRP5	2.15E-07	2.15E-07	-4.17E-10

Appendix 1

ESSS Struts

A1.1 Strut Strain Gauge Installation

As shown in Fig. 4, each of the ESSS struts (which support the ESSS on the aircraft) had a single uniaxial strain gauge. Figure 14 shows the installation in more detail. Initially, strain gauges were placed on the exposed part of the strut and the lug because the RAAF had suggested that strain gauges not be placed in positions which would require disassembly of the aircraft structure. The results from the strain measurements at these locations indicated that the strain signal was too low and hence unreliable. The RAAF agreed to AMRL's request to remove the end fairing to allow access to a better location which is shown in Fig. 14.

Prior to the flight investigation, all the struts were tested in an AMRL tensile testing machine. Loads during these test runs were ±12 kN for the forward struts and ±8 kN for the rear struts. For the forward struts, 12 kN equates to 33% of the tension and compression design loads. For the rear struts, 8 kN equates to 7% of the tensile design load and 5% of the compressive design load (Ref. 12, Sect. A8 and A9). A typical test run is shown in Fig. 15.

A1.2 Strut Damage

The end fairing (Fig. 14) had to be removed from each of the struts to allow the strain gauges to be installed. When these end fairings were removed, damage was discovered in the strut tube. This damage is detailed in Ref. 13, and is summarised below.

(a) For all the struts, damage was present at locations A and B (Fig. 16). These locations are in line with the centreline (C) of the lower rivets.

(b) For the Left-hand Rear strut, this damage was observed before the fairing was removed as there was enough clearance between the fairing and the tube to permit inspection.

(c) For the Left-hand Forward strut, contact was made between the tail of the rivet and the tube (at location A) during removal. However, the contact was slight and not of the level required to produce the damage. Also, the amount of rivet movement was very small, indicating that the tail was only just clear of the tube surface.

(d) For all the other struts and for location B on the Left-hand Forward Strut, there was no contact between the rivet tail and the tube during removal of the rivet centre.

(e) The damage appeared to be of three types: damage that may have been made by a drill bit, impact damage, and "rubbing-type" damage.

(f) The severity of the damage varied, but most of it was more than 0.005 inch deep which was the limit of the allowable damage specified in the Black Hawk Structural Repair Manual (Ref. 14).

(g) The Left-hand Rear strut also has a deep gouge mark at location D.

Damage observed in the struts before removal of the fairing included:

(a) All three struts had a gouge at location E. It appears to be from some type of interference between the strut and the ESSS wing. In addition, the Right-hand Rear strut had a rubbing mark nearby.

(b) The Left-hand Rear strut had corrosion underneath the earth strap for the end-closure fairing.

The damage in the struts, although not severe, was outside the allowable limits as stated in the Structural Repair Manual (Ref. 14) and all four struts were declared unserviceable. A request for more struts was placed with the Army, and four undamaged struts were received. These undamaged struts were used in the flight investigation.

Appendix 2

Range-Pair Analysis

A2.1 Introduction

As mentioned in Section 4.2, a range-pair analysis was undertaken of selected flight data to examine the possibility that, although both ESSS and non-ESSS configurations produced the same max-min strains, there may have been a difference in the number of load cycles applied.

The range-pair analysis was applied to: the raw flight strains; the flight strains converted into principal strains; and the Von Mises equivalent strains. Calibration measurements, taken throughout the flight investigation, were also used to correct the raw data for zero offset effects caused by the drift inherent in the strain gauges. Offset-corrected data were similarly converted into range-pair table format and used with the other processed data to make comparative assessments of gauge drift effects.

Finally, visual comparisons of the range-pair table data were made to determine the effect, if any, of the External Stores Support System (ESSS) and fuel tanks on the stress/strain cycles experienced by the fuselage panels. Prior to the flight investigation, a possible significant source of dynamic loading in the panel was thought to be *"flapping of the ESSS during landing due to the inertial loads of the ESSS and fuel tanks"* (Ref. 3). For this reason, visual comparisons were made on normal, aerodynamically-braked, and operational landings. To aid the comparison, range-pair tables were transformed into 'colour-maps', in which cycle counts were assigned colours indicating their relative magnitudes (ie. the brighter the colour the higher the cycle count).

A2.2 The Range-Pair Method

The Range-Pair method or, alternatively, the Range-Mean-Pair method, is a way of identifying *"load cycles in terms of the stable cyclic stress-strain behaviour of the material concerned (ie. turning points are paired that define closed hysteresis loops)"* (Ref. 15). By extracting and counting the constituent cycles of complex load histories, particular cycles can be evaluated in terms of their severity and fatigue damage contribution. A cycle is bounded by two load values - a maximum load and a minimum load. These are referred to as turning points (TPs).

The range-pair method used here is that developed at AMRL by R.C. Fraser in 1979 (Ref. 15). It is described as a "one-pass" method because the data need to be examined in a single pass to pair all the TPs into cycles. The method is summarised in Appendix 4.

A2.3 A FORTRAN Implementation of the Range-Pair Method

The FORTRAN implementation of the one-pass range-pair method for application to the Black Hawk raw strain data, entitled `BLACK8.FOR`, was an amalgam of new and existing code.

The 'BLACK8.FOR' program is structured in the following way.

(a) A file called `BLKLIST.TXT` (which must be created manually prior to running the program) is accessed. The file contains the MS-DOS 8-character filename prefixes of all files to be processed in the current batch.

(b) The first 8-character filename prefix is read and used to generate the full filenames for all data channels requiring processing (in this case, channels 7 to 21). An accompanying output filename, identical to the input filename with the exception that the first character in the extension is replaced by a letter to distinguish it as an output file (See Table 5), is also generated. An appendable file called RTSFILES.TXT is also opened by the program to hold the names of files which have a range of data that is too small to warrant range-pairing. This file must exist before running the program or an error will result. If the program is being run for the first time, then RTSFILES.TXT should be created as a null (empty) file before running the program. The relationship of the various files used by the program is shown in Fig. 17.

(c) Taking the first input filename created, the program reads the data line-by-line and stores them in an array variable called STORE(). From the data in STORE(), the program removes redundant data points to end up only with the points necessary to define the sequence of peaks and valleys (Fig. 18). These remaining points are stored in another array called VALUE().

(d) Next, the program removes any cycle that has an absolute difference of less than a specified amount, called the discriminator. The size of the discriminator is based on removing cycles that are not fatigue damaging. This process might be viewed as one of smoothing or filtering so as to end up with the information that matters most. A value of 5 με was judged to be suitable for the discriminator in this instance. Cycles found to be larger than 5 με are stored in an array variable called DISC().

(e) A further option that may be activated in the program is a "dead-band" processor. If, for example, we were interested only in cycles falling outside a band ranging between -100 and +100 με, we could specify a dead-band of this size and the program would eliminate all complete cycles falling within it. This feature was part of the existing range-pair code incorporated into BLACK8.FOR, but was not used. It was bypassed by specifying a dead-band ranging between zero and zero.

(f) Before the program can convert the data into range-pairs it must group the TPs according to their relative magnitudes. This is done by breaking the range of data down incrementally into discrete levels and assigning individual TPs to

the level in which they occur. First, the maximum and minimum values of the load history are determined. The range of data between the maximum and minimum is then broken up into segments 100 με wide[3]. Adjustments were made to ensure all segment boundaries were multiples of 100. Load histories having a range of less than 100 με would be treated as a series of TPs, all at the same level and would therefore fail to be paired. Such histories do not undergo further processing, being deleted from the working directory. The names of all files deleted in this way are stored in the file RTSFILES.TXT for future reference.

(g) Once the level boundaries have been established, each TP is assigned to its corresponding level based on which boundaries it lies between. Where a TP falls on a boundary it is automatically assigned to the level of which that boundary is the **upper** bound.

(h) The homogenisation of TPs into 100 με wide levels invariably means there will now be some adjacent points that become indistinct. Adjacent points falling in the same level do not fit into the continuous succession of peaks and troughs required by the program for range-pairing and are therefore degenerate and must be removed. The removal process is carried out by the program whenever the level number of a TP is not different to the one immediately preceding or following it in the level sequence or when a TP does not constitute a level peak or trough. Figure 19 shows a sequence with degenerate data and the same sequence with the degenerate data removed leaving only "valid" points. The valid points are stored in an array called VALIDTP().

(i) As mentioned in Appendix 4, "end effects" must be dealt with to ensure that all TPs are paired correctly. If there is an odd number of valid TPs a "nominal" value is added by the program to the data to ensure pairing of the point which would otherwise be left unpaired. The nominal value used in BLACK8.FOR is zero. Also included is a dummy TP, which is added at the very end of the sequence. The dummy TP is not paired with any of the valid TPs, but it is used to force the pairing of any TPs which are not able to be paired at the end of the load history. If the last point is a peak a large positive number (10^{30}) is used; a large negative number (-10^{30}) is used otherwise.

(j) Having sorted the data, the program commences the range-pair count routine. TPs are loaded into a stack sequentially and used to test if the previous two TPs in the stack can be identified as a range-pair. If a range-pair is not detected using the three-point test the next valid TP is loaded and the process repeated until a range-pair is found. As range-pairs are detected, a two-dimensional array counter is updated to keep a running tally of the number of particular cycles that have been identified. The process continues until all TPs have been accounted for.

---

[3] A level size of 100 με was judged to be appropriate for the Black Hawk data as it provided sufficient detail over the range of strain values recorded without over-simplification or being more refined than necessary to allow conclusions to be drawn.

(k) The final stage of the program is the creation of a range-pair table, such as the example shown in Table 7, which displays the range-pairs that have been extracted from the load history. The table itself is a simple half array with axes of peak (ordinate) and trough (abscissa) load levels obtained by putting the range-pair counts into a number of cells corresponding to their peak and trough values. Header information identifies the number of levels and range of data in the table. Below the table is a line that states: "Unpaired turning points:", followed by a string of zeros (representing levels) and a "1" at either end. The "1" signifies that a "dummy" point has been used by the program to ensure pairing of all data. The use of a "nominal" turning point is signified if such a point was used to make a pairing. Also included is a statement of the total number of range-pairs found and the number of valid turning points that were tested in the process. The range-pair table and accompanying information are written to the output file, the name of which was generated and opened at the start of the program.

The "BLACK8.FOR" source code is provided in Appendix 5.

A2.4. Principal Strains and Von Mises Equivalent Strains

During the Black Hawk flight investigation, panel strains were measured by rosette strain gauges at various locations on the panel surface. A rosette measures strains in three directions and from this information it is possible to determine the maximum and minimum strains that are at the gauge location. These maximum and minimum strains are known as the principal strains.

In addition to determining the principal strains, the strains were converted to Von Mises Equivalent Strains (VMES) so that the strains could be compared against uniaxial test data.

The equations used in both principal strain and VMES calculations are described in Appendix 6. The calculations were performed for all flight conditions, but only on the following channels, which correspond to the sub-elements of the rosette strain gauges:

Gauges	Channels
SLP1 & SRP1	7, 8, & 9
SLP2 & SRP2	10, 11, & 12
SLP3 & SRP3	13, 14, & 15
SLP4 & SRP4	16, 17, & 18
SLP5 & SRP5	19, 20, & 21

Each set of three channels listed above corresponded to arms *a*, *b*, and *c* of the rosette respectively (eg. channel 7 = arm *a*, channel 8 = arm *b*, and channel 9 = arm *c*).

All principal strain and VMES output files were subsequently reformatted into range-pair tables using the "BLACK8.EXE" program in the manner described previously.

Output files were of the form:

ε_{ip}	Infile.bnn	(where 'nn' = channel number of arm 'a')
ε_{iq}	Infile.cnn	
Von Mises	Infile.enn	

A2.5 Zero Offset Correction

Strain gauges often exhibit some degree of drift, which causes a slight offset from the calibrated zero to develop over time. Drift effects can result from small environmental temperature changes and they produce strain measurements that differ from the true values by the amount the gauge is offset. Daily pre-flight and post-flight calibration checks were conducted to check this effect, though it appeared to be small.

Calibration data (contained in files `PORT.CAL` and `STBD.CAL`) were used to make appropriate offset corrections to data files corresponding to all the landings recorded on days 3, 7, and 8 of the flight investigation.[4] The calibration data contained pre-flight gauge zero values for days 3, 7, and 8 and also included post-flight zero measurements taken on day 8. For days 3 and 7 pre-flight zero measurements were used, whilst, for day 8, the average of the pre-flight and post-flight values was used. All corrections were made using Microsoft Excel spreadsheets and, once corrected, the data were range-paired in the established way. Raw offset corrected data were stored in files with a 'z' in the first character place of the filename extension and range-pair data were stored in files with a 'y' in the first character place of the filename extension.

A2.6 Visual Comparison of Data

With the raw, calculated, and offset corrected data all in a convenient range-pair table format, visual comparisons of the tables were made to determine to what extent the carriage of fuel tanks via the ESSS was responsible for the panel cracking. Prior to the flight investigation, it was thought that flapping of the ESSS during landings due to the inertial loads of the ESSS and fuel tanks, was a possible source of dynamic loading on the panel (Ref. 3).

Data presented in the range-pair tables are difficult to compare visually, especially when, as was the case here, the tables are complex and numerous. To make the task easier, a short graphical program was developed to take a given range-pair table and convert it into a 'colour map', the cycle counts being assigned colours to represent their relative magnitudes. With each colour map being scaled to fit the screen, this graphical representation simplified the task of identifying the most frequent and potentially damaging cycles.

The program 'CMAP.FOR' first reads in a single range-pair table data file. The cycle count data are stored in a two dimensional array called `X`(*row, col*), followed by a call

[4] The reasons behind this choice of files will become apparent below.

to set the graphics mode to enable graphical screen output. Range-pair count values are then assigned colours according to their magnitude, with higher counts receiving brighter colours. To keep programming simple, only the 16 default text mode colour attributes were used. Therefore, count values were assigned colours according to the following scheme:

Count Range	Colour Assigned
0 to 50	Grey
51 to 100	Blue
101 to 150	Light Blue
151 to 200	Green
201 to 250	Light Green (Lime)
251 to 300	Cyan
301 to 350	Light Cyan
351 to 400	Yellow
401 to 450	White
> 450	Bright White

As each count is assigned a colour, a rectangular cell is drawn and filled with the assigned colour. X and Y coordinates are automatically updated so that successive cells are positioned on the screen and built up in such a way as to emulate the form of the original range-pair table. A scaling factor is also generated to ensure that the finished "colour-map" fits entirely on the screen. The "CMAP.FOR" source code is provided in Appendix 5 of this report.

Because ESSS-induced dynamic loadings were thought to be most severe during landing operations, comparisons were limited to data recorded during normal, aerodynamically-braked, and operational landings. In addition, only those landings recorded on days 3, 7, and 8 were considered for comparison. On day 3 the ESSS was not used and the aircraft gross weight was 20000 lb. On day 7 the aircraft was flown with two full outboard fuel tanks on the ESSS and on day 8 the aircraft was flown with two 50%-full outboard fuel tanks on the ESSS. The data used correspond to the raw data which earlier underwent zero offset correction (see previous section).

A2.6.1 RESULTS OF VISUAL COMPARISONS.

In total, almost 800 range-pair tables were compared, including 255 tables of offset corrected strain data. With this volume of data, it was not practical to include, in this document, all of the colour-maps that were generated in the process. A complete record of the colour-maps was made by noting down colours and their locations as well as table size and first cell strain values. Where first cell strain values were not equal for day 3, day 7, and day 8 colour-maps, cell colour coordinate corrections were manually made and noted down. However, even this abbreviated record of the comparisons is too unwieldy to warrant inclusion here. Instead, an overall impression of the findings can be gained by examining a few selected examples, which were typical of the bulk of the colour maps generated.

A typical comparison was that shown in Fig. 20 which comprises colour-maps produced for normal-landing right-panel raw data. By considering cell 2A (corresponding in this instance to peak strains ranging between 0 and +100 με and trough strains ranging between -100 and 0 με) it can be seen that there was a change in the colour representing the cycle count. For N200NMLR.A07 there was no ESSS and a relatively low cycle count was registered, hence the relatively dark blue colour of the cell. Then for E22HNMLR.A07, where the aircraft was flown with ESSS supporting two 50%-full outboard fuel tanks, the cycle count jumped considerably in cell 2A and so a much brighter lime colour can be seen filling the cell. Finally, E22FNMLR.A07 shows that when the ESSS supporting two full outboard fuel tanks was fitted, there was a drop in the number of cycles recorded as evidenced by the light blue colour. The slight increase in the number of cycles for the E22FNMLR.A07 case over the N200NMLR.A07 case would seem to indicate that, in this example at least, the use of the ESSS does increase the number of cycles experienced. However, this same example also shows the reverse happening in cell 4C (corresponding to peak strains between +200 and +300 με and trough strains between +100 and +200 με). Here the count assigned colour changes from light blue to green to grey, indicating that the cycle count for the E22FNMLR.A07 case is lower than that for the N200NMLR.A07. This behaviour was typical and occurred over the entire spectrum of data comparisons carried out.

Another observation to be made from the example in Fig. 20 is that there was a significant increase in the strain counts measured during day 8, when the ESSS was used to support two 50%-full outboard fuel tanks, compared to either of the other two days' data. Even operation with full fuel tanks, which might be expected to produce a greater inertial dynamic loading, did not produce such high strain counts. This trend was observed in about half of the visual comparisons made. An approximately equal number of comparisons showed no such trend at all or sometimes the opposite. Part of the cause of the higher cycle counts that were observed for day 8 data might be the sloshing motion of fuel inside the tanks, which might be occurring despite damping by internal baffles. Figure 21 shows another example taken from the principal stress table comparisons.

Another contributing factor could be pooling of the fuel in the rear half of the tanks when the aircraft comes in to land because the tanks are then in a nose-high situation. This shifts the C.G. of the fuel rearwards and increases the torsional moment produced by the fuel mass on the ESSS (Fig. 22).

Comparisons made between raw data colour-maps and offset-corrected data colour-maps showed that the effect of zero offsets was insignificant, an occurrence that might have been because offsets had mostly been less than 100 με (ie. raw data turning points were generally translated by only one level or not at all when corrected for offsets). Observations were also made using offset corrected data in support of the fuel sloshing and moment arm theories born out of the other raw and calculated data comparisons.

A final example is shown in Fig. 23. This example is indicative of the overall trends observed from these comparisons. Taken from raw data range-pair tables measured during aerodynamically-braked landings, the colour-maps show that the ESSS has no significant effect on either the strain cycle counts or the strain magnitudes. Cell 4C in Fig. 23 maintained a blue colour fill regardless of whether the ESSS was present. Cell 2A again supports the theory that sloshing motion was occurring in the half-full fuel tanks, with higher strain counts being registered than in the other two cases. Yet, cells 2B and 3C show more cycles in the non-ESSS case than in the other two cases.

The trends identified by these few examples were unanimously supported by the rest of the data comparisons.

A2.7. Concluding Remarks

(a) Black Hawk internal panel raw strain data files have been converted to range-pair table format using a FORTRAN computer program implementation of R.C. Fraser's (Ref. 15) one-pass range-pair method. This has been done to make the data easier to utilise in the future for fatigue analysis purposes.

(b) The raw strain data have also been used to calculate principal strains and VMES, thereby determining the strain at each point on the panel surface where rosettes strain gauges were positioned. These calculated data were subsequently range-paired for analysis.

(c) Zero offsets arising from drift effects inherent in the strain gauges used during the flight investigation, have been corrected in the raw strain data corresponding to landing conditions for several aircraft configurations. Offset corrections were typically less than 100 $\mu\varepsilon$ and were obtained from calibration data recorded throughout the flight investigation. Offset-corrected data have also been range-paired.

(d) Range-paired raw data, calculated data, and offset-corrected raw data, corresponding to landing conditions only, have been visually compared to determine the extent of dynamic loading resulting from the carriage of fuel tanks via the External Stores Support System (ESSS). A computer "colour-mapping" technique was developed as a useful tool in making these comparisons. Two main trends were observed. Firstly, comparisons revealed that generally neither cycle counts nor load magnitudes varied appreciably between operation with no ESSS and the ESSS with two full outboard fuel tanks. Secondly, approximately one half of the comparisons indicated that when the aircraft was flown with two 50%-full outboard fuel tanks supported by the ESSS, the number of load cycles applied to the panel increased. A probable cause of this phenomenon has been suggested which relates to the increased moment at the fuel tank attachment point due to the displaced centre of gravity of the 50%-full fuel tank. There is also the possibility that the cause was fuel sloshing inside the tank. However, the other half of the comparisons showed either no effect or the opposite effect.

Appendix 3

Analysis of New Rigging Procedure for ESSS Ejector Racks

A3.1 INTRODUCTION

The ESSS fuel tanks are mounted on the ESSS wings via ejector racks which are fixed to the wings. The ejector racks are fastened to the wings by bolts which have castellated nuts. In August 1992, the procedure for fastening the ejector racks to the wings (called the "rigging procedure") was altered by a Special Technical instruction (STI) (Ref. 11). Some pilots had reported that the new method was causing higher vibrations so the Army requested that one of the aims of the flight investigation was to determine if the new rigging procedure had any detrimental effect on the panel cracking.

The old (pre-STI) rigging procedure was as follows: when fastening the castellated nuts, they were hand-tightened as far as possible and then the nut was **advanced, with a spanner, to the next castellation** to line up with the hole in the bolt and a cotter pin was installed.

The new (post-STI) rigging procedure is as follows: when fastening the castellated nuts, they are hand-tightened as far as possible and then the nut is **backed off** to the first castellation and the cotter pin is installed. The alteration in the rigging procedure was made because it was suspected that the pre-STI procedure may have led to cracked bushings in the ejector racks due to over-torquing of the bolts.

To determine the effects of the old and new rigging procedures, one flight during the flight investigation was conducted with the ejector racks fitted in accordance with the old procedure. The aircraft was configured with two full tanks on the ESSS and some typical flight conditions were flown (Table 4(j)).

The data from this flight were compared to the data obtained from the equivalent aircraft configuration, with the ejector racks fitted according to the new procedures. Two approaches were attempted in comparing the data collected for the two rigging methods: the Fast Fourier Transform technique and an indicative fatigue damage method.

A3.2 ANALYSIS

A3.2.1 Fast Fourier Transform Method

Fast Fourier Transforms (FFTs) were performed on the flight data and it appeared that there might be a difference in the panel strain environment induced by the two rigging

methods. However, the FFTs contain no phase information about the strain signal so the difference in terms of fatigue damage could not be found directly from them.

A3.2.1 Indicative Fatigue Damage Method

(a) Indicative Fatigue Damage

The term *indicative fatigue damage calculation* has been used because the calculations are similar to, but **not** the same as Sikorsky fatigue damage calculations. Specifically, material data from MIL-HDBK-5F have been used rather than Sikorsky material data. Also, an average endurance curve instead of a conservative endurance curve has been used. An average endurance curve is acceptable for the purposes of comparing the two rigging methods.

(b) Material Data and Endurance Curve

The material data in MIL-HDBK-5F Fig. 3.7.4.1.8(d) (Ref. 10) were selected as appropriate. The Figure defines an equivalent stress equation for 7075-T6 aluminium to calculate the allowable cycles (N_f) for a given equivalent stress level (S_{eq}):

$$\log N_f = 14.86 - 5.80 \log S_{eq}$$

$$S_{eq} = S_{max}(1-R)^{0.49}$$

$$R = S_{min} / S_{max}$$

Where S_{eq} is an equivalent stress for a load which varies from a low of S_{min} to a high of S_{max}, and R is the stress ratio.

(c) Range-Pair Conversion and Discretisation Level

Range-pair tables (Appendix 2) were completed for each of the data files and these were used as the load cycles in the indicative fatigue damage calculations. The range-pair method discretised the flight data into 100 με steps which corresponds to a stress of 1 ksi. Thus if a strain history did not vary by more than 100 με then a range-pair would not be found. Conceivably a strain at a nominal level of, say, 3000 με would not yield any load cycles from the range-pair process if the strain history for the manoeuvre stayed between 2950 and 3050 με. Thus, such a strain history would not produce any range-pairs and hence not be considered as fatigue damaging.

Since aluminium has no endurance limit, Sikorsky set the load (or stress) corresponding to an endurance of 10^8 cycles as the endurance limit. That is, if a load has an endurance of greater than 10^8 cycles, then the load is not considered to be fatigue damaging. To test that the discretisation process did not hide potentially damaging load cycles, the following calculation was performed to determine the stress

level required for a strain amplitude of less than 100 με (i.e. equivalent to 1 ksi stress in aluminium) to be damaging.

From the equations above, we can state, for a stress amplitude of 1 ksi, that:

$$S_{\min} = S_{\max} - 1$$

$$\text{and therefore } R = \frac{S_{\max} - 1}{S_{\max}}$$

Substituting for R in the equation for S_{max} gives:

$$S_{eq} = S_{\max}\left(1 - \frac{S_{\max} - 1}{S_{\max}}\right)^{0.49} = S_{\max}^{0.51}$$

Substituting for S_{max} in the equation for log N_f and setting $N_f = 10^8$ gives:

$$\log 10^8 = 14.86 - 5.80 \log\left(S_{\max}^{0.51}\right)$$

$$S_{\max} = 208 \text{ ksi}$$

Hence, an endurance of 10^8 cycles would be achieved for stress cycles varying between 207 ksi and 208 ksi. This level of stress is well in excess of the ultimate strength of the material and shows that a discretisation level of 1 ksi (100 με) is not too coarse for the analysis.

(d) Indicative Fatigue Damage Calculation

Having found that the range-pairs had an adequate level of accuracy the next step was to evaluate the indicative fatigue damage occurring for the duration of each flight condition.

A FORTRAN program was written which: took the RP information (strain levels, and number of cycles (n_i) at each strain level); converted the strains to stresses by multiplying by Young's Modulus for aluminium (10 000 ksi); calculated the allowable number of cycles (N_f) from the MIL-HDBK equation (Ref. 10, Fig. 3.7.4.1.8(d)); and then used Miner's Rule to evaluate the fatigue damage as follows:

$$\text{Proportion of life expended} = \sum_i \frac{n_i}{N_{fi}}$$

where n_i is the number of cycles completed and N_{fi} is the allowable number of cycles to failure, at the i^{th} stress level.

The results of the damage calculations are shown in Table 8 and Fig. 24.

(e) Statistical Analysis

For the rigging methods to be essentially the same in terms of the fatigue damage induced in the panel, the mean of the differences of the damage caused by each method needs to equal zero.

From Ref. 16 the most appropriate statistical test is the Student's t-test. This will be used to test the hypothesis that the mean (μ) of the differences between the damage caused by the old rigging method and the new rigging method is zero (ie, $\mu = 0$ will be tested).

The formula for the test-statistic T to be used for the t-test is:

$$T = \sqrt{n}\left(\frac{X - \mu}{S}\right)$$

where n is the number of samples, X is the average of the samples, μ is the expected average ($\mu = 0$ in this case) and S is the standard deviation of the sample.

Considering the last column (marked "Old - New") in Table 8, there are 50 samples so $n = 50$, the average $X = 3.34 \times 10^{-9}$, and the standard deviation $S = 9.63 \times 10^{-9}$.

This yields $T = 2.45$.

For the t-test comparison, a significance level must be chosen. The significance level indicates the probability that the hypothesis may be rejected even though it is correct. Thus a 0.1% significance level equates to a 1 in 1000 chance of a false rejection of the hypothesis while a 1% level equates to a 1 in 100 chance. The 0.1% significance level is the preferred level given the following factors:

- There was only one set of measurements made with the old rigging and they were made over a small number of flight conditions.
- Although repeatability between corresponding flight conditions for the old and new rigging method measurements could be assured at the gross level, slight variations would have existed. Such variations could have led to differences in the fatigue damage calculated for flights flown on different days, but with the same rigging method for the ESSS tanks.
- If an experiment is conducted under tightly controlled (e.g. laboratory) conditions, then high significance levels of 1%, 5%, or even 10% might be acceptable. However, for experiments in which conditions cannot be tightly controlled, lower significance levels are necessary so that, if two sets of data are concluded to be different at these lower significance levels, then it is likely that the difference is real and not due to small variations in the experimental conditions.

Hence, given the number of variables involved which could not be controlled (e.g. atmospheric temperature) then a 0.1% significance level is considered appropriate for

this analysis. The results for a 1% significance level have been included for comparison.

Table A11 of Ref. 16 indicates, for $n = 50$, the following values for t:

Significance Level	t
0.1 %	3.26
1%	2.40

The hypothesis that we have is that there is no difference in the fatigue damage caused by the two rigging procedures. To accept the hypothesis, and thus indicate that there is no difference between rigging methods, then the value of T must be less than t at the chosen level of significance.

Since $T = 2.45$, then at the 0.1% significance level the hypothesis is accepted and the rigging change cannot be proven to have had any effect on the amount of fatigue damage to the panel. In comparison, at the 1% level, the hypothesis is on the borderline between rejection and acceptance.

Hence, the data do not support the contention that the change in the ESSS ejector rack rigging procedure had any detrimental effect on the panel cracking. This result indicates that if there is a difference in the fatigue damage produced by the two rigging methods, then the difference is smaller than that which could be deduced from the data recorded during the flight investigation.

A3.3 Concluding Remarks

One of the aims of the flight investigation was to determine if the new rigging procedure for the Black Hawk ESSS ejector racks was an improvement over the old rigging procedure.

One flight was made with the ejector racks rigged according to the old procedure and five flight conditions were covered.

An indicative fatigue damage calculation was performed which compared the fatigue damage to the panel for the two rigging methods. The damage values produced were then statistically analysed to determine if there was a difference between the two methods.

At a significance level of 0.1% (where the significance level indicates the probability that the conclusion drawn is incorrect), the conclusion is that there is no difference between the two rigging methods.

Appendix 4

The Range-Pair Counting Method

Note: The following summary of the range-pair method is essentially paraphrased or quoted from R.C. Fraser's original, and more comprehensive report on the subject, (Ref. 15).

The basic method is to select and remove from a time-ordered list of load maxima and minima (turning points), the adjacent pair having the smallest absolute difference. This is repeated until all possible pairs are removed. Each pair is then considered to constitute the peak and trough of one load cycle for which a mean and alternating load can be determined.

Unfortunately, there is a drawback to this otherwise simple method: the method obtains only one range-pair for each pass through a given data record, making it inefficient, especially when applied to long complex load histories. The Black Hawk data records were typically between 16 - 30 seconds in duration and often contained over 1000 load cycles.

A first step in reducing the number of passes required is achieved by recognising that the minimum difference condition is satisfied by cycles which are themselves components or perturbations of larger cycles. This observation can be expressed algebraically in terms of absolute differences as follows and is called a 'four-point' or 'perturbation' (Ref. 15):

For a sequence of four turning points (TPs) denoted TP_{k-3}, TP_{k-2}, TP_{k-1}, and TP_k, if

$$| TP_{k-3} - TP_{k-2} | \geq | TP_{k-1} - TP_{k-2} | \leq | TP_k - TP_{k-1} | \qquad \text{equation (A)}$$

then the cycle TP_{k-2} to TP_{k-1} constitutes a range-pair (Ref. 15). This is illustrated in Fig. 25.

By advancing through the load history and considering the data in blocks of four-point rather than as one large block, a considerable increase in the number of pairs obtained per pass is made although several passes are still necessary to process the entire load history. To obtain complete processing in a single pass, a further refinement is made by using equation (A) repetitively. According to Fraser (Ref. 15):

'As each turning point is passed it is loaded into a turning point stack and equation (A) used to test if it identifies the previous two turning points in the stack as a range mean pair. If a range mean pair is not detected the next turning point in the load history is loaded into the stack and the process repeated until a range mean pair is found. When this occurs the range mean pair turning points are removed from the stack, the gap closed and equation (A) used again to detect as many range mean pairs as possible.'[5]

[5] Note: the terms "range pair" and "range mean pair" are used here synonymously. The inclusion of "mean" is a reminder that each pair of TPs has both a range and a mean.

Figure 26 illustrates this concept.

In this way cycle counting proceeds through the load history with the turning point stack being progressively loaded and emptied.

Finally, we can further improve the method described so far by examining the single pass characteristic itself. Consider Fig. 27:

As in Fig. 25, the four-point test would pair TP_{k-1}, TP_{k-2} in Fig. 27(a). But if TP_{k-3} is moved to a different position, as in Fig. 27(b), the:

'one-pass four point procedure would not reach TP_k with the given sequence undisturbed since it would have removed the pair TP_{k-3}, TP_{k-2} when it reached TP_{k-1}. Thus the turning point TP_{k-3} can only lie where it is depicted in [Fig. 27(a)] *(ie. below the load values of TP_{k-2} and TP_{k-1}) if it is to remain in the history unpaired when the four point one-pass method reaches TP_k. Hence, the use of the fourth point, TP_{k-3} is unnecessary in this situation and only the right hand portion of equation (A) need be used as the range-pair test (hereafter called the three point test). The same argument applies to the mirror image of* [Fig. 27] *if "below" is replaced by "above" so that the three point test suffices for all cases.'*

Due to the relative simplicity and efficiency of the three-point test, it was chosen over the four-point test for use herein.

End Effects

Whilst the vast majority of TPs in a practical load history will be successfully paired by the three-point test, there are always a small number of points that elude the process and remain unpaired at the end. These end effects occur because load histories are finite in length and thus there exist TPs which cannot be identified as perturbations of larger cycles because the TPs of these larger cycles do not appear in the given record.

Some of the possible 'residuals' for the three-point test are shown in Fig. 28. The absence of more information at the ends of the sequences prevents the turning points being paired in the normal manner. However, the problem can be solved in a way which avoids having to change to a different pairing process. By including a large 'dummy' turning point at the end of sequences (a) to (d) and applying the three-point method as before to pair right to left, it can be seen that pairing of the turning points at the end of the load history can be accomplished (see Fig. 29). When the last TP is a peak the 'dummy' TP is a large negative number and vice versa for a trough. The 'dummy' TP typically has a magnitude of 10^{30}, a convention adhered to in the FORTRAN implementation of the method in this report.

Another end effect is the failure to pair one TP whenever a load history contains an odd number of turning points. This is dealt with by adding an extra TP to the TP stack to ensure its pairing (this is sometimes called closing the sequence). When this nominal TP is used it is added to the stack before the dummy to obtain conservative pairing.

Appendix 5
Program Code (BLACK8.FOR and CMAP.FOR)

```
      Program BLACK8
c     This program takes in a single column of strain measurement data
c     and generates a range-mean-pair table of that data.  In doing so,
c     the program first filters the data to remove consecutive turning
c     points that are within a specified discriminant range (5uE).  This
c     reduces the data to a clear procession of peaks and troughs. The
c     program then discretises the data, breaking the data range
c     (from maximimum value to minimum value) into 100uE wide segments
c     or 'levels.'  Each strain reading is then assigned a level.  If
c     any two consecutive turning points are found to be in the same
c     level, the second is removed as a degenerate point to again ensure a
c     clear procession of peaks and troughs.  The 'three-point' method
c     is then used to pair the data points.  A dummy turning point and
c     a nominal turning point are added to ensure range pairing of any
c     unpaired data which are not picked up by the fundamental pairing
c     process.  The paired data are output in the form of a table that is
c     written to an output file which uses the same name as the input file
c     but with an 'z' in the extension e.g. 'n200adll.z22'.
c
c     The program was written/modified/merged by Luther Krake to be used
c     as an aid to a Black Hawk panel cracking investigation but uses a
c     significant amount of code from two existing range pair programs
c     written by Geoff Swanton, namely peakval.for and rptnew.for.
c     Variable declaration
c
      DIMENSION itp(0:50),irp(0:50,0:50),VALIDTP(10000)
      DIMENSION degen(10000),STORE(10000),VALUE(10000),DISC(10000)
      DIMENSION ian(2)
      CHARACTER NAME*8,OUTFILE*12,GAUGENAME*12,dline(50)*6
      REAL NZ,X,MAX,MIN,NZZ(10000),by(50),NOMINAL,PSTAR,VSTAR,NLEV,ba
      REAL L,LEVEL(10000),Tem(10000),NEXT,DBVAL,DBPEAK,RANGE
      REAL POINT1,POINT2,POINT3,Xi,Xc,DISCMNT,DBLO,DBHI,BOUNDS,dummin
      INTEGER v,totrec,recsel,pcount,JJ,kk,pawn
      INTEGER COUNT,K,i,NOMIND,NUMDISC,FIRSTPT,p1,p2,n
c     File 'blklist.txt' contains names of all strain gauges used in
c     Black Hawk flight investigation.  These are used to ensure that the file
c     prefix entered by the user is valid.  If it is not valid an error
c     message is displayed to screen and the program terminated.
c
      open(unit=4,file='blklist.txt',status='old')
13    read(4,'(a)',end=14)NAME
c     The following code (rather cumbersomely) forms the "main" program
c     block.  No doubt it would have been better from an aesthetic and
c     stylistic point of view to write all this as subroutines.  However
c     because much of the code presented herein was 'borrowed,' the form
c     of the new program was largely predetermined.
c     The following do loop encapsulates the entire main program.  It
c     generates input filenames for all channels (7 to 23) using the filename
c     prefix currently stored in the variable NAME.
15    do 102 pawn=7,23
      i=0
      if (pawn.eq.7) then
          GAUGENAME=NAME(1:8)//'.0'//'07'
      elseif (pawn.eq.8) then
          GAUGENAME=NAME(1:8)//'.0'//'08'
      elseif (pawn.eq.9) then
```

```
            GAUGENAME=NAME(1:8)//'.0'//'09'
          elseif (pawn.eq.10) then
            GAUGENAME=NAME(1:8)//'.0'//'10'
          elseif (pawn.eq.11) then
            GAUGENAME=NAME(1:8)//'.0'//'11'
          elseif (pawn.eq.12) then
            GAUGENAME=NAME(1:8)//'.0'//'12'
          elseif (pawn.eq.13) then
            GAUGENAME=NAME(1:8)//'.0'//'13'
          elseif (pawn.eq.14) then
            GAUGENAME=NAME(1:8)//'.0'//'14'
          elseif (pawn.eq.15) then
            GAUGENAME=NAME(1:8)//'.0'//'15'
          elseif (pawn.eq.16) then
            GAUGENAME=NAME(1:8)//'.0'//'16'
          elseif (pawn.eq.17) then
            GAUGENAME=NAME(1:8)//'.0'//'17'
          elseif (pawn.eq.18) then
            GAUGENAME=NAME(1:8)//'.0'//'18'
          elseif (pawn.eq.19) then
            GAUGENAME=NAME(1:8)//'.0'//'19'
          elseif (pawn.eq.20) then
            GAUGENAME=NAME(1:8)//'.0'//'20'
          elseif (pawn.eq.21) then
            GAUGENAME=NAME(1:8)//'.0'//'21'
          elseif (pawn.eq.22) then
            GAUGENAME=NAME(1:8)//'.0'//'22'
          elseif (pawn.eq.23) then
            GAUGENAME=NAME(1:8)//'.0'//'23'
          endif
c         Having generated an input file name it opens the file:
          open(unit=1,file=GAUGENAME,ERR=17,status='unknown')
c         The code listed above was replaced with that listed below when range pairing
c         of principle strains and Von Mises Equivalent strains was required.
c         do leta=1,3
c         if (leta.eq.1) then
c             leti='P'
c             letr='B'
c         elseif (leta.eq.2) then
c             leti='Q'
c             letr='C'
c         elseif (leta.eq.3) then
c             leti='V'
c             letr='E'
c         endif
c15       do 102 pawn=7,19,3
c         i=0
c         if (pawn.eq.7) then
c             GAUGENAME=NAME(1:8)//'.'//leti//'07'
c         elseif (pawn.eq.10) then
c             GAUGENAME=NAME(1:8)//'.'//leti//'10'
c         elseif (pawn.eq.13) then
c             GAUGENAME=NAME(1:8)//'.'//leti//'13'
c         elseif (pawn.eq.16) then
c             GAUGENAME=NAME(1:8)//'.'//leti//'16'
c         elseif (pawn.eq.19) then
c             GAUGENAME=NAME(1:8)//'.'//leti//'19'
c         endif
c         open(unit=1,file=GAUGENAME,ERR=17,status='unknown')
          goto 18
17        write(*,*)'THERE ARE NO FILES OF THAT KIND IN THE CURRENT'
          write(*,*)'DIRECTORY.  CHECK FILENAME AND TRY AGAIN.'
```

```
      stop
c
c     An output filename is also generated with a 'a' in the extention
c     to designate it as an output file.  The file is then opened.
18    OUTFILE=GAUGENAME(1:9)//'a'//GAUGENAME(11:12)
      open(unit=2,file=OUTFILE,status='unknown')
c
c     The rtsfiles.txt (rts=range-too-small) file is opened.  This file
c     must already exist as an empty file in the working directory ie. it must
c     be created by the user.  Data files that are found to have a strain range
c     of less than 100 uE will be deleted from the working directory and the filename
c     appended to rtsfiles.txt.
      open(unit=3,file='rtsfiles.txt',status='old',access='append')
c
c     Initialise variables
      NOMINAL=0.0
      Discmnt=5
      dblo=0
      dbhi=0
      M=1
      I=1
c     Read in data from input file (ie. GAUGENAME (see above)).
      READ(1,*) Xi
      STORE(1)=Xi
60    READ(1,*,end=65)Xc
      M=M+1
      if(Xi.EQ.Xc) then
          goto 60
      else
          I=I+1
          STORE(I)=Xc
          Xi=Xc
          goto 60
      endif
c
c     COUNT is the number of data points read and stored.
65    COUNT=I
      K=1
      VALUE(1)=STORE(1)
C     * PEAK-VALLEY EXTRACTION *
C     THIS SECTION EXTRACTS THE PEAKS & VALLEYS FROM THE STRING OF
C     NUMBERS IN THE ARRAY "STORE( )" & PUTS THEM INTO THE ARRAY "VALUE( )".
      do 20,j=1,COUNT-2
          POINT1=STORE(j)
          POINT2=STORE(j+1)
          POINT3=STORE(j+2)
          if (POINT2.GE.POINT1.AND.POINT2.LE.POINT3) then
              POINT1=POINT2
              POINT2=POINT3
          elseif (POINT2.GT.POINT1.AND.POINT2.GT.POINT3) then
              K=K+1
              VALUE(K)=POINT2
          elseif (POINT2.LE.POINT1.AND.POINT2.GE.POINT3) then
              POINT1=POINT2
              POINT2=POINT3
          elseif (POINT2.LT.POINT1.AND.POINT2.LT.POINT3) then
              K=K+1
              VALUE(K)=POINT2
          endif
20    CONTINUE
      K=K+1
      VALUE(K)=POINT3
```

```
C     * DISCRIMINATOR PROCESS *
C     THIS SECTION KEEPS ONLY THOSE PEAKS & VALLEYS THAT ARE GREATER
C     THAN THE SPECIFIED DISCRIMINANT VALUE, STORING THEM IN THE ARRAY
C     "DISC( )".
      if (value(1).LT.value(2)) then
          vstar=value(1)
          X=vstar
      elseif (value(1).GT.value(2)) then
          pstar=value(1)
          X=pstar
      endif
      j=1
      N=1
30    j=j+1
      if (X.EQ.pstar) goto 25
      if (X.EQ.vstar) goto 35
25    if (value(j).GT.X) then
          pstar=value(j)
          X=pstar
      elseif (value(j).LT.pstar) then
          if (abs(value(j)-pstar).GT.discmnt) then
              vstar=value(j)
              X=vstar
              DISC(N)=pstar
              N=N+1
          endif
      endif
      if (J.EQ.K) GOTO 40
          goto 30
35    if (value(j).LT.X) then
          vstar=value(j)
          X=vstar
      elseif (value(j).GT.vstar) then
          if (abs(value(j)-vstar).GT.discmnt) then
              pstar=value(j)
              X=pstar
              DISC(N)=vstar
              N=N+1
          endif
      endif
      if (J.EQ.K) GOTO 40
      goto 30
40    DISC(N)=X
      NUMDISC=N
C     * DEAD-BAND PROCESSOR *
C     THIS PART OF THE PROGRAM USES THE DEAD-BAND.  ANY COMPLETE CYCLES
C     FALLING WITHIN THIS DEAD-BAND ARE ELIMINATED.  THOSE TURNING POINTS
C     STILL VALID AFTER THIS PROCESS ARE WRITTEN TO THE ARRAY "NZZ( )".
      K=1
      if(DISC(1).LT.DISC(2)) then
          if(DISC(1).LE.DBHI.AND.DISC(1).GE.DBLO) then
              DBVAL=DISC(1)
              X=DBVAL
              FIRSTPT=0
              DBPEAK=DBLO
          else
              VSTAR=DISC(1)
              X=VSTAR
              NZZ(K)=X
              K=K+1
              FIRSTPT=1
          endif
```

```
      elseif(DISC(1).GT.DISC(2)) then
          if(DISC(1).LE.DBHI.AND.DISC(1).GE.DBLO) then
              DBPEAK=DISC(1)
              X=DBPEAK
              FIRSTPT=0
              DBVAL=DBHI
          else
              PSTAR=DISC(1)
              X=PSTAR
              NZZ(K)=X
              K=K+1
              FIRSTPT=1
          endif
      endif
      J=1
45    J=J+1
      if(J.GT.NUMDISC) GOTO 50
      if(DISC(J).GT.X) then
          if(DISC(J).GT.DBHI.OR.DISC(J).LT.DBLO) then
              if(FIRSTPT.EQ.0) then
                  if(DISC(J-1).LE.DBHI.AND.DISC(J-1).GE.DBLO) then
                      NZZ(K)=DBVAL
                      K=K+1
                  endif
                  PSTAR=DISC(J)
                  X=PSTAR
                  NZZ(K)=X
                  K=K+1
                  FIRSTPT=1
              elseif(NZZ(K-1).GT.DBHI) then
                  if(DISC(J-1).LE.DBHI.AND.DISC(J-1).GE.DBLO) then
                      NZZ(K)=DBVAL
                      K=K+1
                  endif
                  PSTAR=DISC(J)
                  X=PSTAR
                  NZZ(K)=X
                  K=K+1
              elseif (NZZ(K-1).LT.DBLO) then
                  PSTAR=DISC(J)
                  X=PSTAR
                  NZZ(K)=X
                  K=K+1
              endif
          elseif (DISC(J).LE.DBHI.AND.DISC(J).GE.DBLO) then
              if (DISC(J-1).GT.DBHI.OR.DISC(J-1).LT.DBLO) then
                  DBPEAK=DISC(J)
              elseif (DISC(J).GT.DBPEAK) then
                  DBPEAK=DISC(J)
              endif
              X=DISC(J)
          endif
      elseif (DISC(J).LT.X) then
          if (DISC(J).GT.DBHI.OR.DISC(J).LT.DBLO) then
              if (FIRSTPT.EQ.0) then
                  if (DISC(J-1).LE.DBHI.AND.DISC(J-1).GE.DBLO) then
                      NZZ(K)=DBPEAK
                      K=K+1
                  endif
                  VSTAR=DISC(J)
                  X=VSTAR
                  NZZ(K)=X
```

```
                    K=K+1
                    FIRSTPT=1
                elseif (NZZ(K-1).LT.DBLO) then
                    if (DISC(J-1).LE.DBHI.AND.DISC(J-1).GE.DBLO) then
                        NZZ(K)=DBPEAK
                        K=K+1
                    endif
                    VSTAR=DISC(J)
                    X=VSTAR
                    NZZ(K)=X
                    K=K+1
                elseif (NZZ(K-1).GT.DBHI) then
                    VSTAR=DISC(J)
                    X=VSTAR
                    NZZ(K)=X
                    K=K+1
                endif
            elseif (DISC(J).LE.DBHI.AND.DISC(J).GE.DBLO) then
                if (DISC(J-1).GT.DBHI.OR.DISC(J-1).LT.DBLO) then
                    DBVAL=DISC(J)
                elseif (DISC(J).LT.DBVAL) then
                    DBVAL=DISC(J)
                endif
                    X=DISC(J)
            endif
        endif
        GOTO 45
50      if (DISC(NUMDISC).LE.DBHI.AND.DISC(NUMDISC).GE.DBLO) then
            if (NZZ(K-1).EQ.PSTAR) then
                NZZ(K)=DBVAL
            elseif  (NZZ(K-1).EQ.VSTAR) then
                NZZ(K)=DBPEAK
            endif
        endif
c       * RANGE-PAIRING *
c       ************************************************************
c       THIS SECTION DETERMINES THE MAXIMUM AND MINIMUM DATA VALUES
55      COUNT=K-1
        BOUNDS=0
        MAX=0
        MIN=0
        Tem(1)=NZZ(1)
        do JJ=1,COUNT-1
            NEXT=NZZ(JJ+1)
            do kk=JJ,1,-1
                if (NEXT.ge.Tem(kk)) then
                    Tem(kk+1)=NEXT
                    goto 80
                else
                    Tem(kk+1)=NEXT
                    call SWAP (Tem(kk+1),Tem(kk))
                endif
            end do
80      end do
        MAX=Tem(COUNT)
        MIN=Tem(1)
        write(*,*)'FILE= ',GAUGENAME
c       THE RANGE OF DATA, FROM MAX TO MIN, IS BROKEN UP INTO SEGMENTS 100 uE
c       WIDE.  IF THE DATA RANGE IS FOUND TO BE LESS THAN 100 uE THE FILE IS
c       DELETED FORM THE WORKING DIRECTORY AND THE NAME OF THE FILE IS STORED
c       IN rtsfiles.txt.  IF THE RANGE CAN NOT BE SPLIT CLEANLY INTO 100 uE
c       SEGMENTS (ie. RANGE DIVIDED BY ba IS NOT AN INTEGER VALUE) THEN AN
```

```
c     EXTRA SEGMENT IS ADDED TO ENSURE THAT ALL THE DATA CAN BE ALLOTTED TO
c     AN APPROPRIATE LEVEL.
      ba=100.0
      RANGE=abs(MAX-MIN)
      if (RANGE.le.ba) then
          write(3,*)GAUGENAME
          close(unit=2,Status='delete')
          goto 102
      else
          if (MIN.lt.SIGN(INT(ABS(MIN)/ba)*ba,MIN)) then
              MIN=SIGN(INT(ABS(MIN)/ba)*ba,MIN)-100
          else
              MIN=SIGN(INT(ABS(MIN)/ba)*ba,MIN)
          endif
          if (MAX.lt.SIGN(INT(ABS(MAX)/ba)*ba,MAX)) then
              MAX=SIGN(INT(ABS(MAX)/ba)*ba,MAX)
          else
              MAX=SIGN(INT(ABS(MAX)/ba)*ba,MAX)+100
          endif
      endif
      RANGE=abs(MAX-MIN)
      NLEV=RANGE/ba
      dummin=int(MIN-ba)
      BOUNDS=NLEV+1
      i=1
84    by(i)=dummin+(ba*i)
      if (by(i).gt.MAX+1) then
          goto 86
      else
      if (i.lt.BOUNDS) then
          i=i+1
          goto 84
      endif
      endif
c
c     * NEXT, EACH DATA POINT IS ASSIGNED A LEVEL BASED ON WHICH BOUNDARY
c     VALUES IT FALLS BETWEEN *
86    do I=1,COUNT
      if (NZZ(I).EQ.MIN) then
          LEVEL(I)=1
      else if (NZZ(I).EQ.MAX) then
          LEVEL(I)=BOUNDS-1
      else
          j=1
85        if ((NZZ(I).GT.by(j)).AND.(NZZ(I).LE.by(j+1))) then
              LEVEL(I)=j
          else
              j=j+1
              goto 85
          end if
      endif
      end do
c     * DEGENERATE AND NON-DEGENERATE DATA ARE SEPARATED *
      if (LEVEL(1).LT.LEVEL(2)) then
          VSTAR=LEVEL(1)
          X=VSTAR
      else
          PSTAR=LEVEL(1)
          X=PSTAR
      endif
      Q=2
      J=1
```

```
      L=1.0
      VALIDTP(1)=NZZ(1)
90    J=J+1
      if (LEVEL(J).eq.X) then
          degen(L)=LEVEL(J)
          L=L+1
          if (J.eq.COUNT) then
              goto 95
          endif
      elseif (LEVEL(J).gt.X) then
          if (J.EQ.COUNT) then
              PSTAR=LEVEL(J)
              X=PSTAR
              goto 95
          endif
          if (LEVEL(j+1).lt.LEVEL(j)) then
              PSTAR=LEVEL(J)
              X=PSTAR
              VALIDTP(Q)=NZZ(J)
              Q=Q+1
          else
              degen(L)=LEVEL(j)
              L=L+1
          endif
      elseif (LEVEL(J).lt.X) then
          if (J.EQ.COUNT) then
              VSTAR=LEVEL(J)
              X=VSTAR
              goto 95
          endif
          if (LEVEL(j+1).gt.LEVEL(j)) then
              VSTAR=LEVEL(J)
              X=VSTAR
              VALIDTP(Q)=NZZ(J)
              Q=Q+1
          else
              degen(L)=LEVEL(j)
              L=L+1
          endif
      endif
      goto 90
c
c     ian(i)=assigned number; 1=prev line, 2=current line
95    ian(2)=0
c     totrec=COUNT for total records in file
c     recsel=COUNT for records selected
      totrec=0
      recsel=0
c     * ADD A "NOMINAL" OR "DUMMY" DATA POINT TO END OF DATA SEQUENCE *
          Z=AMOD((Q-1),2.)
          if (Z.NE.0) then
              VALIDTP(Q)=NOMINAL
              NOMIND=1
              Q=Q+1
              if (VALIDTP(Q-1).GT.VALIDTP(Q-2)) then
                  VALIDTP(Q)=-10E30
              elseif (VALIDTP(Q-1).LT.VALIDTP(Q-2)) then
                  VALIDTP(Q)=10E30
              endif
          elseif (Z.EQ.0) then
              if (VALIDTP(Q-1).GT.VALIDTP(Q-2)) then
                  VALIDTP(Q)=-10E30
```

```
            elseif (VALIDTP(Q-1).LT.VALIDTP(Q-2)) then
                VALIDTP(Q)=10E30
            endif
        endif
c     * READ IN THE SORTED DATA *
      do i=1,BOUNDS-1
          do j=1,BOUNDS-1
              irp(i,j)=0
          end do
      end do
      m=0
      A=0
100   A=A+1
      NZ=VALIDTP(A)
c     Count total records
      totrec=totrec+1
c     Count total number of records selected
      recsel=recsel+1
c     * RANGE-PAIR COUNT ROUTINE *
      ian(1)=ian(2)
      if (NZ.le.by(1)) then
          ian(2)=1
      elseif (NZ.gt.by(BOUNDS-1)) then
          ian(2)=BOUNDS-1
      else
          j=1
105       if (NZ.gt.by(j).and.NZ.le.by(j+1)) then
              ian(2)=j
          else
              j=j+1
              goto 105
          endif
      endif
      if (recsel.lt.3) then
          itp(ian(2))=1
          goto 100
      endif
      if (ian(2).gt.ian(1)) then
          ns=ian(1)+1
          nf=ian(2)
          iv=1
      else
          ns=ian(1)-1
          nf=ian(2)
          iv=-1
      endif
      do j=ns,nf,iv
          if (itp(j).eq.1) then
              p1=j
              if (IAN(2).gt.IAN(1)) then
                  k=1
110               ic=p1-k
                  if (ic.le.0) then
                      goto 116
                  endif
                  if (itp(ic).eq.1) then
                      p2=ic
                  else
                      k=k+1
                      goto 110
                  endif
              else
```

```
                    p2=p1
                    k=p2+1
115                 if (k.le.0) then
                        goto 116
                    endif
                    if (itp(k).eq.1) then
                        p1=k
                    else
                        k=k+1
                        goto 115
                    endif
                endif
                itp(p1)=0
                itp(p2)=0
                irp(p1,p2)=irp(p1,p2)+1
            endif
116     end do
        itp(ian(2))=1
        if (A.EQ.Q) then
            goto 120
        else
            goto 100
        endif
c
c       * GENERATE OUTPUT *
120     write (2,130) int(BOUNDS-1)
        write (2,135) int(MIN),int(MAX)
        write (2,140) ba
130     format (5x,'RANGE MEAN PAIR TABLE with ',i2,' levels.')
135     format (5x,'Range:',i6,'  to',i6)
140     format (5x,'The increment between levels is',f8.2,' uE')
        write (2,*)' '
c       Add degenerate range pairs into the range pair
c       table by adding them into array 'irp'
        do k=1,L-1
            if (amod(k,2.).eq.0) then
                n=int(degen(k))
                irp(n,n)=irp(n,n)+1
            endif
        end do
        write(2,*)'      PEAKS (uE)         |'
        write(2,*)'-----------------------|-----'
        write(2,159)'LEVEL 1           |',irp(1,1)
159     format(6x,A19,1x,i4)
        write(2,160)'(',by(1),' to',(by(2)-0.01),')    |'
160     format (A1,f8.2,A3,f8.2,A5)
        do v=1,BOUNDS-1
            dline(v)='------'
        end do
        write(2,163)(dline(v),v=1,2)
        ic=2
        i=2
141     write(2,162)'LEVEL ',i,'|',(irp(i,j),j=1,ic)
162     format(6x,A6,i2,10x,A1,50(i5))
        write(2,161)'(',by(i),' to',(by(i+1)-0.01),')    |'
161     format(A1,f8.2,A3,f8.2,A5)
        if (i.lt.BOUNDS-1) then
            write(2,163)(dline(v),v=1,i+1)
163         format('-----------------------|',50(A5))
            i=i+1
            ic=ic+1
            goto 141
```

```
      else
          write(2,164)(dline(v),v=1,i)
164       format('------------------------|',50(A5))
      endif
      write (2,165)'|',(i,i=1,BOUNDS-1)
165   format (24x,A1,50(i5),/)
      write (2,167)
167   format (25x,'TROUGHS',/)
      write (2,170) (itp(i),i=1,BOUNDS-1)
170   format (/5x,'Unpaired turning points: ',50(i3))
      do i=1,BOUNDS
          by(i)=0
      end do
c     Count total number of range pairs (pcount) and
c     print this and the total number of data points
c     (int(count)) beneath the table
      pcount=0
      do i=1,BOUNDS-1
          do j=1,BOUNDS-1
              pcount=pcount+irp(i,j)
          end do
      end do
      write (2,*)' '
      write (2,180) pcount,int(count)
180   format (/5x,'A total of',i5,' range pairs were derived from',
     &i5,' data points.')
      if (NOMIND.eq.1) then
          write(2,181)'However the nominal value was used to pair',int(Q
     &-1),' pts.'
181   format(/5x,A42,i4,A5)
      endif
c
c     NOTE: END OF "MAIN" DO LOOP:
102   continue
c
c     WHEN FINISHED ALL DATA CHANNELS FOR PREVIOUS FILE PREFIX READ FROM
c     blklist.txt READ NEXT ONE AND REPEAT PROCESS UNTIL FINISHED:
      goto 13
14    write(*,*)'Done!'
      stop
      end
      SUBROUTINE JPLEN(STRG,ILEN)
C     THIS SUBROUTINE OBTAINS THE LENGTH OF A STRING
C     INPUT:  STRG - STRING TO HAVE LENGTH DETERMINED
C     OUTPUT: ILEN - LENGTH OF STRING
      CHARACTER*(*) STRG
C     FIND LENGTH OF STRING.
      ILEN = LEN(STRG)
70    if (STRG(ILEN:ILEN).EQ.' ') then
       ILEN = ILEN - 1
       if (ILEN.GT.0) GOTO 70
      end if
      RETURN
      end

      SUBROUTINE SWAP(X,YY)
      real X,YY
      AUX=X
      X=YY
      YY=AUX
      return
      end
```

```
c     COLOURMAP.FOR  written by Luther Krake (July 1995)
c
c     This program reads in data from a formatted range-pair table
c     and uses this data to generate a colour plot representation
c     of the table.  Colours are assigned to range-pair counts based
c     on the count size eg. the higher the count the brighter the
c     colour.  The "colourmaps" are used to facillitate easier visual
c     comparisons of range-pair table data.
c     NOTE: This program was written to be used in tandem with range-
c           pair tables generated using BLACK8.for.  Modifications
c           may be required to run the program on tables generated by
c           other means.

      INCLUDE 'FGRAPH.FI'
      INCLUDE 'FGRAPH.FD'

      CHARACTER FILENAME*40,LEV*5
      INTEGER I,ROW,COL,X(50,50),COUNT,Xord,Yord
      INTEGER*4 colour

c     Enter the name of the filename containing relevant range-pair
c     table.
      WRITE(*,*)'Enter FILENAME:'
      READ(*,'(a)')FILENAME
      OPEN(UNIT=2,FILE=FILENAME,STATUS='OLD')

c     Read range-pair count data into a 2-D array X(ROW,COL), skipping
c     over irrelevant formatted text.
      DO I=1,6
          READ(2,*)
      END DO

      ROW=1
10    READ(2,15,END=20)LEV,(X(ROW,COL),COL=1,ROW)
15    FORMAT(6x,A5,14x,50(i5))
      IF (LEV.NE.'LEVEL') THEN
          GOTO 20
      ELSE
          DO I=1,2
              READ(2,*)
          END DO
          ROW=ROW+1
          GOTO 10
      ENDIF
20    COUNT=ROW-1
      CALL graphicsmode()

c     Assign range-pair count values colours appropriate to
c     their size ie. higher values receive brighter colours.
      Yord=0
      DO ROW=1,COUNT
          Xord=0
          DO COL=1,ROW
              IF (X(ROW,COL).GE.0) THEN
                  IF (X(ROW,COL).LT.50) THEN
                  colour=SETCOLOR(8)
                  ELSEIF (X(ROW,COL).LT.100) THEN
                  colour=SETCOLOR(1)
                  ELSEIF (X(ROW,COL).LT.150) THEN
                  colour=SETCOLOR(9)
                  ELSEIF (X(ROW,COL).LT.200) THEN
                  colour=SETCOLOR(2)
                  ELSEIF (X(ROW,COL).LT.250) THEN
```

```
                colour=SETCOLOR(10)
                ELSEIF (X(ROW,COL).LT.300) THEN
                colour=SETCOLOR(3)
                ELSEIF (X(ROW,COL).LT.350) THEN
                colour=SETCOLOR(11)
                ELSEIF (X(ROW,COL).LT.400) THEN
                colour=SETCOLOR(14)
                ELSEIF (X(ROW,COL).LT.450) THEN
                colour=SETCOLOR(7)
                ELSE
                colour=SETCOLOR(15)
                ENDIF
            ENDIF
            CALL drawtable(Xord,Yord,COUNT)
            Xord=Xord+639/COUNT
        END DO
        Yord=Yord+479/COUNT
    END DO

    CALL endprogram()
    END

    SUBROUTINE graphicsmode()
c   Sets the videomode of the computer.
        INCLUDE 'FGRAPH.FD'

        INTEGER*2 modestatus,maxx,maxy
        RECORD /videoconfig/ myscreen
        COMMON maxx,maxy


        modestatus=SETVIDEOMODE($MAXCOLORMODE)
        IF(SETVIDEOMODE($MAXCOLORMODE).EQ.0)
     +  STOP 'Error: no color graphics capability'

        CALL GETVIDEOCONFIG(myscreen)
        maxx=myscreen.numxpixels-1
        maxy=myscreen.numypixels-1
        END

    SUBROUTINE drawtable(Xord,Yord,COUNT)
c   Generates the colour map as a series of appropriately coloured
c   rectangles.
    INCLUDE 'FGRAPH.FD'

    INTEGER Xord,Yord,maxx,maxy,COUNT
    INTEGER*2 status
    RECORD /xycoord/ xy
    COMMON maxx,maxy

    CALL MOVETO(0,0,xy)
    status=RECTANGLE($GFILLINTERIOR,Xord,Yord,Xord+639/COUNT,Yord+479/
   +COUNT)

    END

    SUBROUTINE endprogram()
c   Resets videomode to its default setting.
    INCLUDE 'FGRAPH.FD'
    INTEGER*2 dummy

    READ(*,*)   !Wait for ENTER to be pressed
    dummy=SETVIDEOMODE($DEFAULTMODE)
    END
```

Appendix 6

Calculation of Principal Strains and Von Mises Equivalent Strains

The outputs from the five rosette strain gauges (channels 7 to 21) on each panel were converted into principal strains using the following method:

Let the measured strains ε_{ia}, ε_{ib} and ε_{ic} be the strains in the OA, OB and OC directions respectively for gauge i where OA and OC are at right angles (Fig. 30). For the rosette strain gauges used in this investigation, angle AOB is 45°.

Theta is the angle between OD and OC and is positive with OD lying between OC and OA. The principal strains, ε_{ip} and ε_{iq}, acting along OD and its normal respectively, are then calculated from the following formulae (Ref. 17):

$$\varepsilon_{ip} = \frac{1}{2}\left[\varepsilon_{ic} + \varepsilon_{ia} + \sqrt{(\varepsilon_{ic} - \varepsilon_{ia})^2 + (2\varepsilon_{ib} - \varepsilon_{ic} - \varepsilon_{ia})^2}\right]$$

$$\varepsilon_{iq} = \frac{1}{2}\left[\varepsilon_{ic} + \varepsilon_{ia} - \sqrt{(\varepsilon_{ic} - \varepsilon_{ia})^2 + (2\varepsilon_{ib} - \varepsilon_{ic} - \varepsilon_{ia})^2}\right]$$

The calculated strains take account of the combined tensile, compressive and shear stresses acting at the strain gauge locations. The calculation of theta was not required.

The Von Mises Equivalent Strain (VMES) is given by the following formula (Ref. 17):

$$VMES = \sqrt{\varepsilon_{ip}^{\ 2} + \varepsilon_{iq}^{\ 2} - \varepsilon_{ip}\varepsilon_{iq}}$$

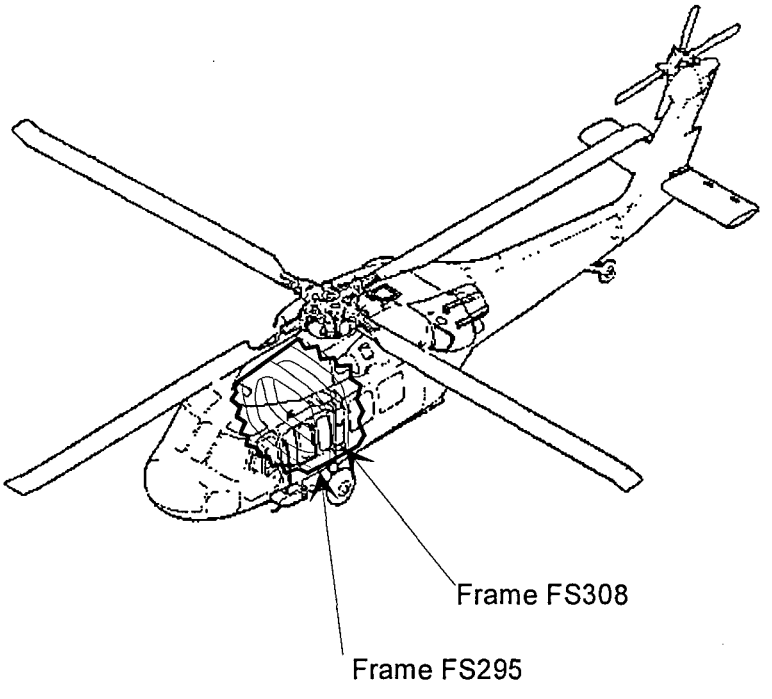

Figure 1: Location of frames FS295 and FS308.

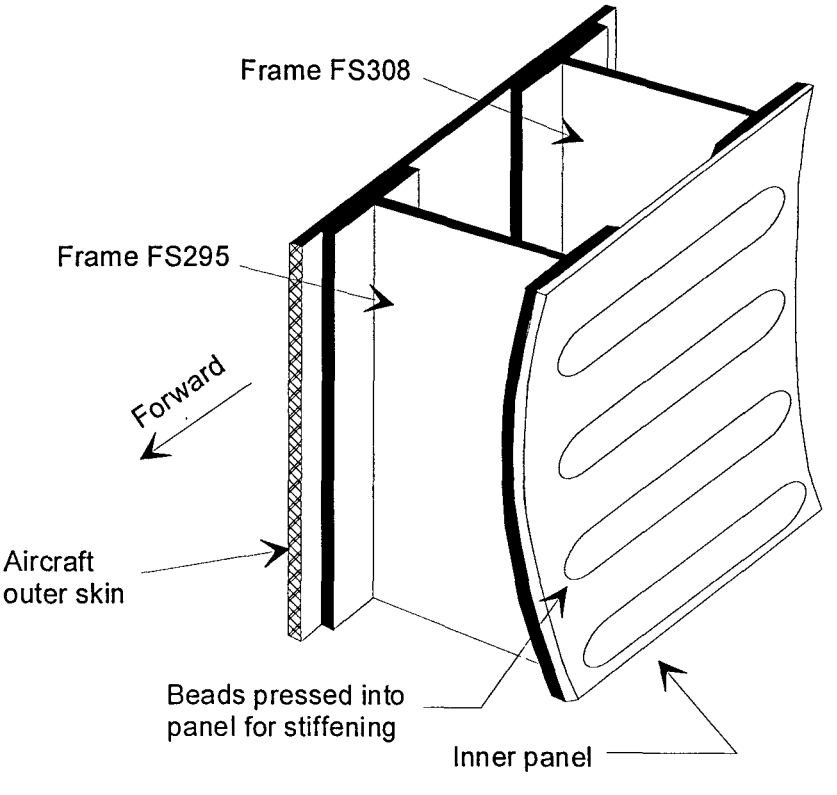

Figure 2: Close-up view of the panel.

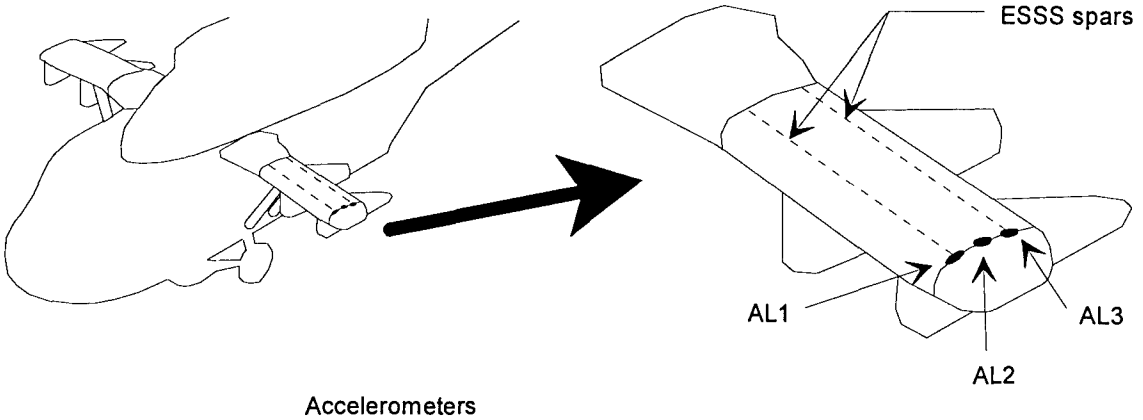

Figure 3: Accelerometer locations.

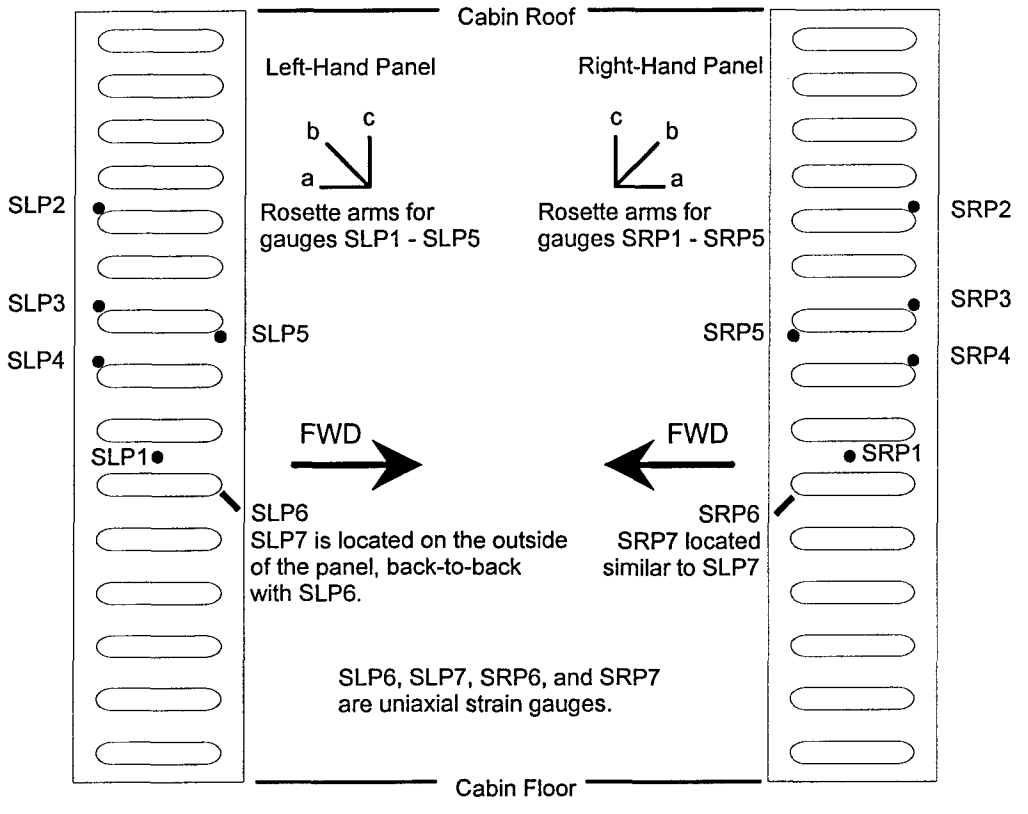

INTERNAL PANEL STRAIN GAUGES

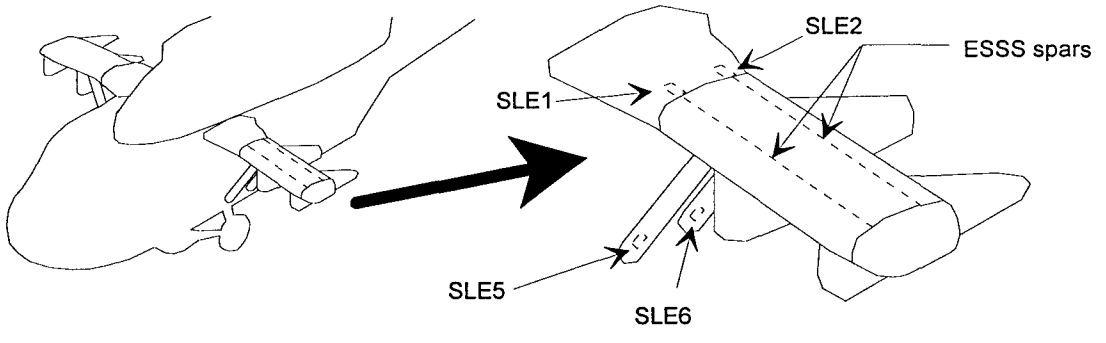

SLE1 and SLE2- Located at the root of the ESSS spars on the upper surface of the "wing"
SLE3 - Located on the lower surface of the "wing", under SLE1
SLE4 - Located on the lower surface of the "wing", under SLE2
SLE5 - Located on the back face of the forward strut tube, 110 mm from lower end of composite tube
SLE6 - Located on the back face of the rear strut tube 140 mm from lower end of composite tube

Left-hand side strain gauges shown. Right-hand side strain gauges are located in equivalent positions and are known as SRE1, SRE2, ..., SRE6.

ESSS STRAIN GAUGES

Figure 4: Strain gauge locations.

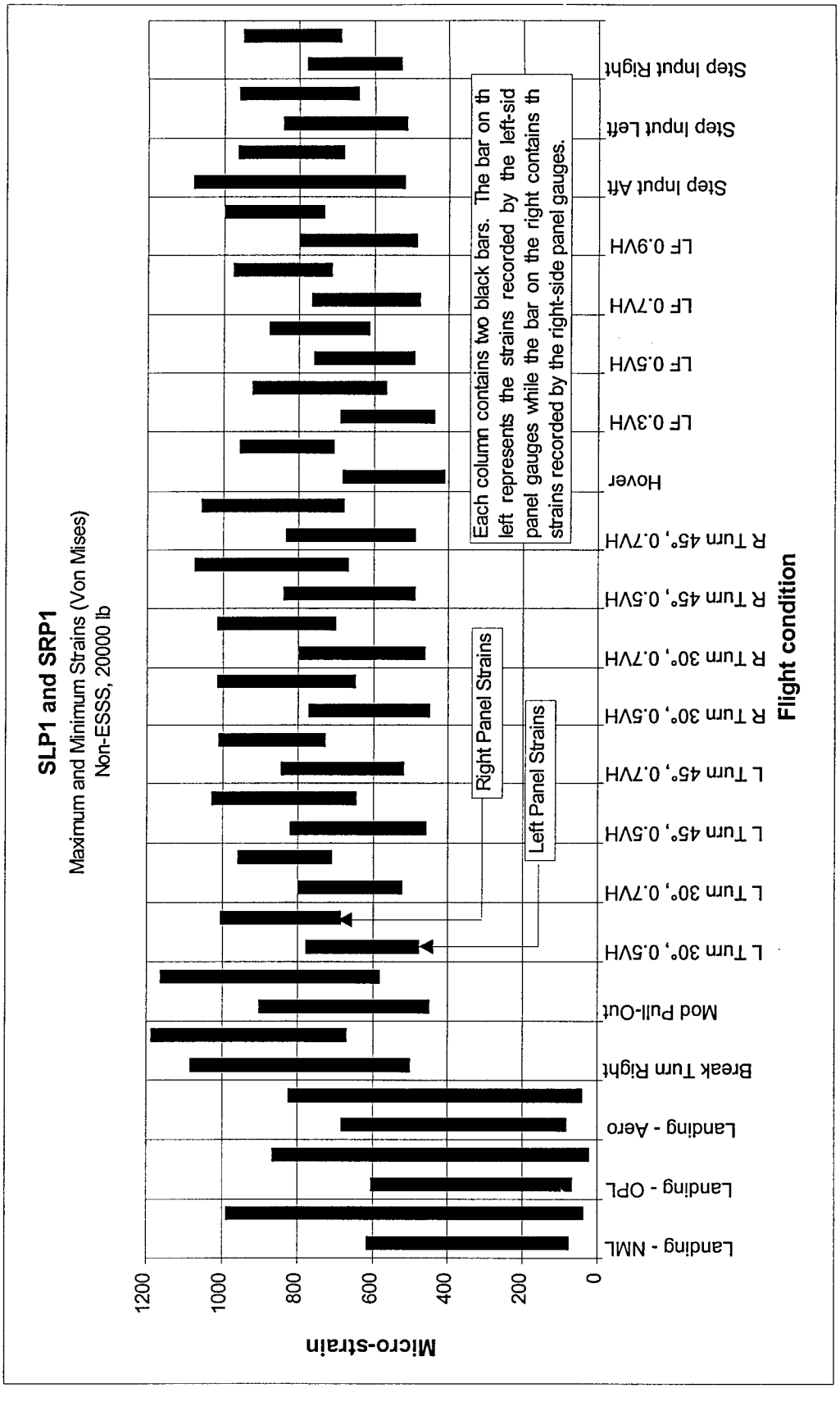

Figure 5(a): Maximum and minimum strains for the non-ESSS aircraft configuration at a gross weight of 20000 lb.

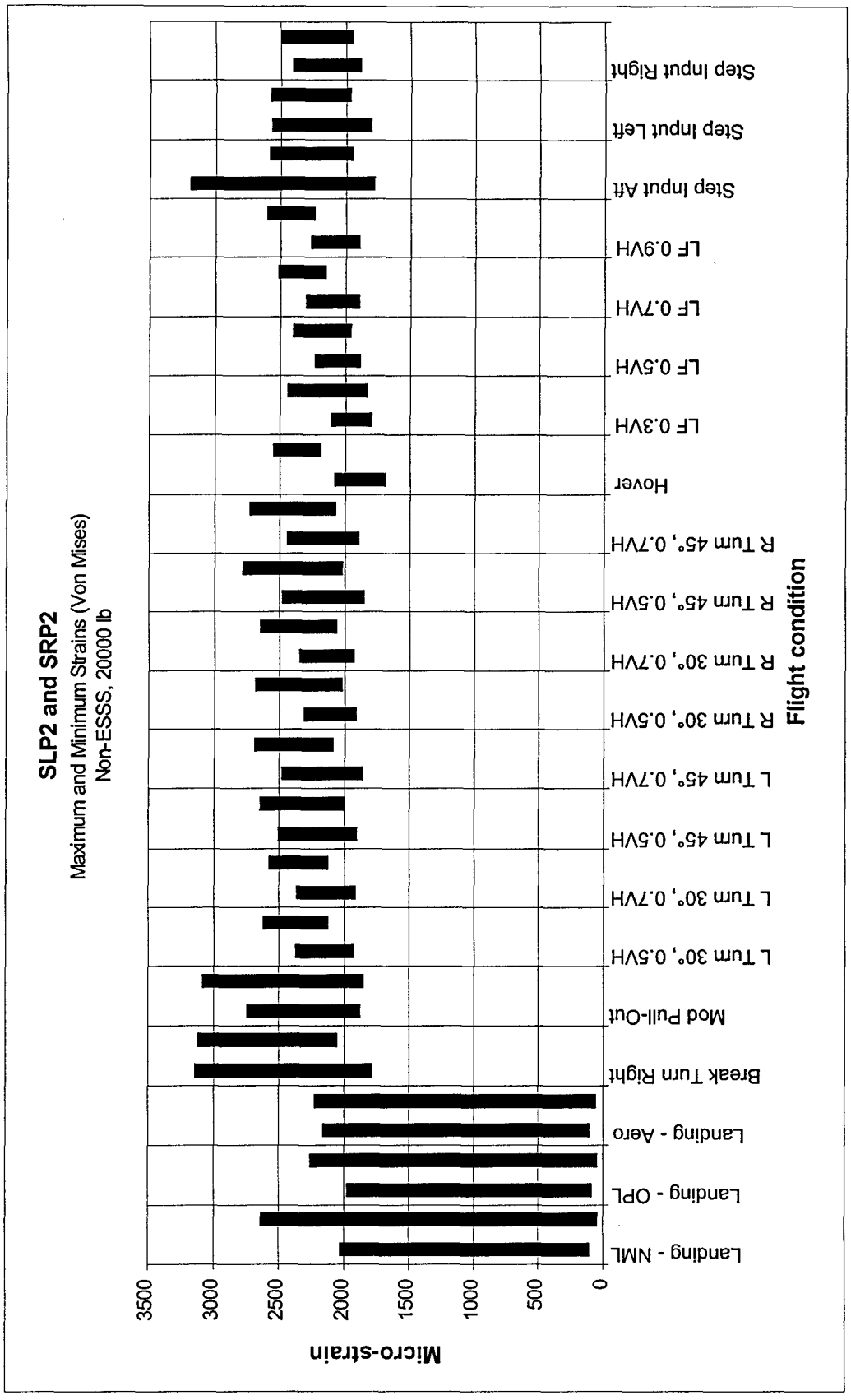

Figure 5(b): Maximum and minimum strains for the non-ESSS aircraft configuration at a gross weight of 20000 lb.

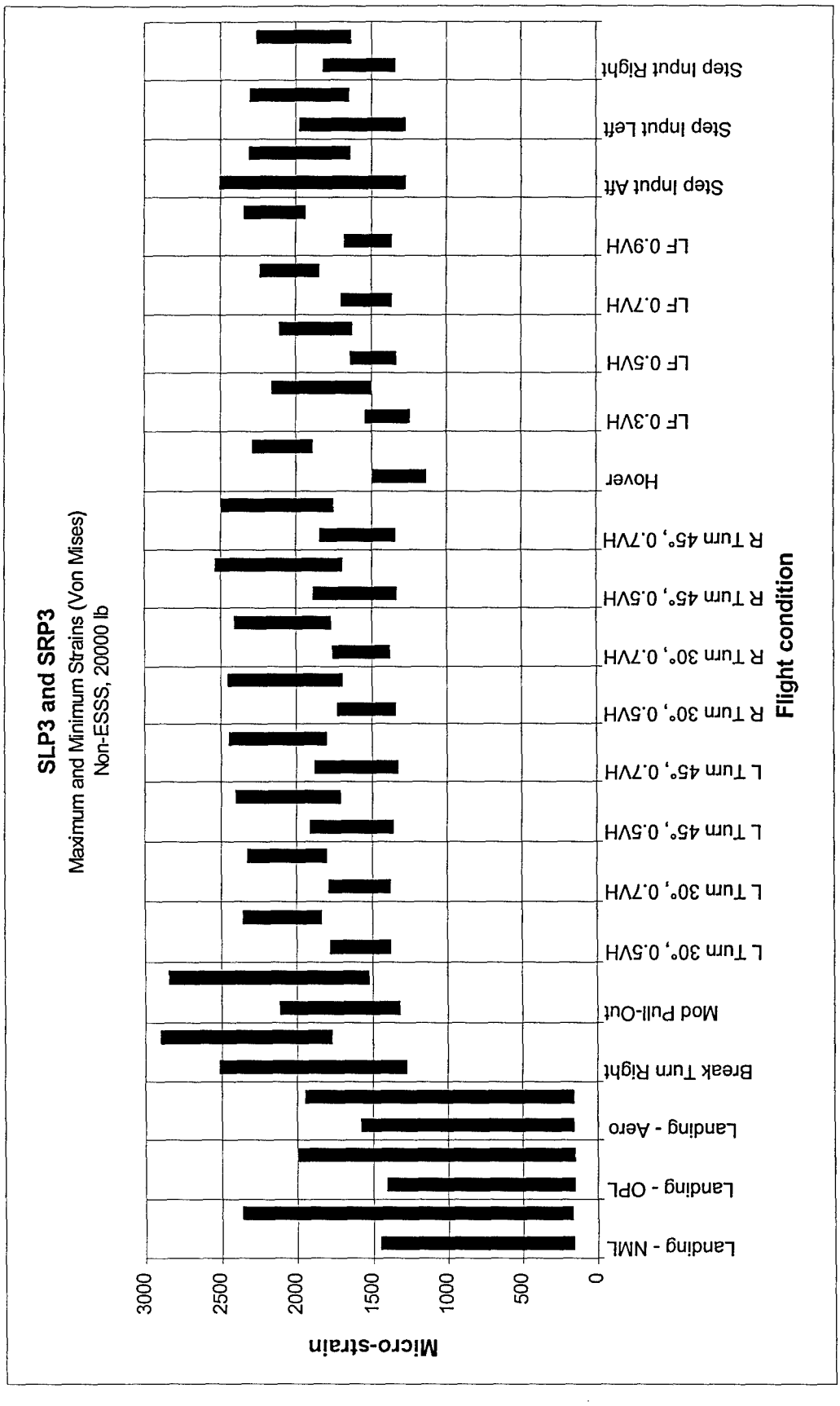

Figure 5(c): Maximum and minimum strains for the non-ESSS aircraft configuration at a gross weight of 20000 lb.

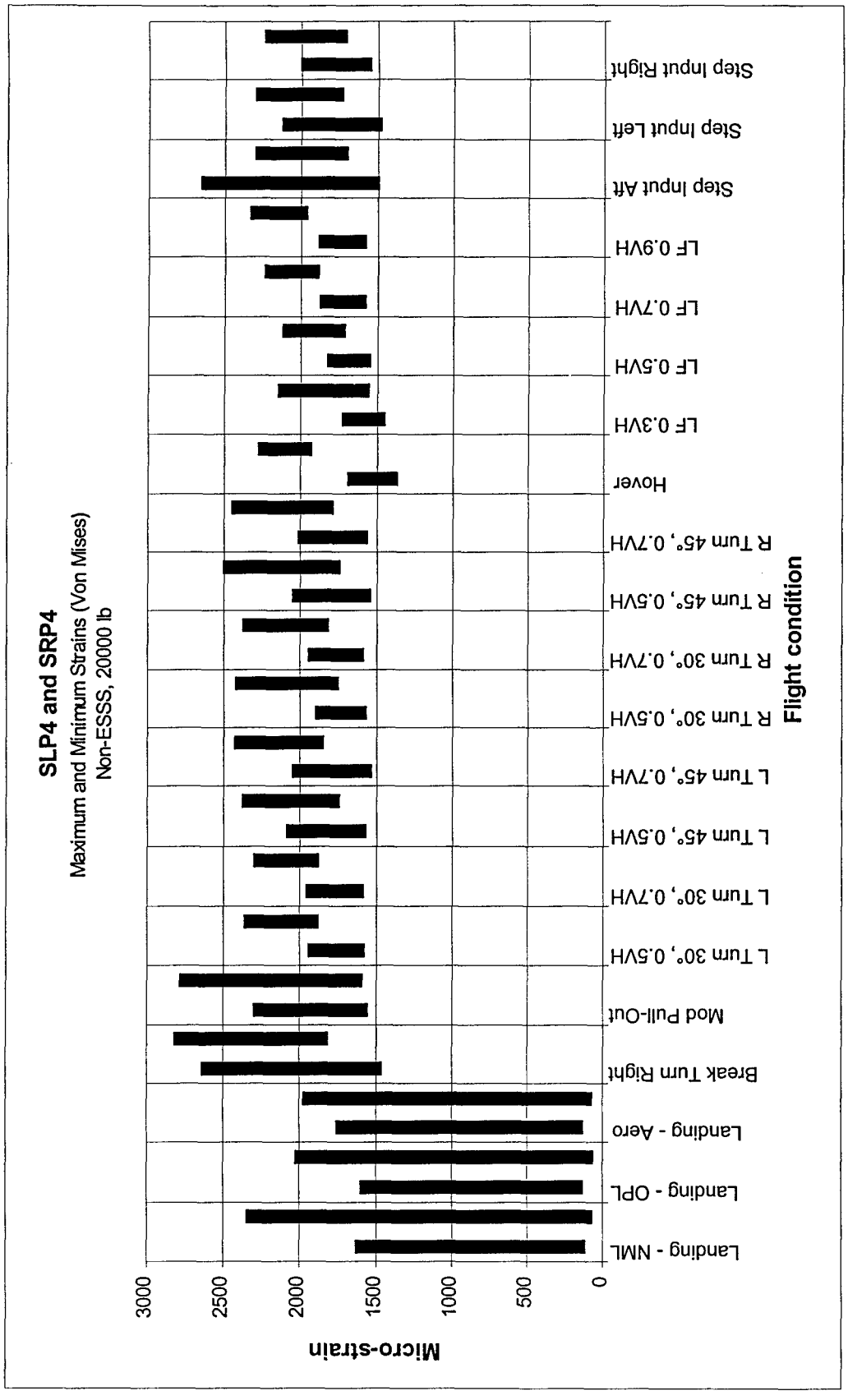

Figure 5(d): Maximum and minimum strains for the non-ESSS aircraft configuration at a gross weight of 20000 lb.

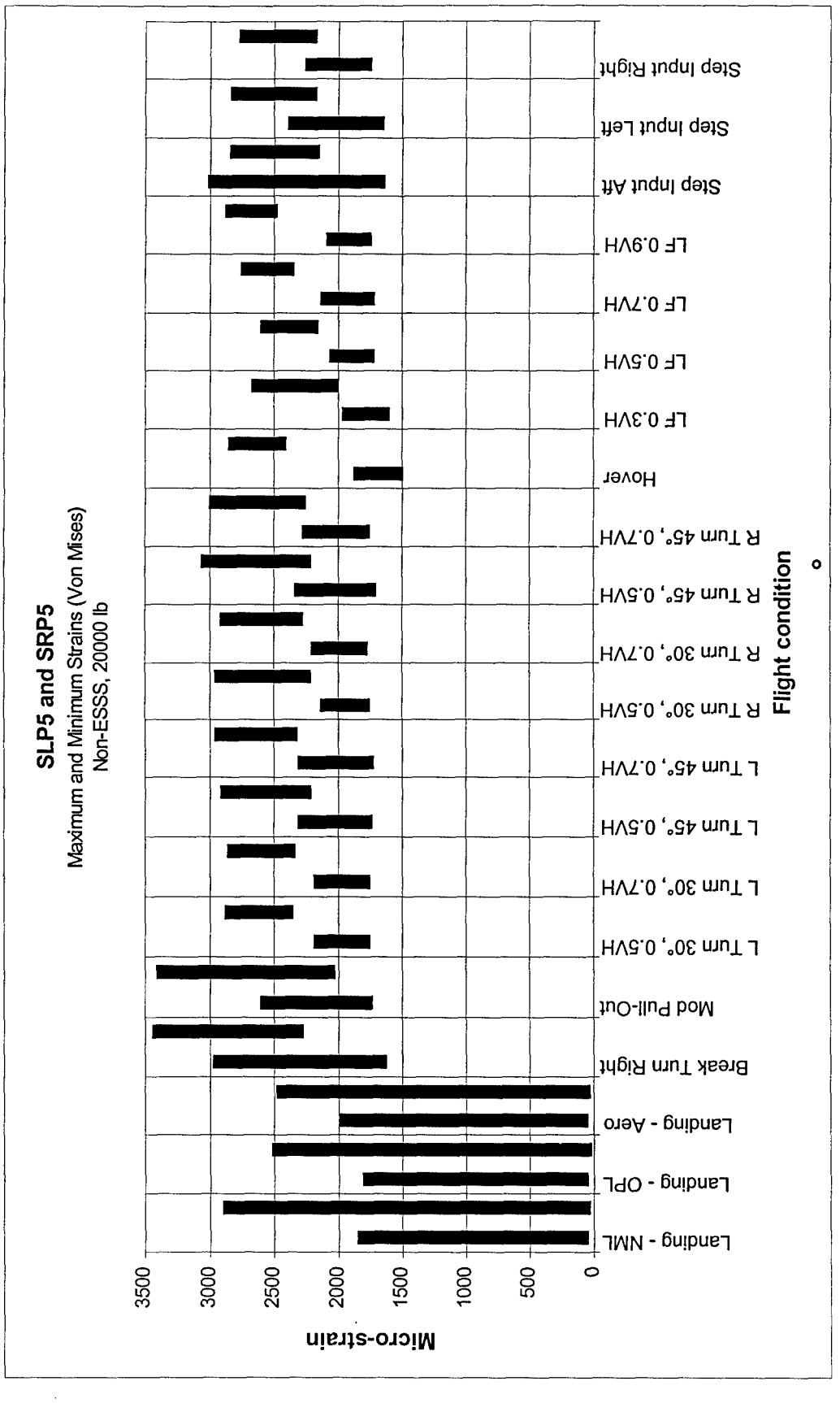

Figure 5(e): Maximum and minimum strains for the non-ESSS aircraft configuration at a gross weight of 20000 lb.

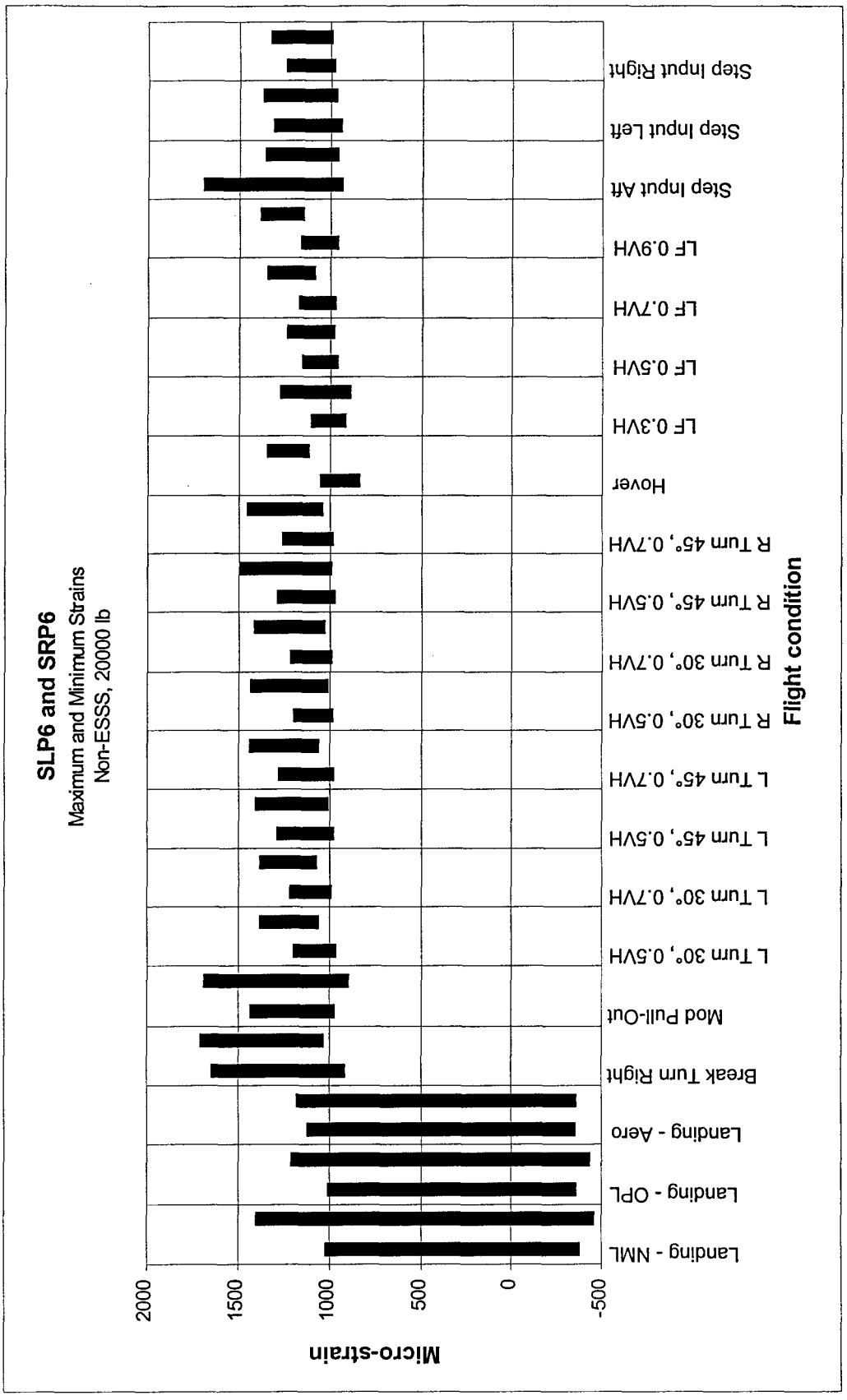

Figure 5(f): Maximum and minimum strains for the non-ESSS aircraft configuration at a gross weight of 20000 lb.

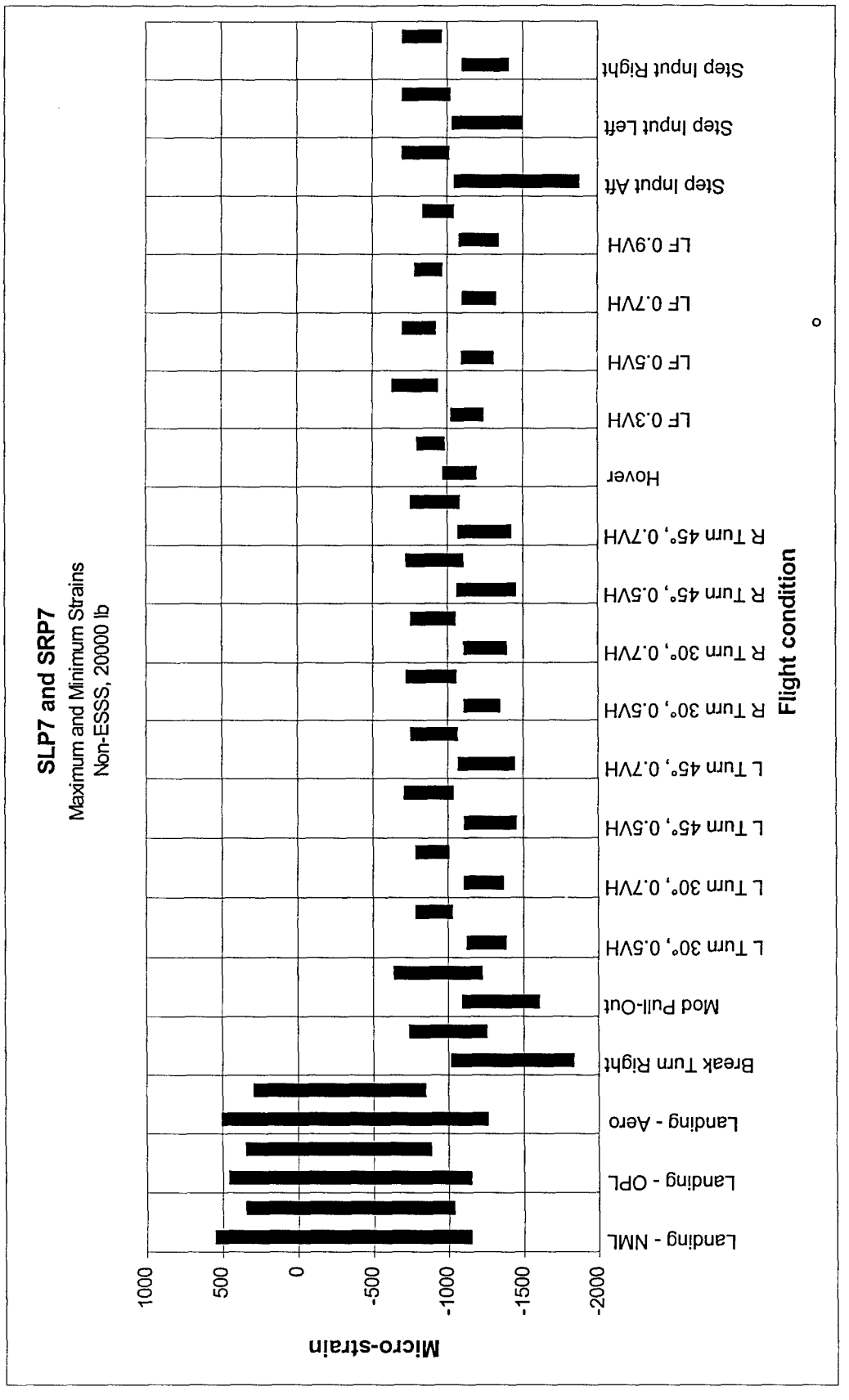

Figure 5(g): Maximum and minimum strains for the non-ESSS aircraft configuration at a gross weight of 20000 lb.

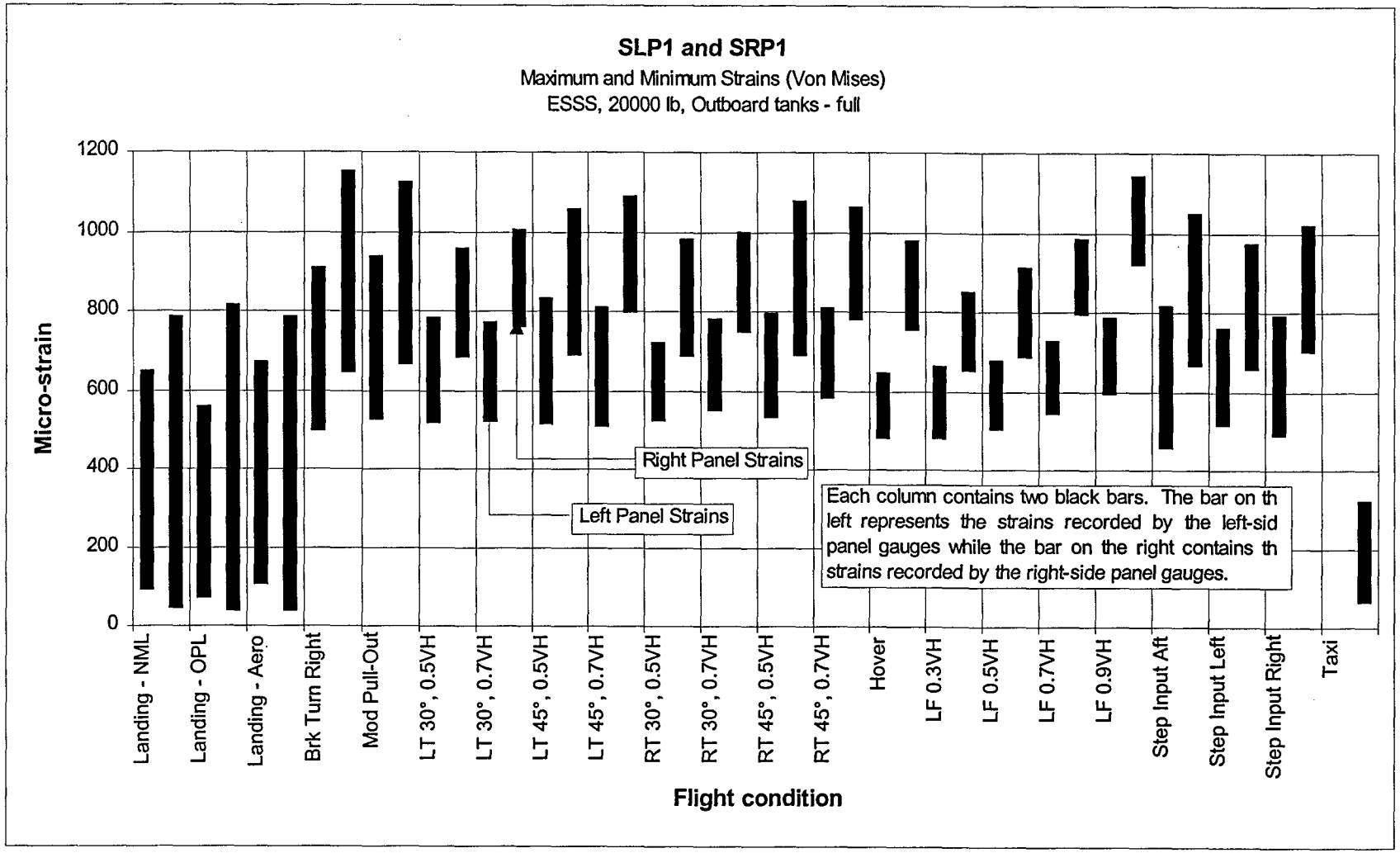

Figure 6(a): Maximum and minimum strains for the ESSS aircraft configuration with two outboard tanks (full of fuel) at a gross weight of 20000 lb.

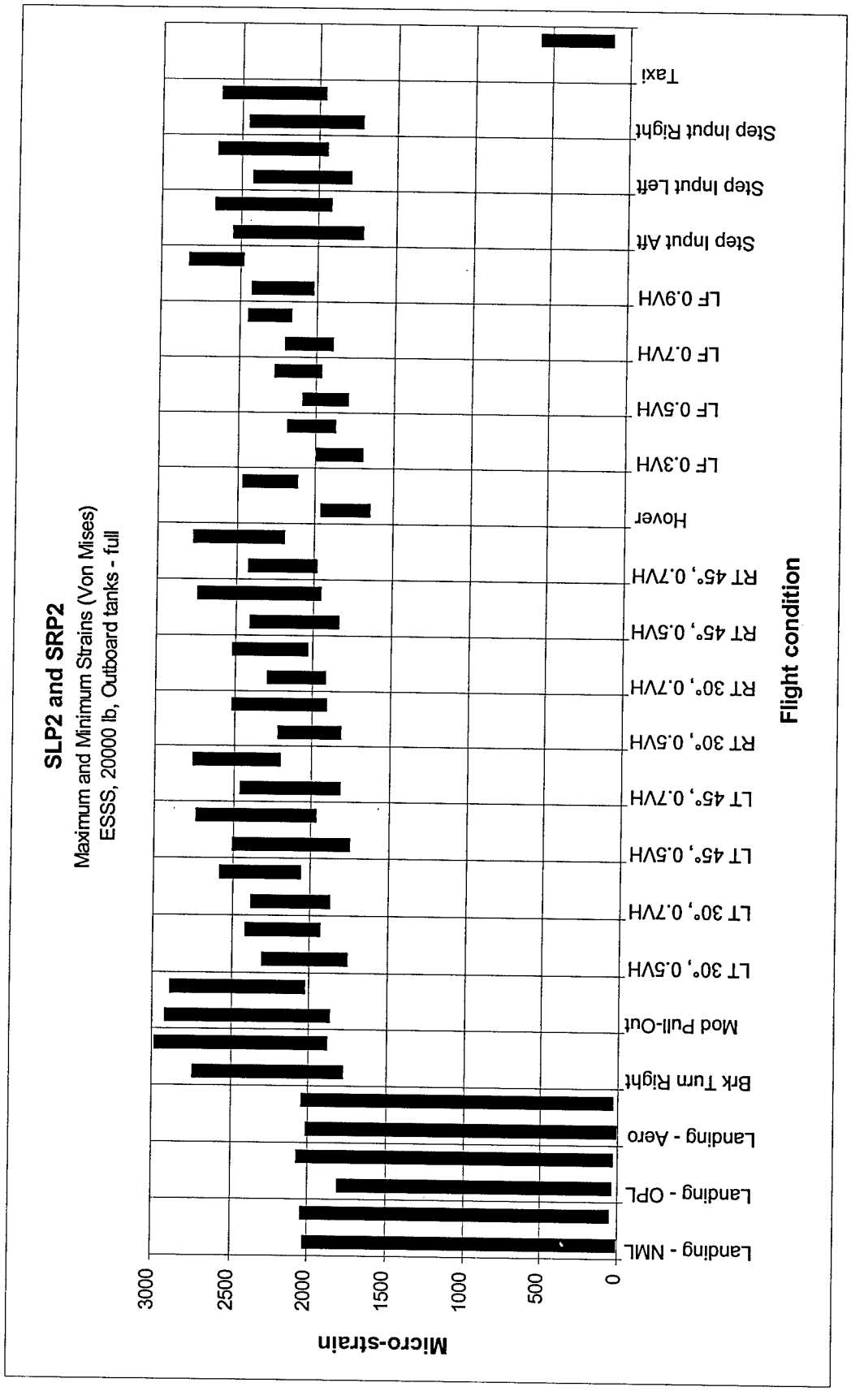

Figure 6(b): Maximum and minimum strains for the ESSS aircraft configuration with two outboard tanks (full of fuel) at a gross weight of 20000 lb.

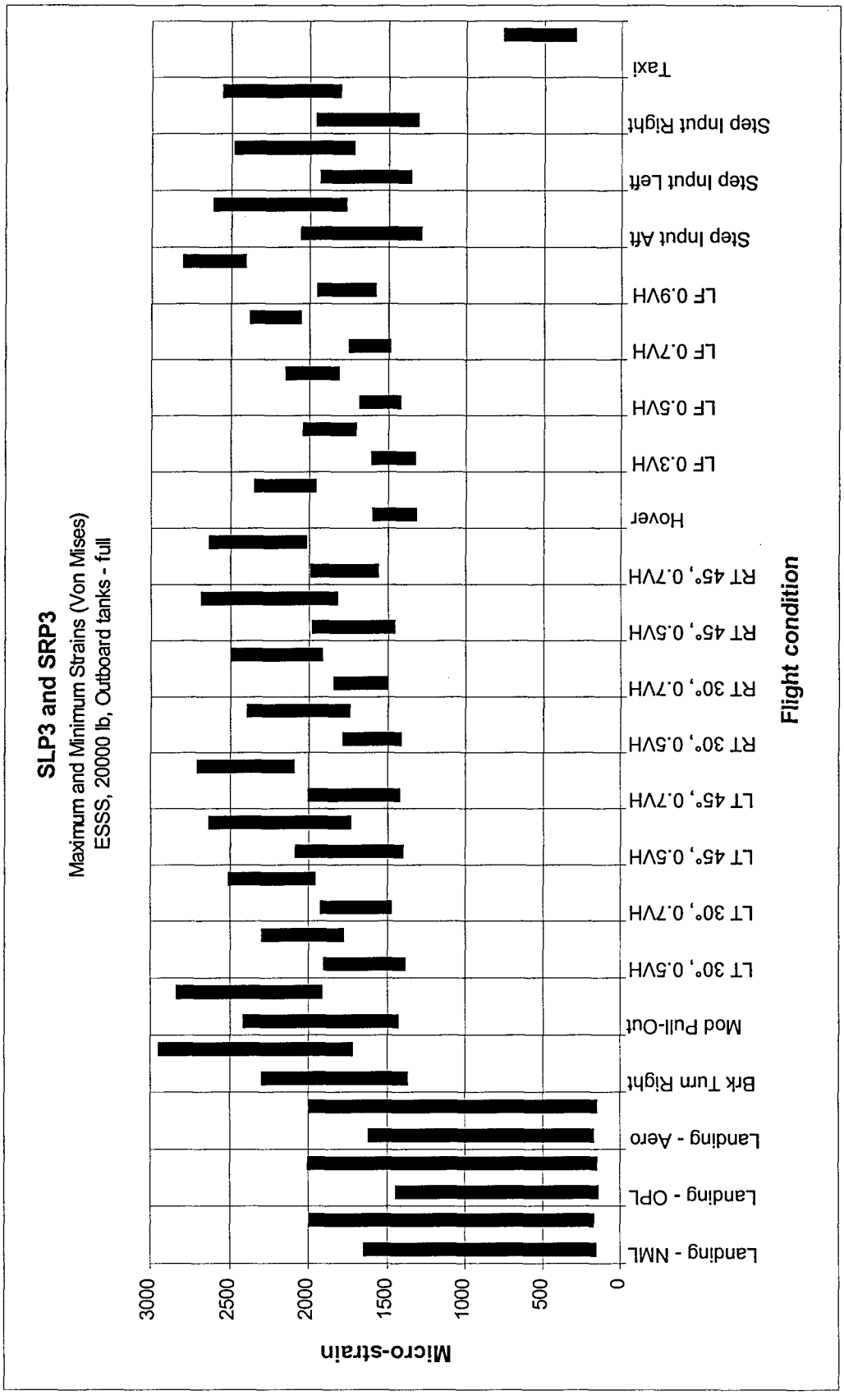

Figure 6(c): Maximum and minimum strains for the ESSS aircraft configuration with two outboard tanks (full of fuel) at a gross weight of 20000 lb.

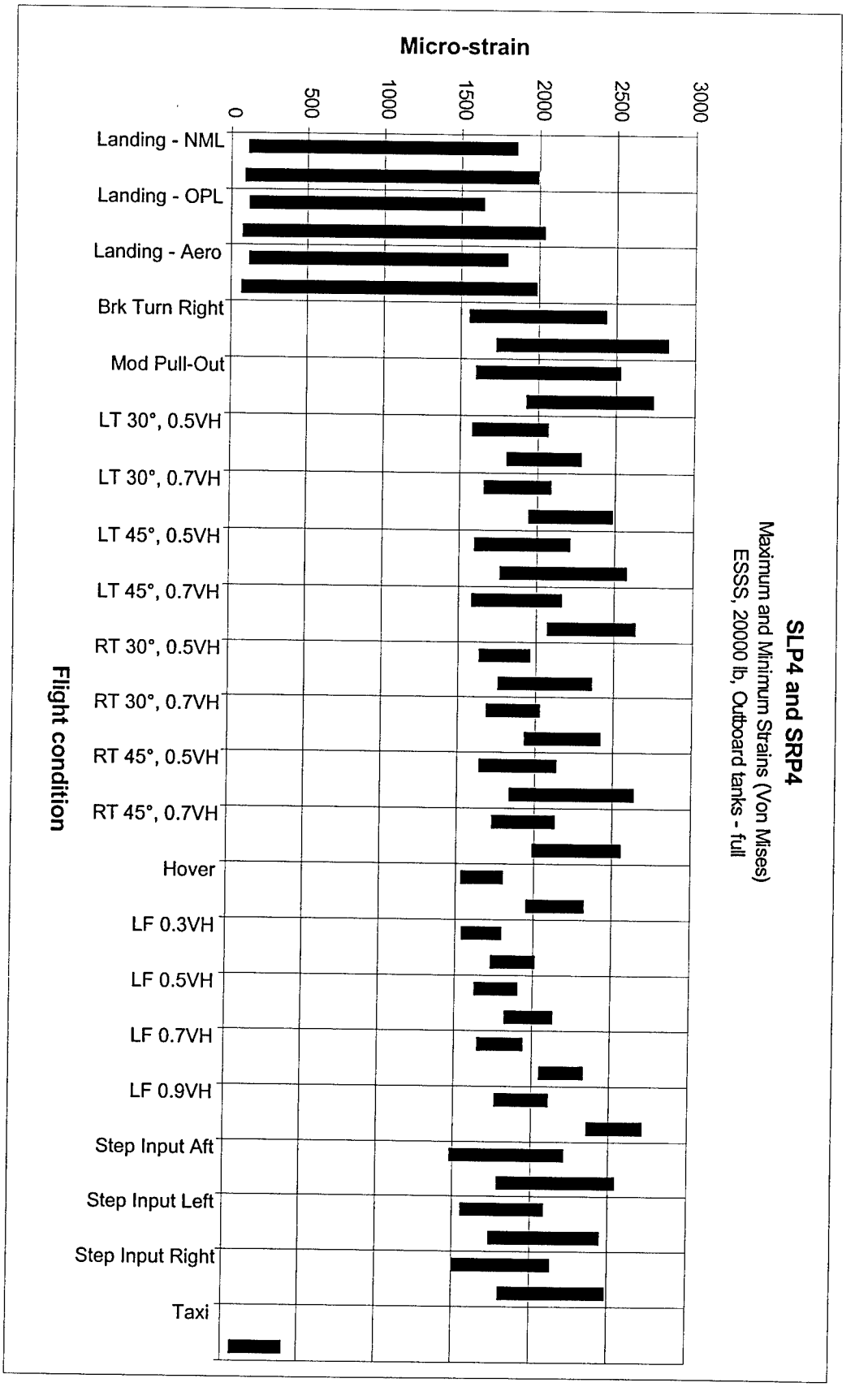

Figure 6(d): Maximum and minimum strains for the ESSS aircraft configuration with two outboard tanks (full of fuel) at a gross weight of 20000 lb.

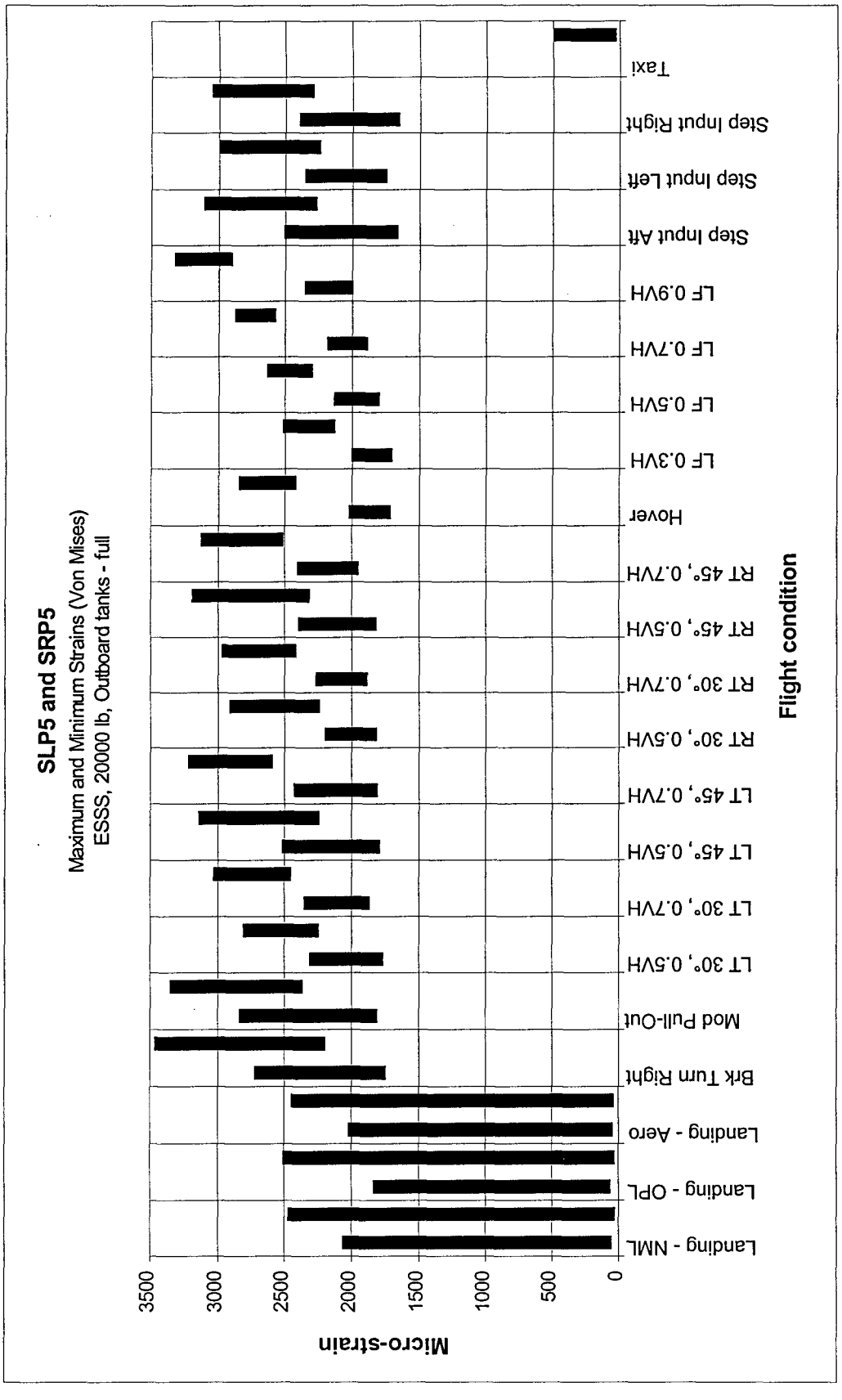

Figure 6(e): Maximum and minimum strains for the ESSS aircraft configuration with two outboard tanks (full of fuel) at a gross weight of 20000 lb.

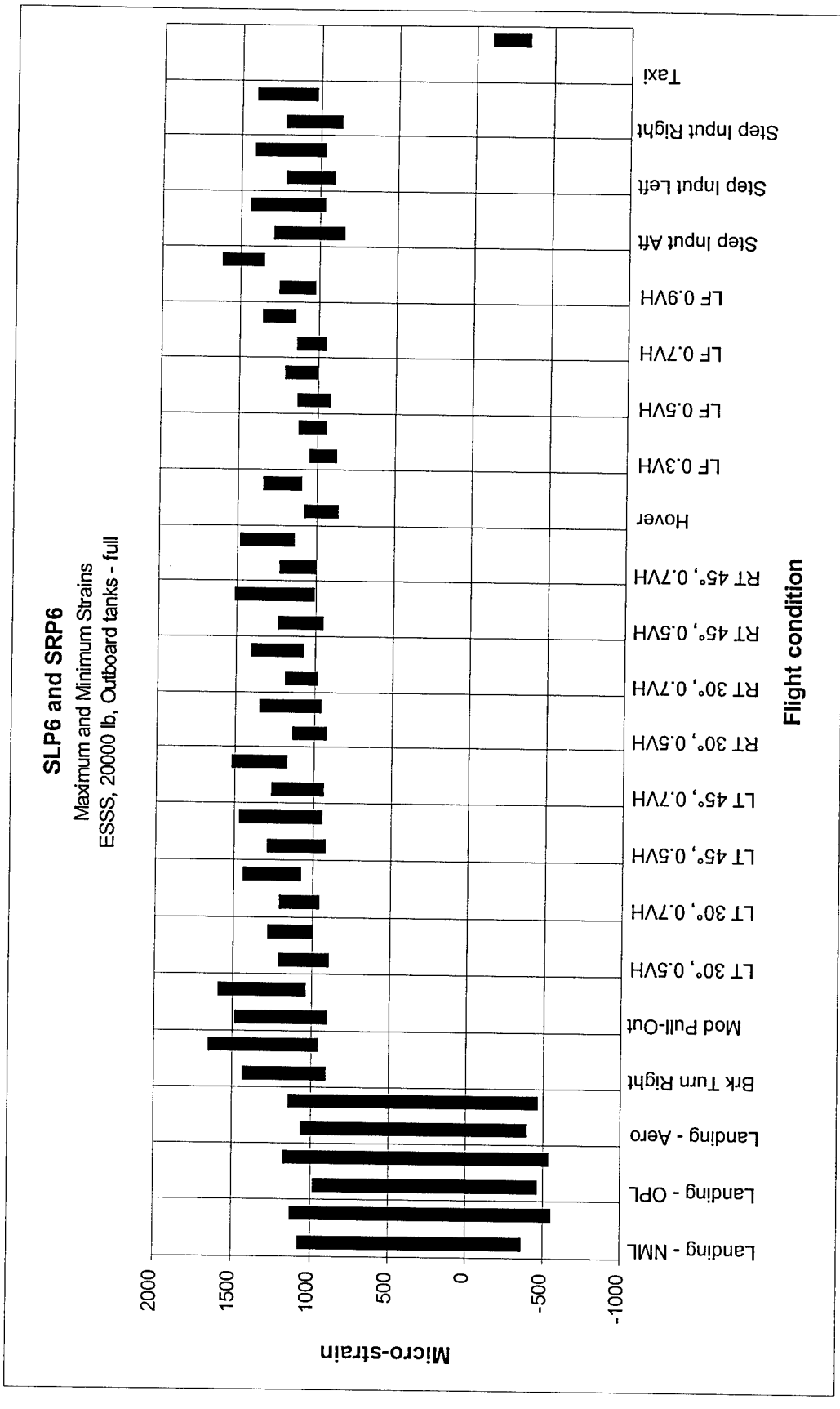

Figure 6(f): Maximum and minimum strains for the ESSS aircraft configuration with two outboard tanks (full of fuel) at a gross weight of 20000 lb.

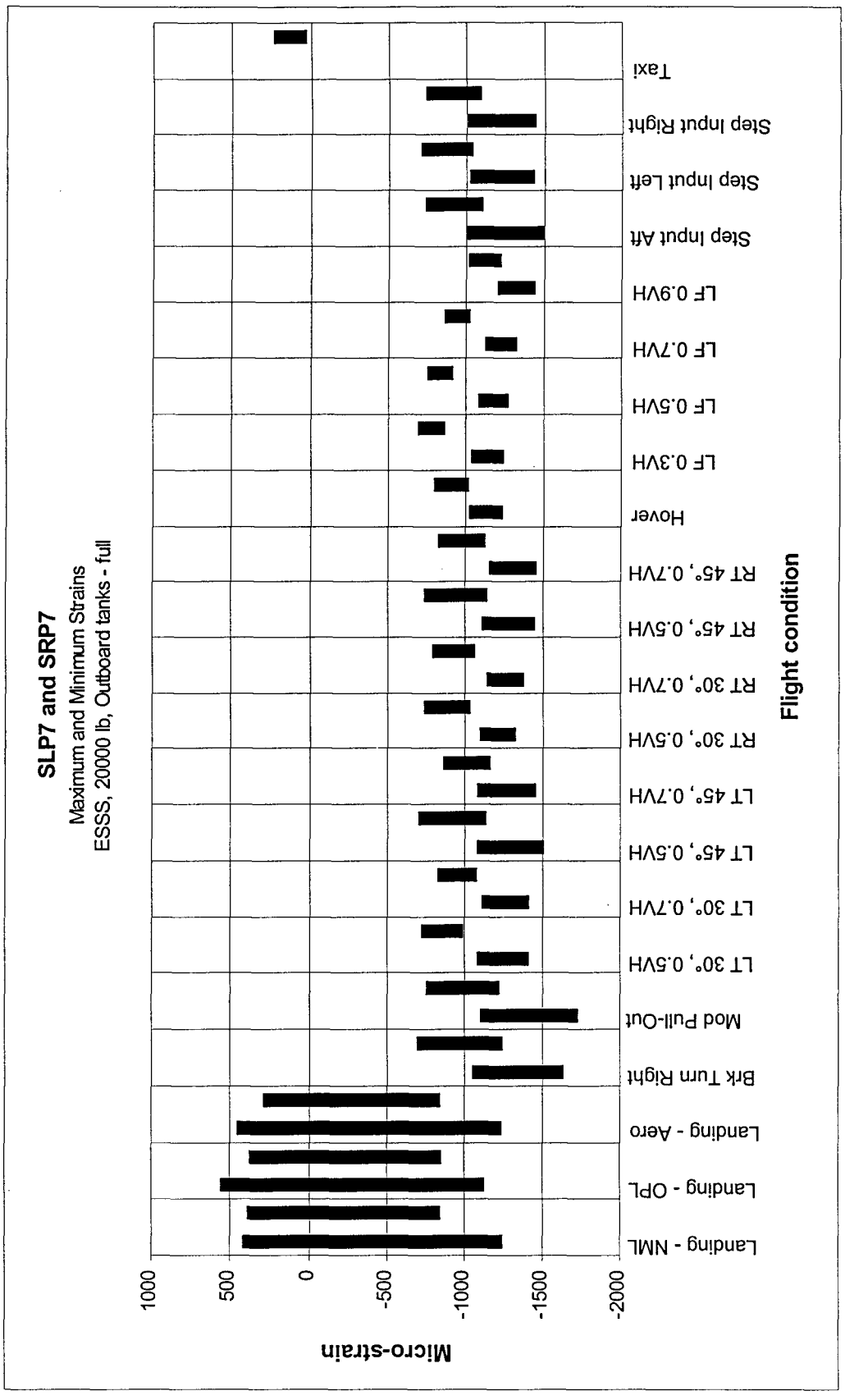

Figure 6(g): Maximum and minimum strains for the ESSS aircraft configuration with two outboard tanks (full of fuel) at a gross weight of 20000 lb.

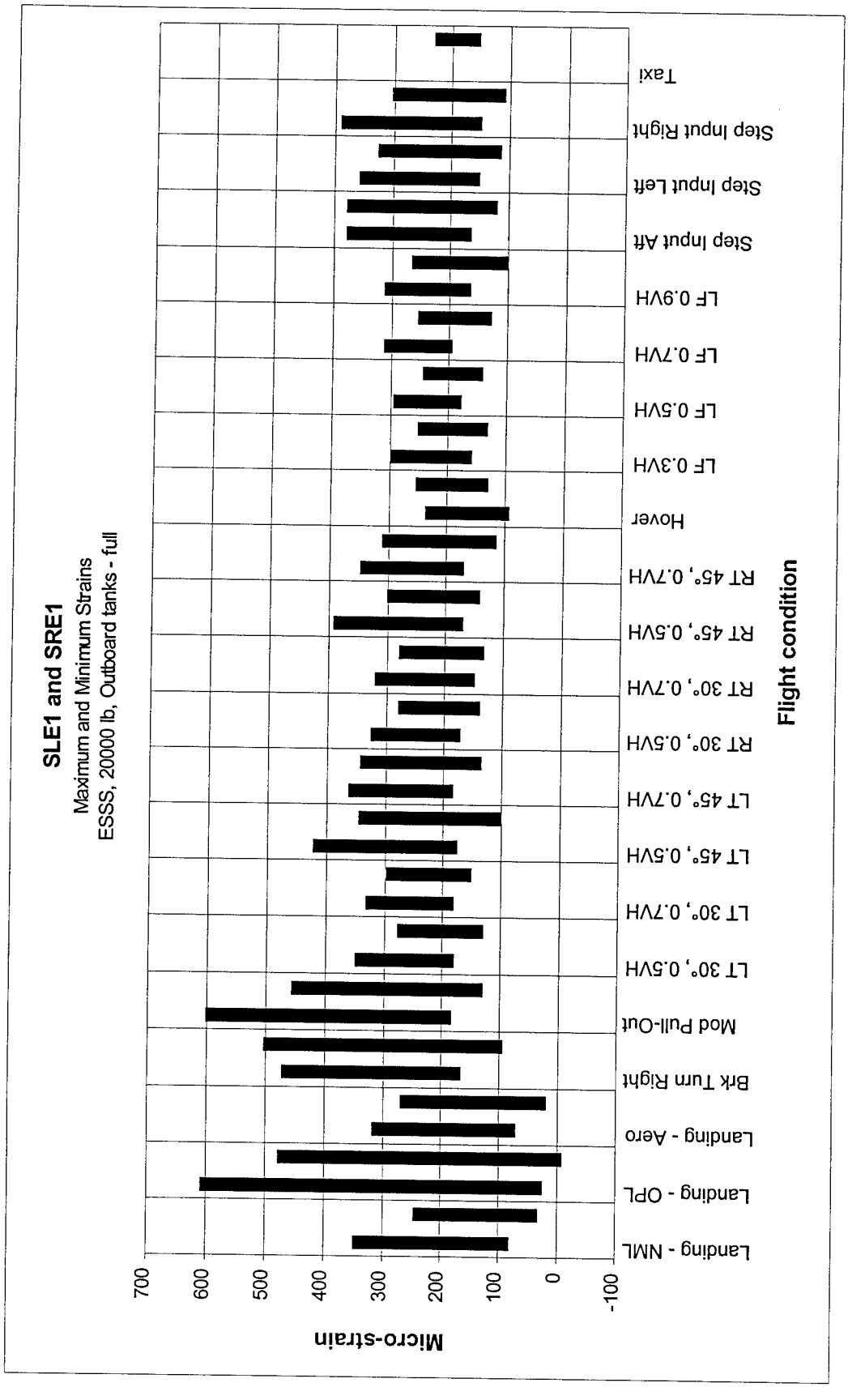

Figure 6(h): Maximum and minimum strains for the ESSS aircraft configuration with two outboard tanks (full of fuel) at a gross weight of 20000 lb.

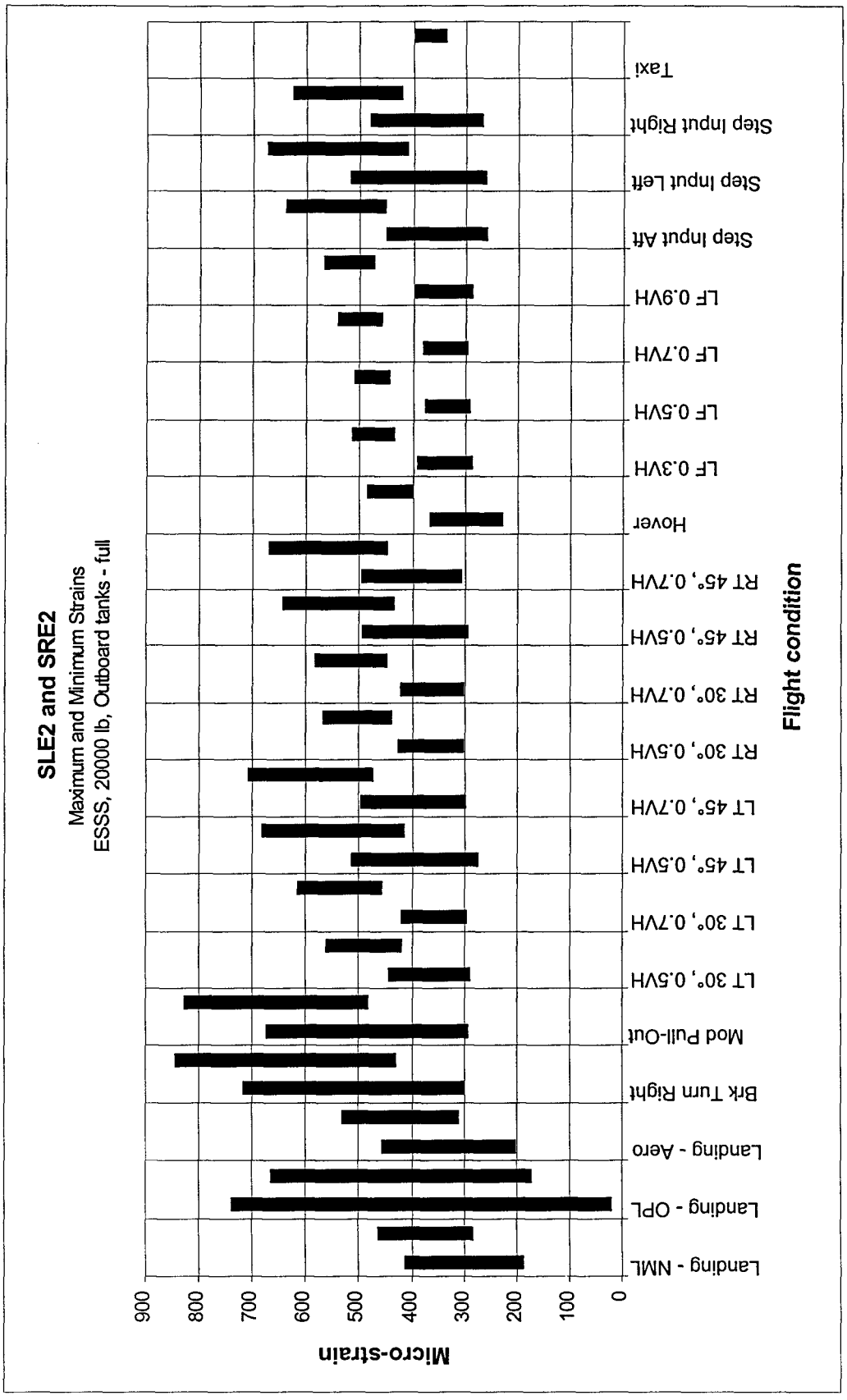

Figure 6(i): Maximum and minimum strains for the ESSS aircraft configuration with two outboard tanks (full of fuel) at a gross weight of 20000 lb.

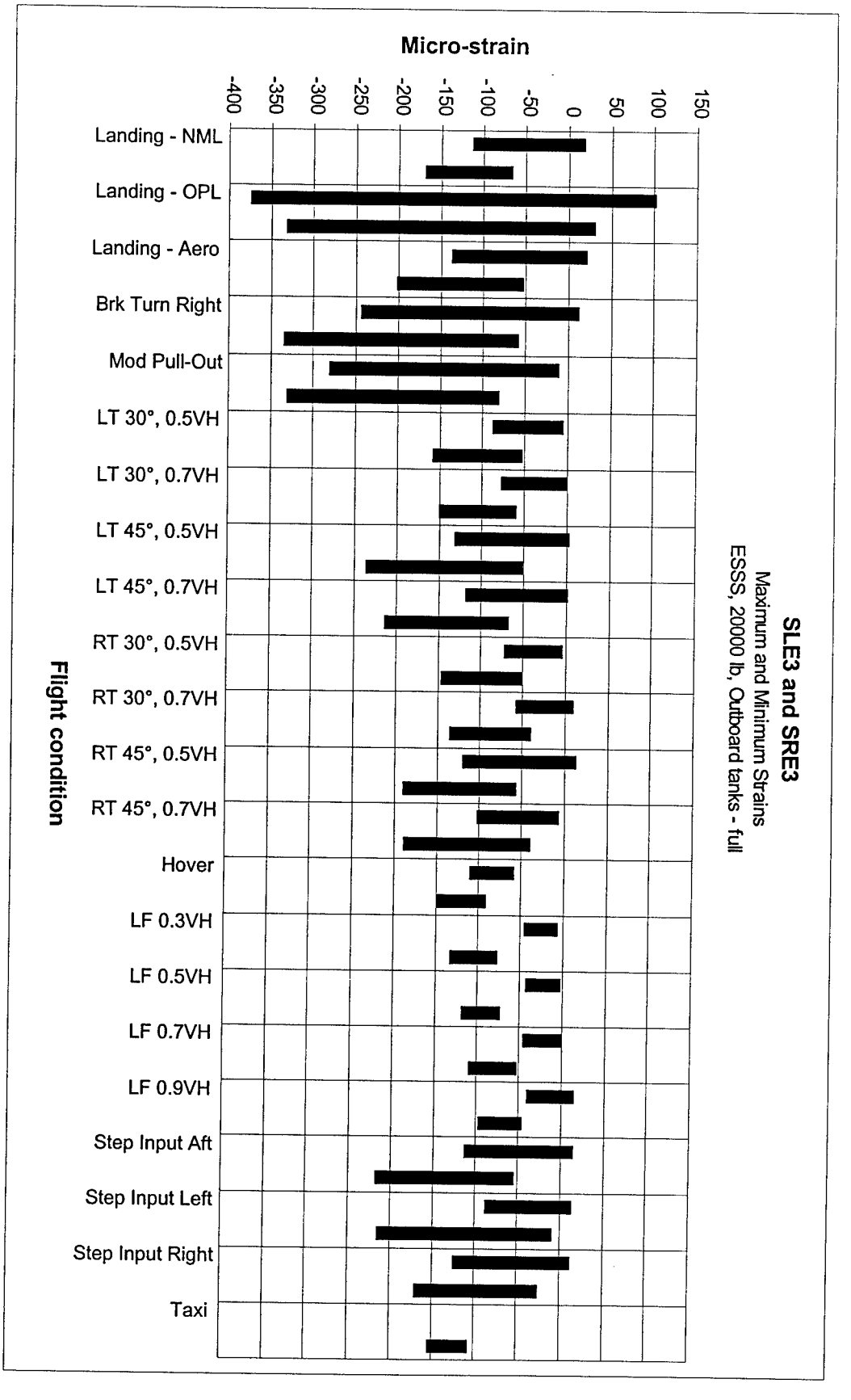

Figure 6(j): Maximum and minimum strains for the ESSS aircraft configuration with two outboard tanks (full of fuel) at a gross weight of 20000 lb.

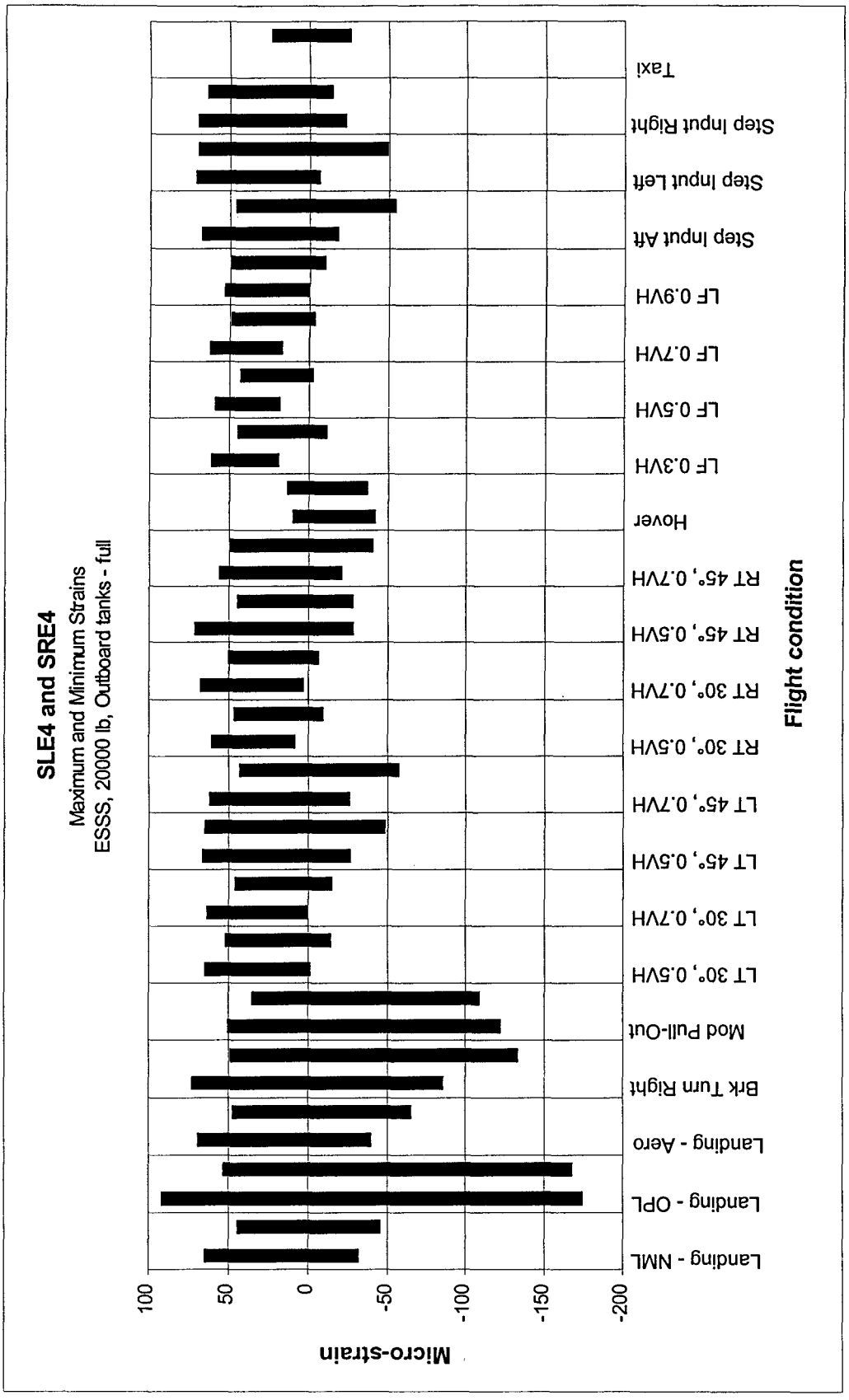

Figure 6(k): Maximum and minimum strains for the ESSS aircraft configuration with two outboard tanks (full of fuel) at a gross weight of 20000 lb.

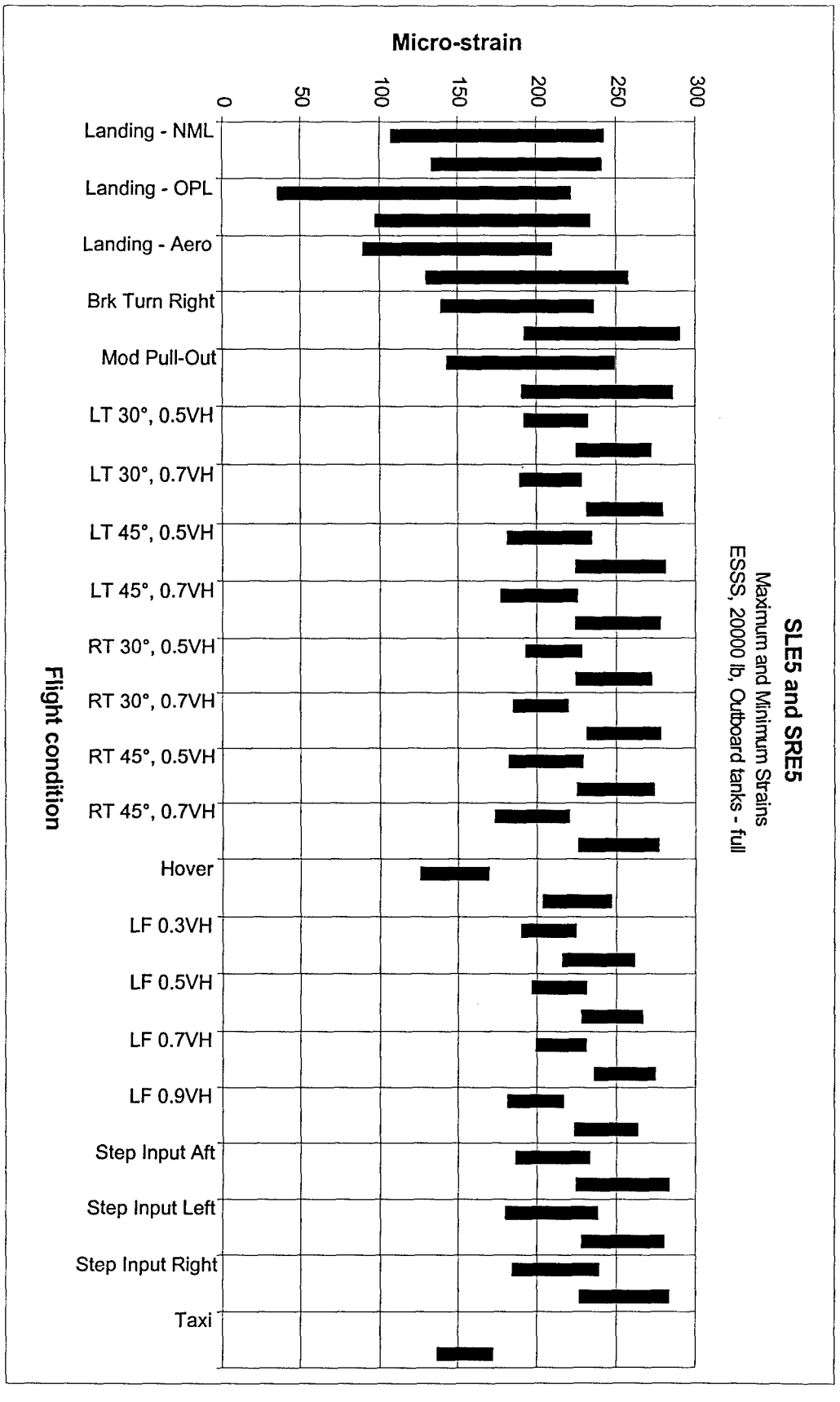

Figure 6(1): Maximum and minimum strains for the ESSS aircraft configuration with two outboard tanks (full of fuel) at a gross weight of 20000 lb.

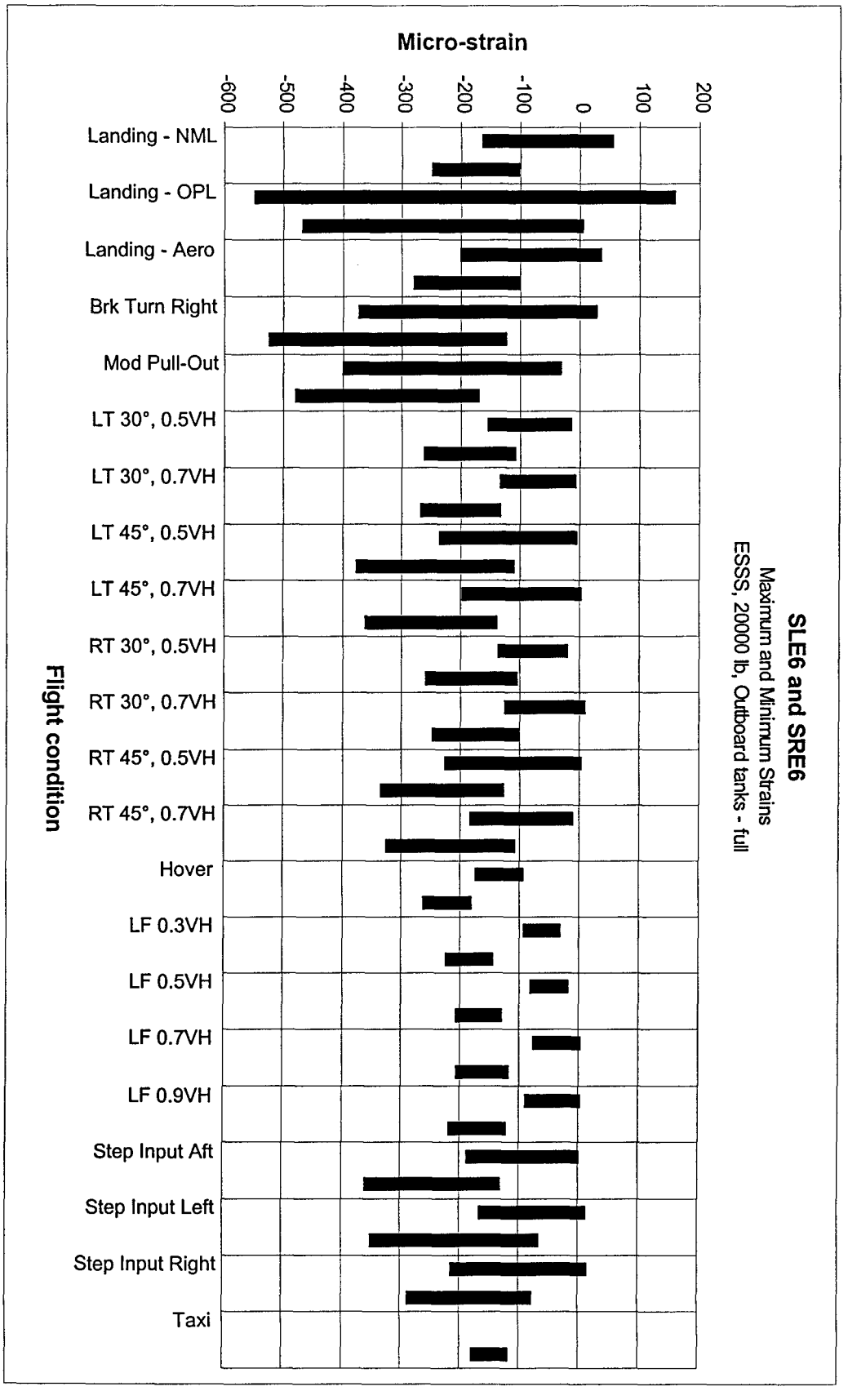

Figure 6(m): Maximum and minimum strains for the ESSS aircraft configuration with two outboard tanks (full of fuel) at a gross weight of 20000 lb.

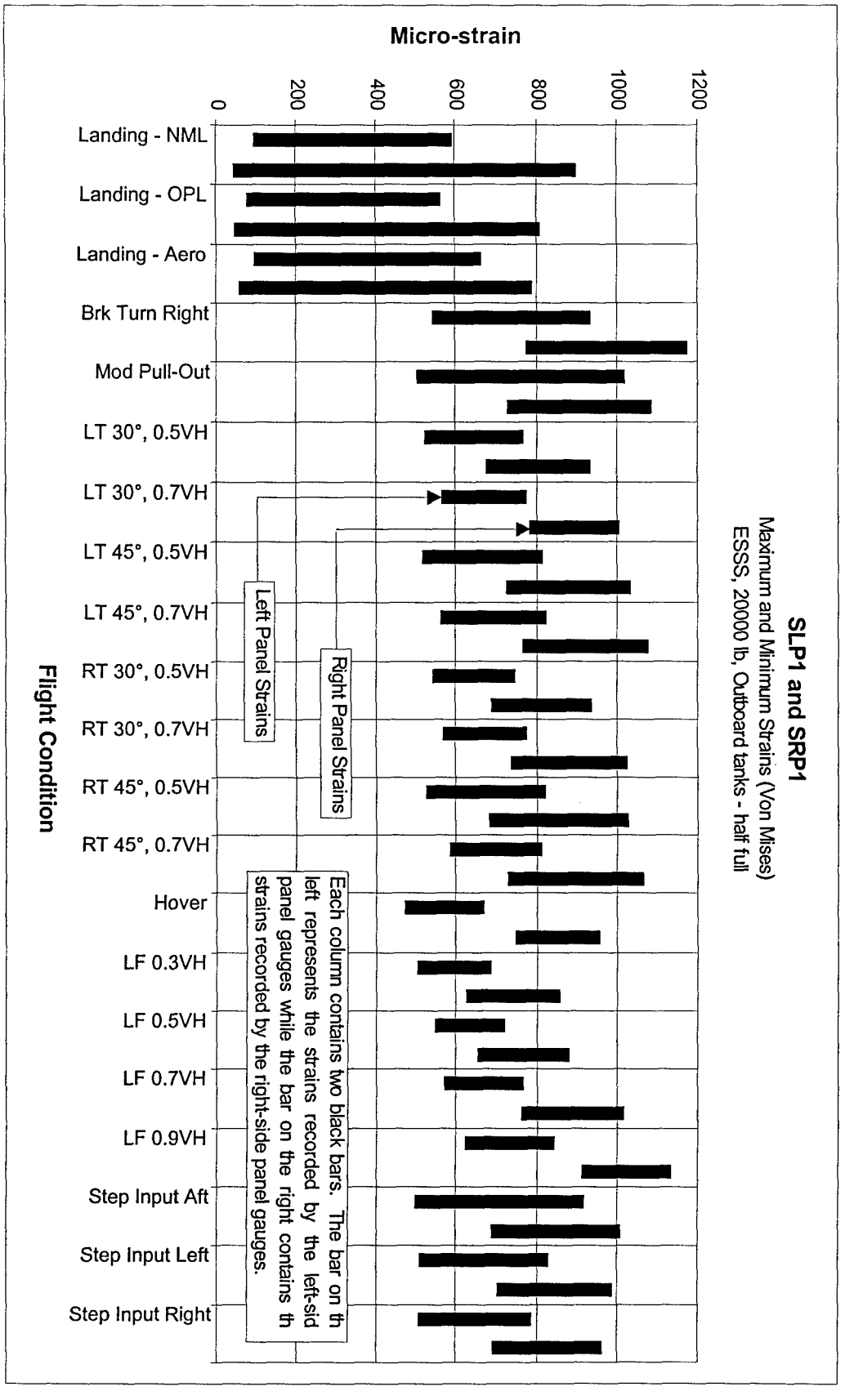

Figure 7(a): Maximum and minimum strains for the ESSS aircraft configuration with two outboard tanks (half full of fuel) at a gross weight of 20000 lb.

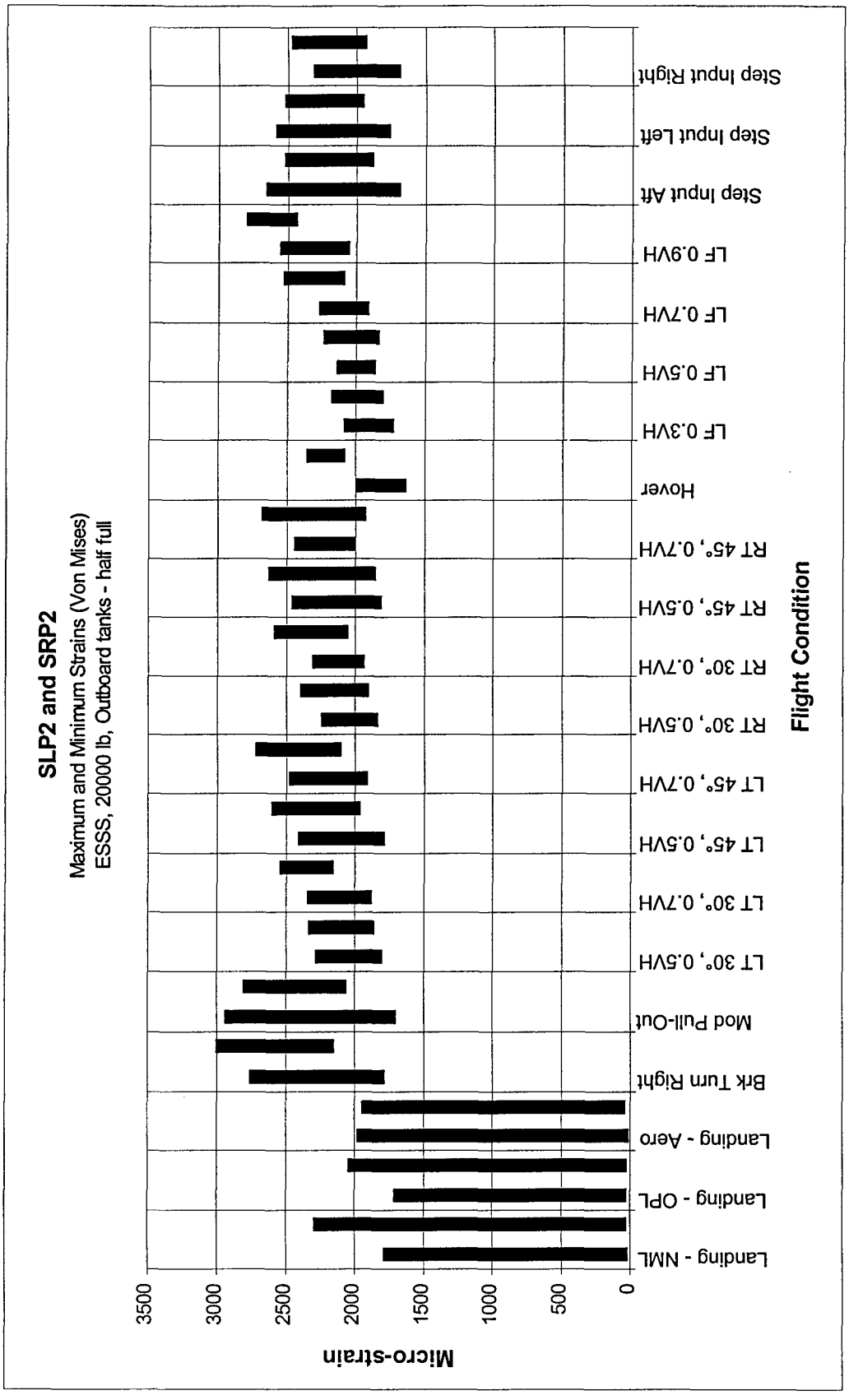

Figure 7(b): Maximum and minimum strains for the ESSS aircraft configuration with two outboard tanks (half full of fuel) at a gross weight of 20000 lb.

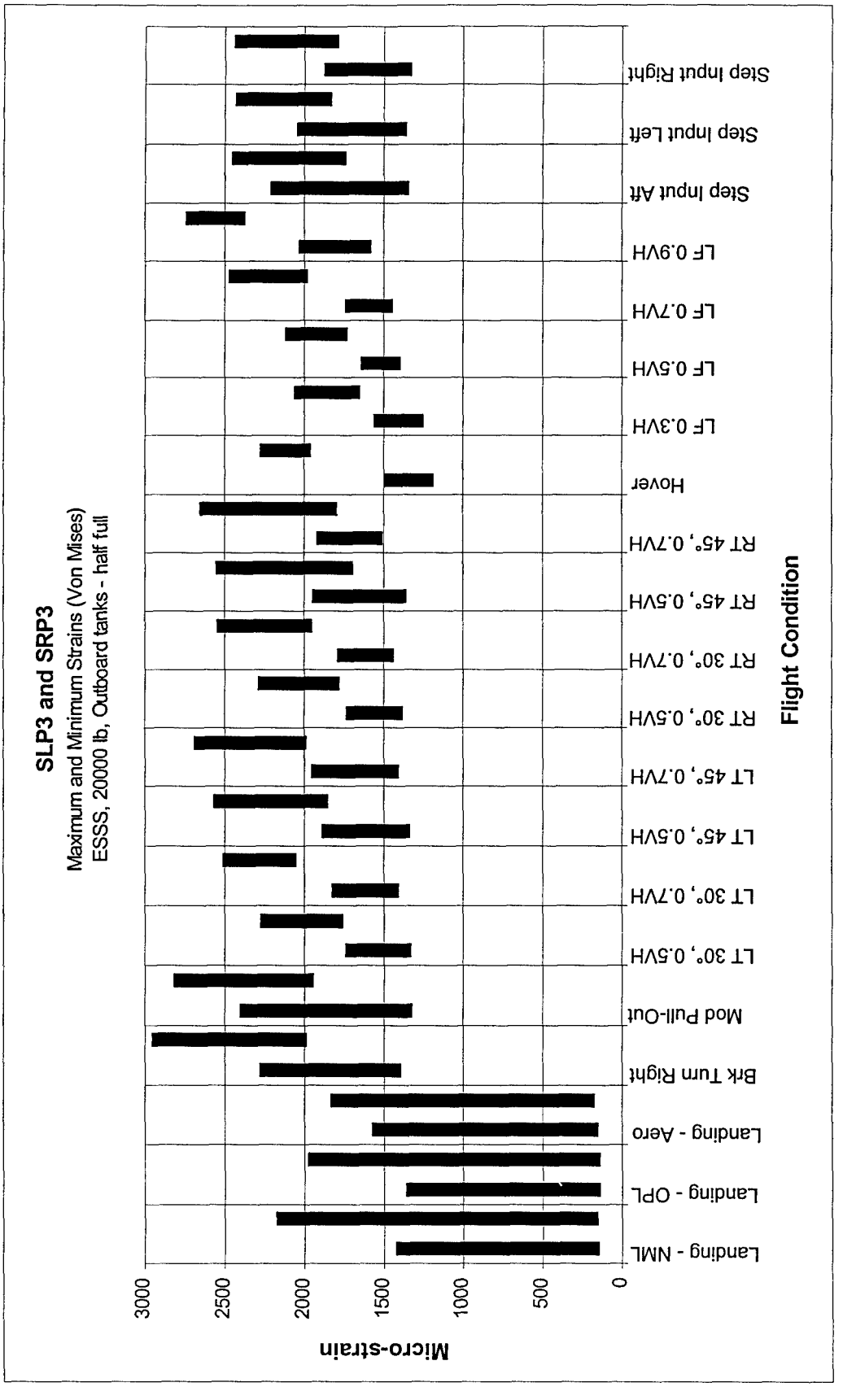

Figure 7(c): Maximum and minimum strains for the ESSS aircraft configuration with two outboard tanks (half full of fuel) at a gross weight of 20000 lb.

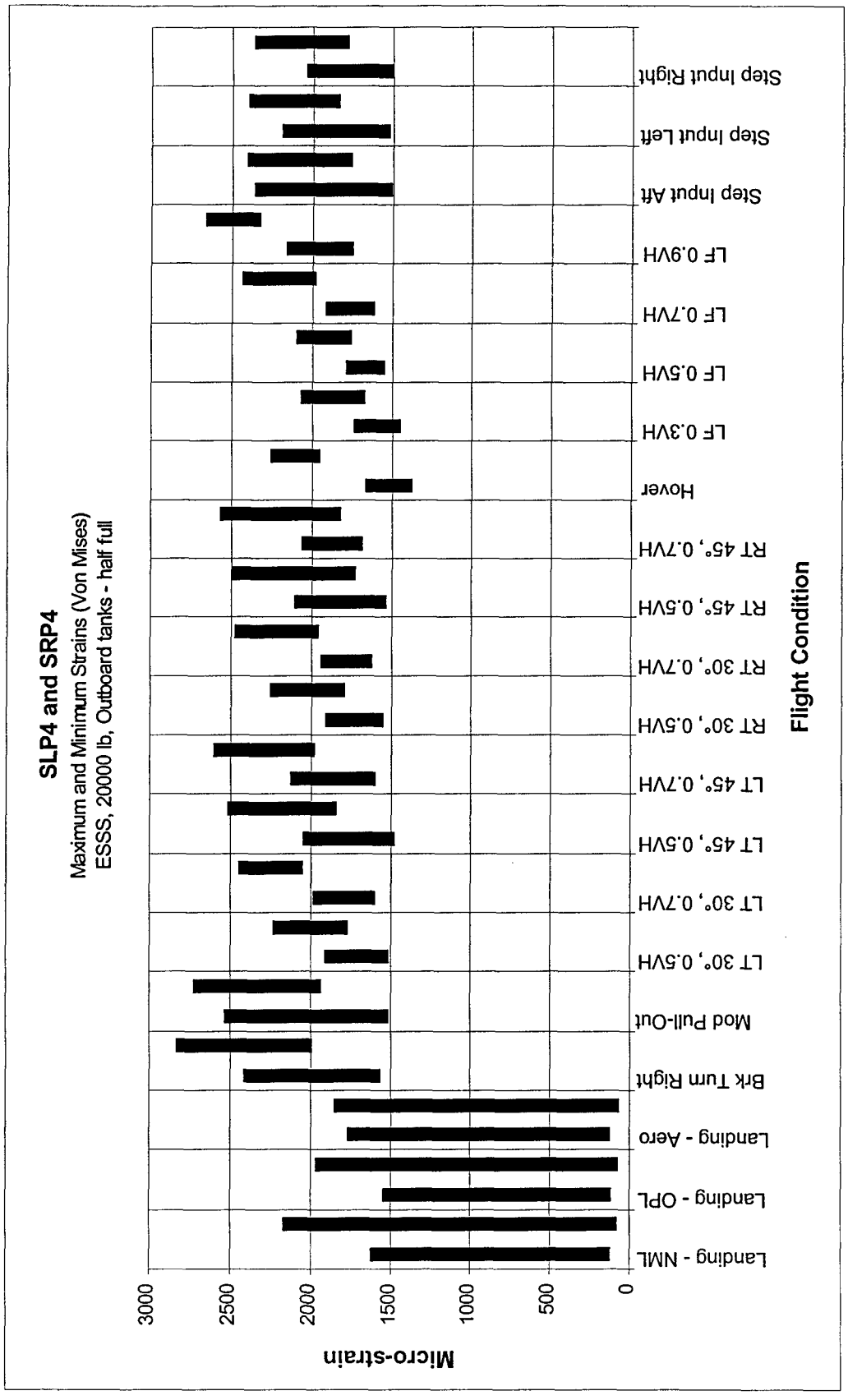

Figure 7(d): Maximum and minimum strains for the ESSS aircraft configuration with two outboard tanks (half full of fuel) at a gross weight of 20000 lb.

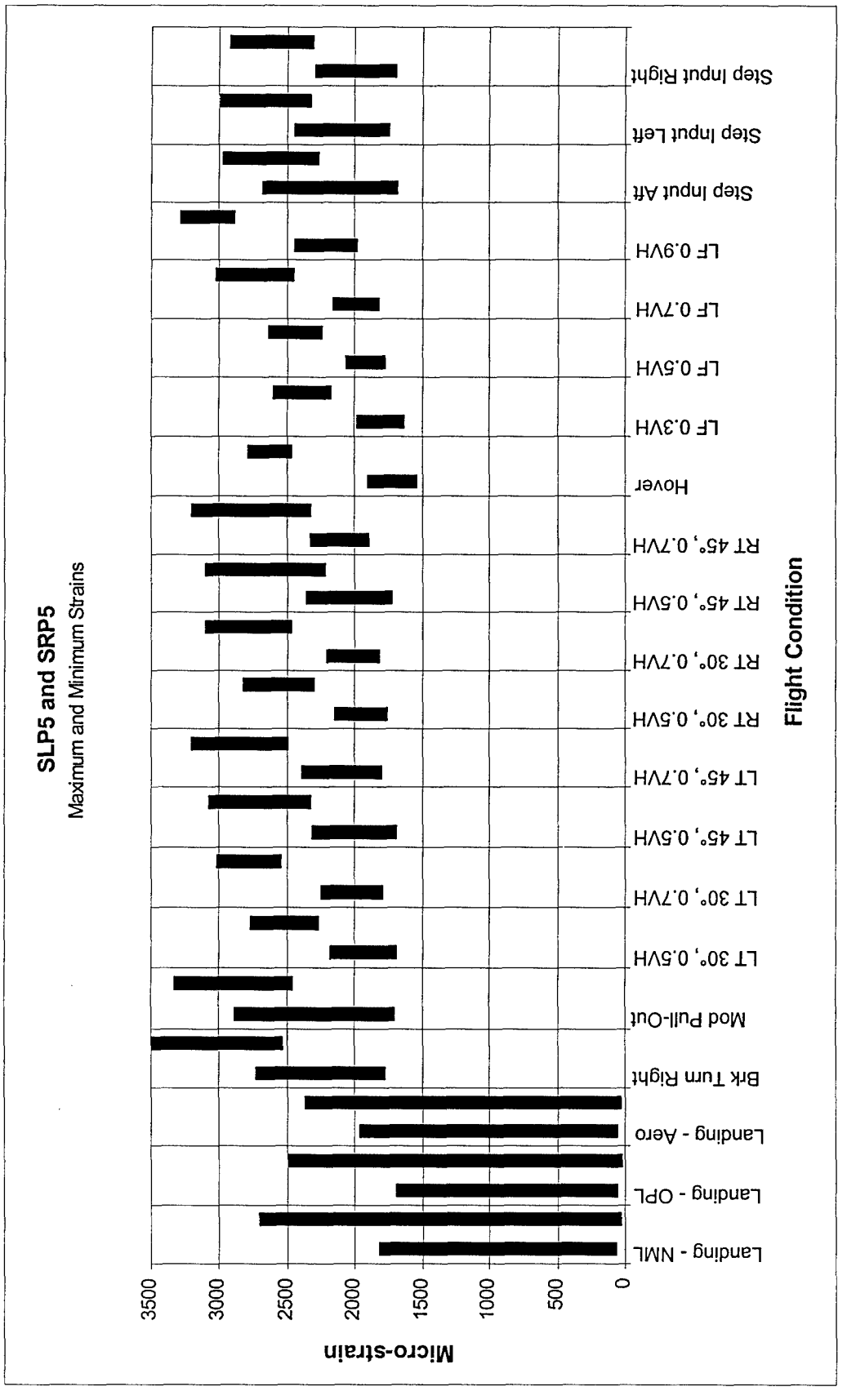

Figure 7(e): Maximum and minimum strains for the ESSS aircraft configuration with two outboard tanks (half full of fuel) at a gross weight of 20000 lb.

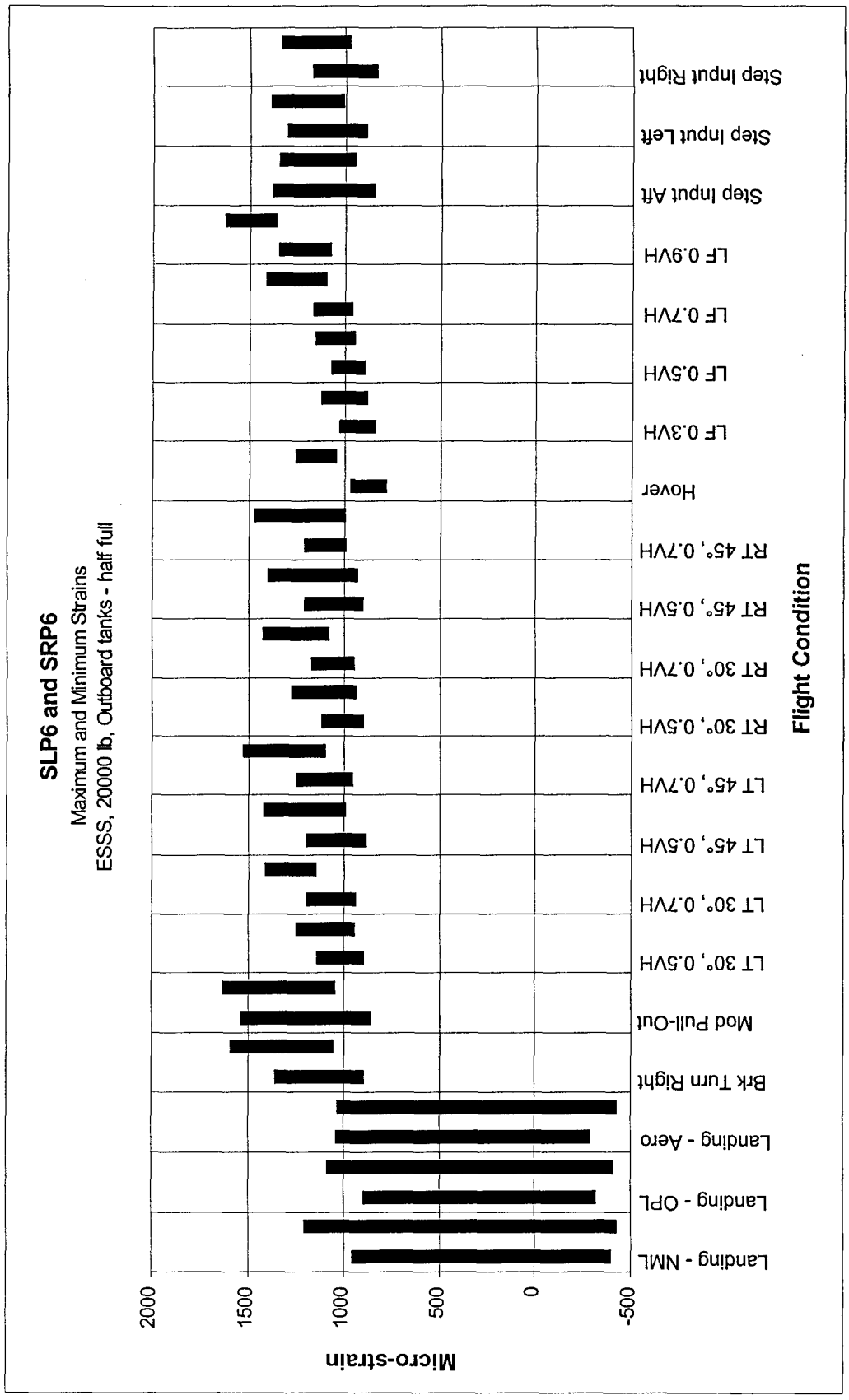

Figure 7(f): Maximum and minimum strains for the ESSS aircraft configuration with two outboard tanks (half full of fuel) at a gross weight of 20000 lb.

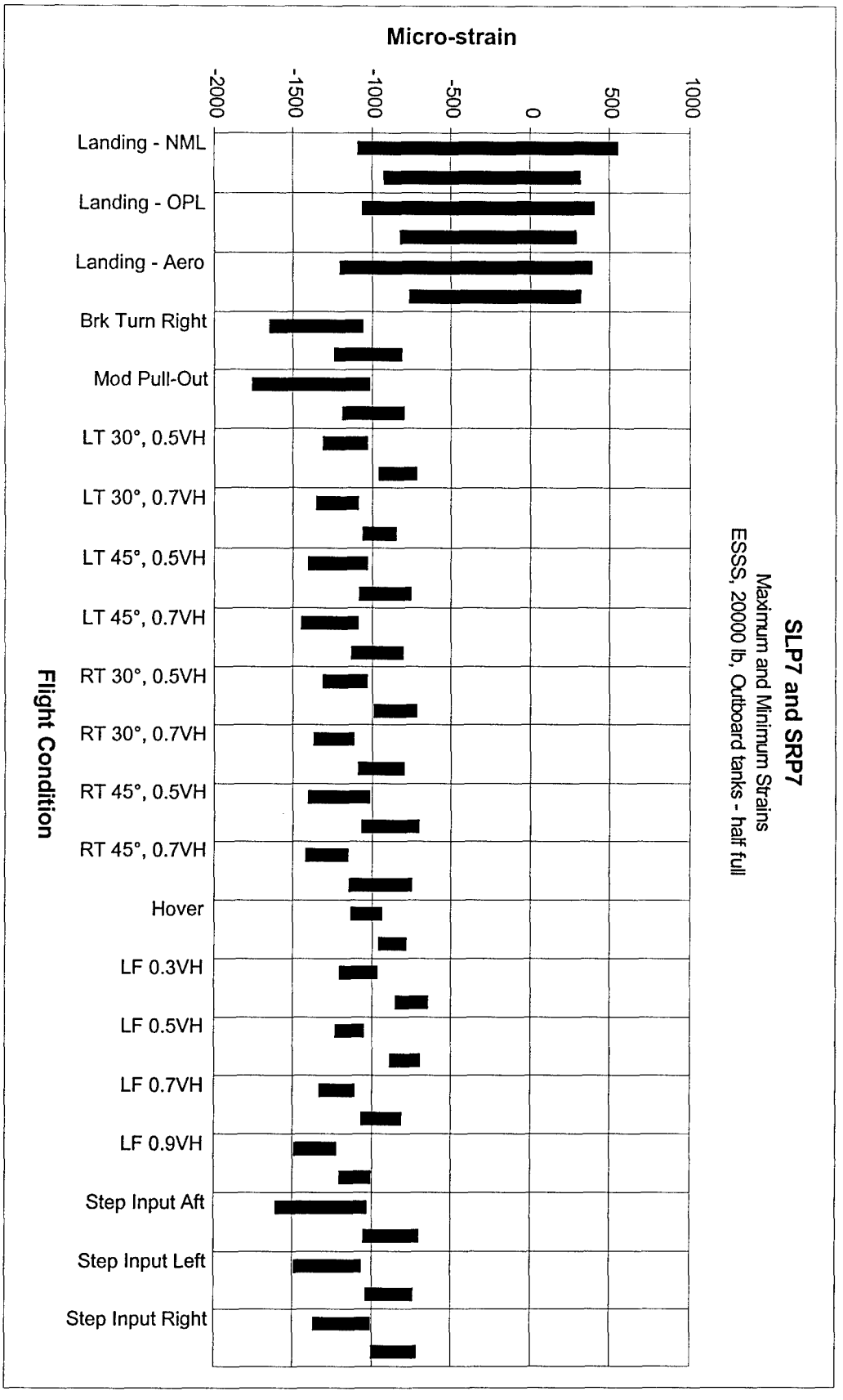

Figure 7(g): Maximum and minimum strains for the ESSS aircraft configuration with two outboard tanks (half full of fuel) at a gross weight of 20000 lb.

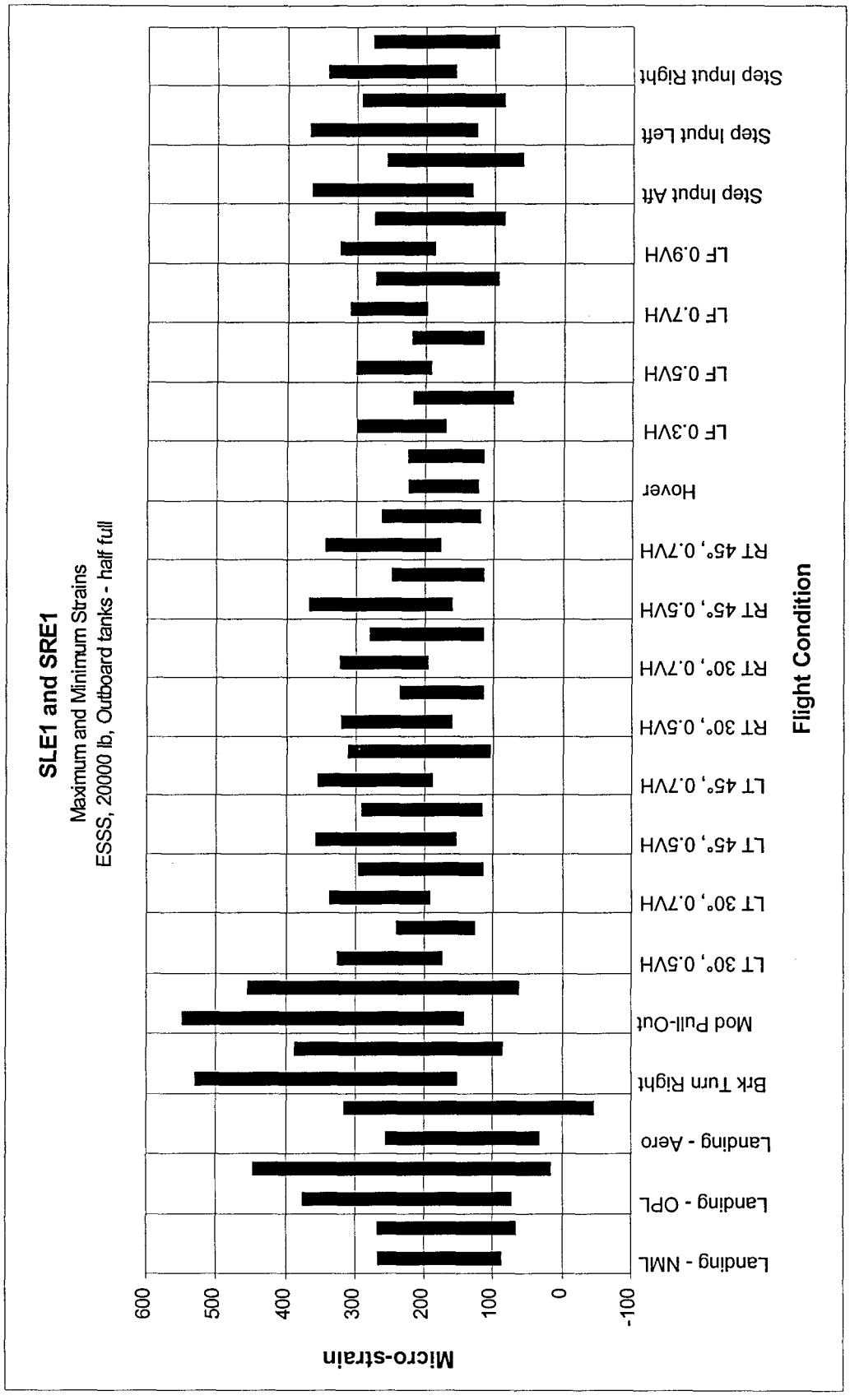

Figure 7(h): Maximum and minimum strains for the ESSS aircraft configuration with two outboard tanks (half full of fuel) at a gross weight of 20000 lb.

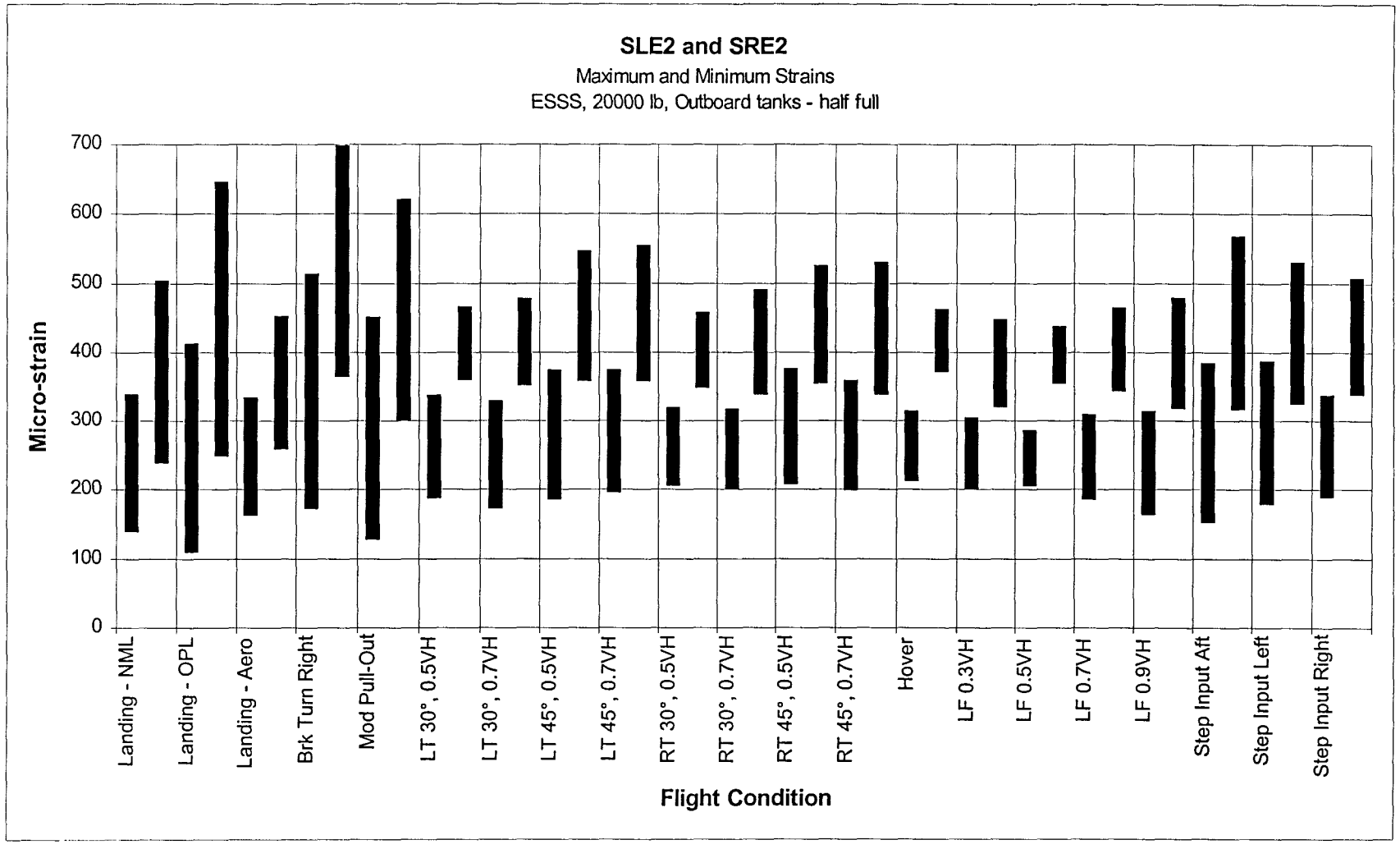

Figure 7(i): Maximum and minimum strains for the ESSS aircraft configuration with two outboard tanks (half full of fuel) at a gross weight of 20000 lb.

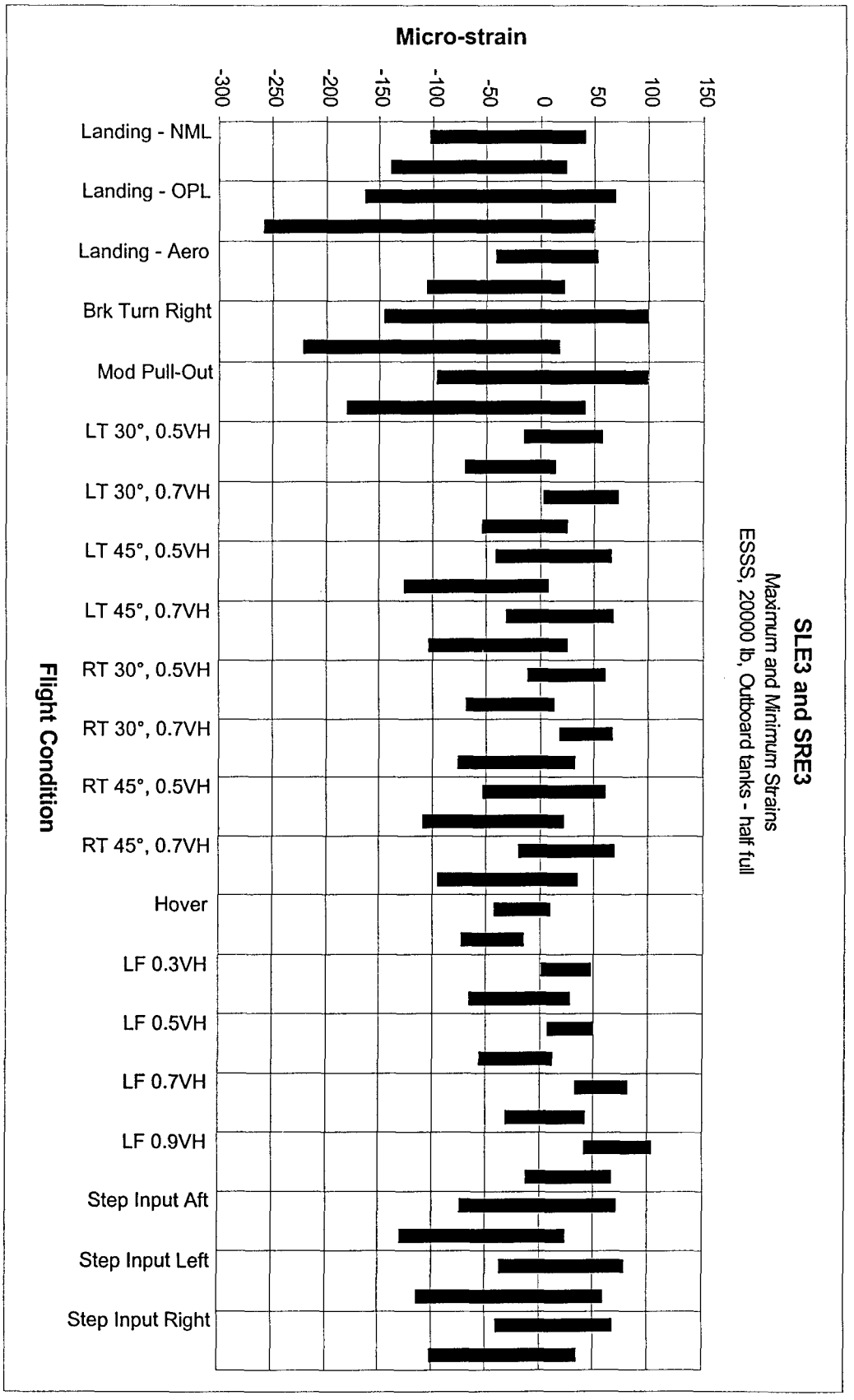

Figure 7(j): Maximum and minimum strains for the ESSS aircraft configuration with two outboard tanks (half full of fuel) at a gross weight of 20000 lb.

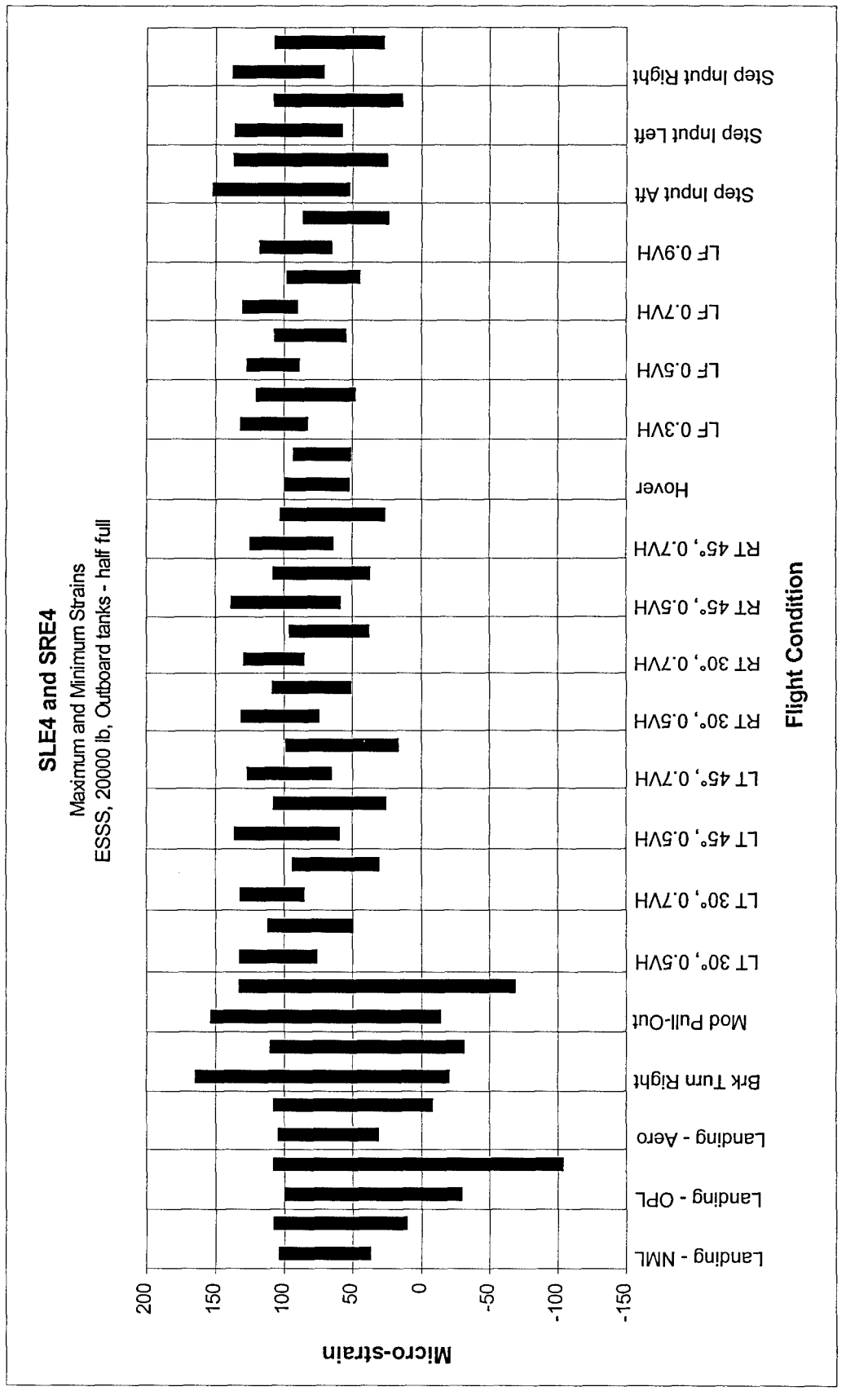

Figure 7(k): Maximum and minimum strains for the ESSS aircraft configuration with two outboard tanks (half full of fuel) at a gross weight of 20000 lb.

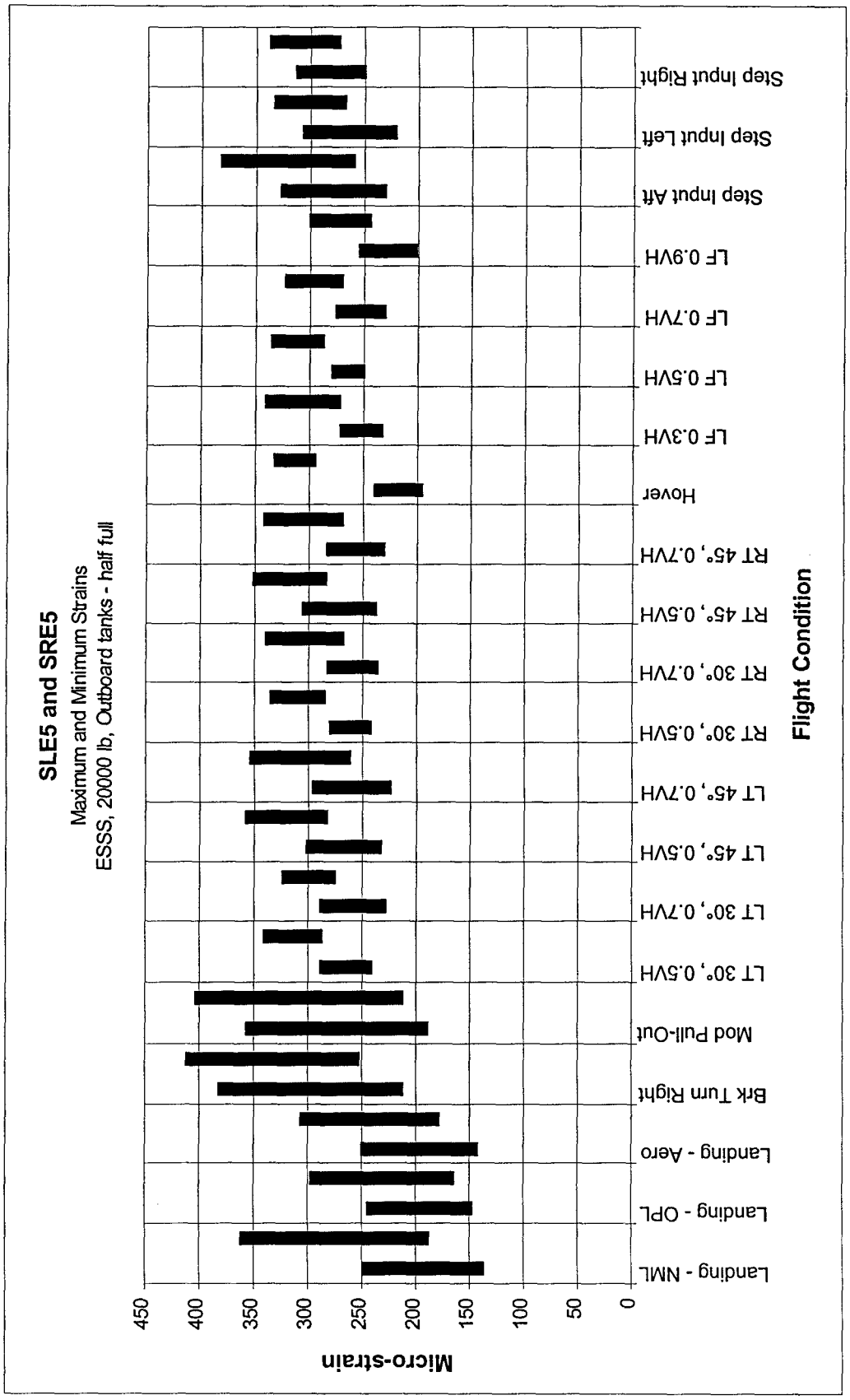

Figure 7(l): Maximum and minimum strains for the ESSS aircraft configuration with two outboard tanks (half full of fuel) at a gross weight of 20000 lb.

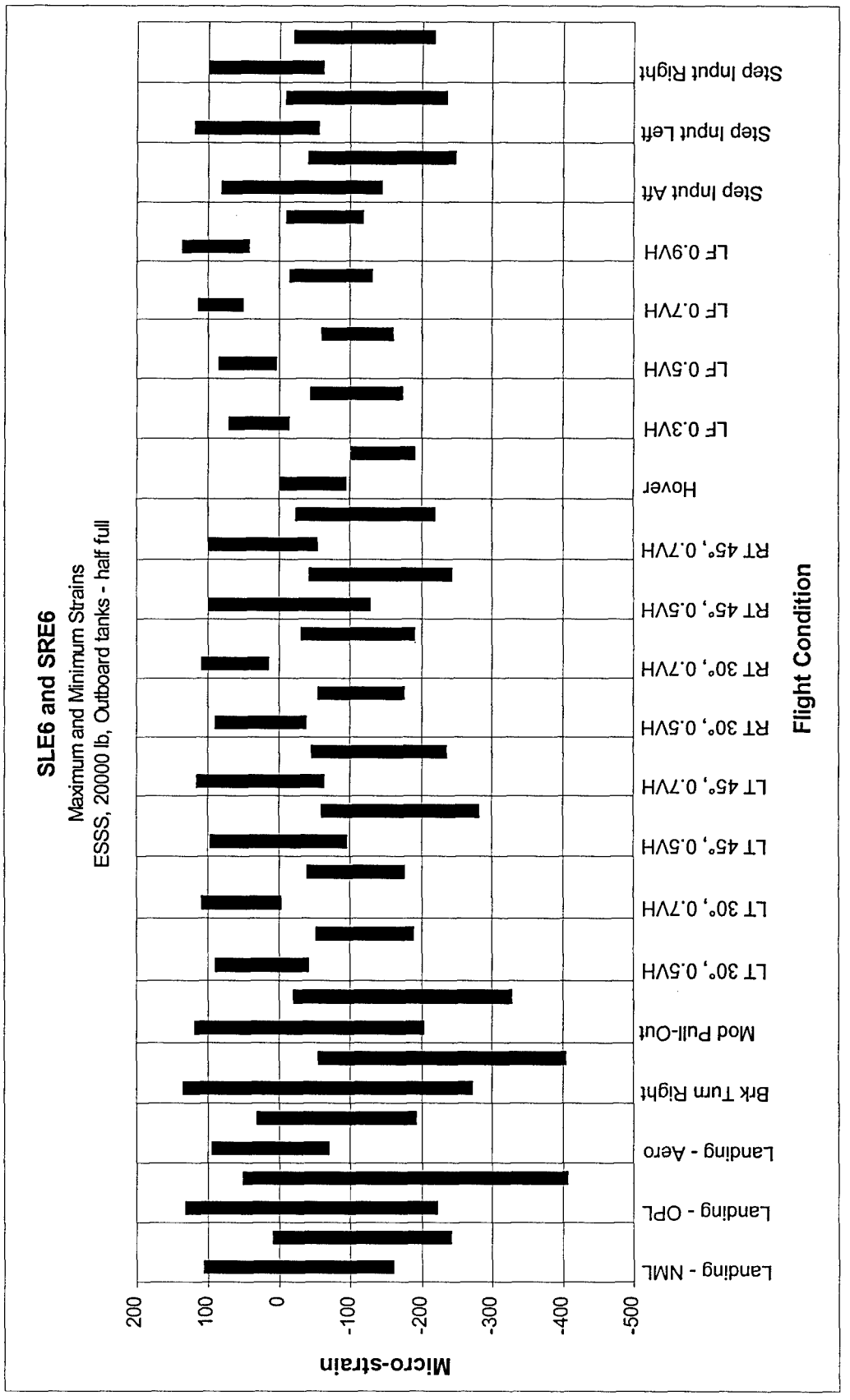

Figure 7(m): Maximum and minimum strains for the ESSS aircraft configuration with two outboard tanks (half full of fuel) at a gross weight of 20000 lb.

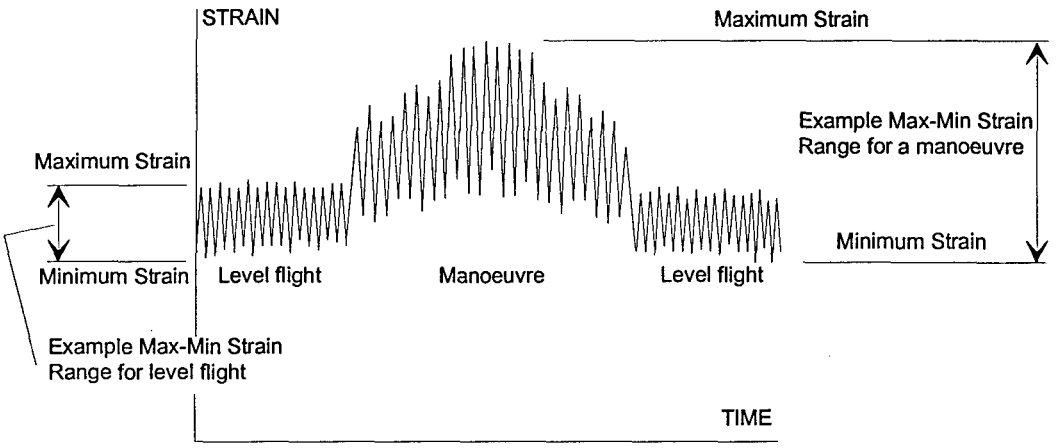

Figure 8: Examples of how the maximum and minimum strains were obtained in Figs 5, 6, and 7

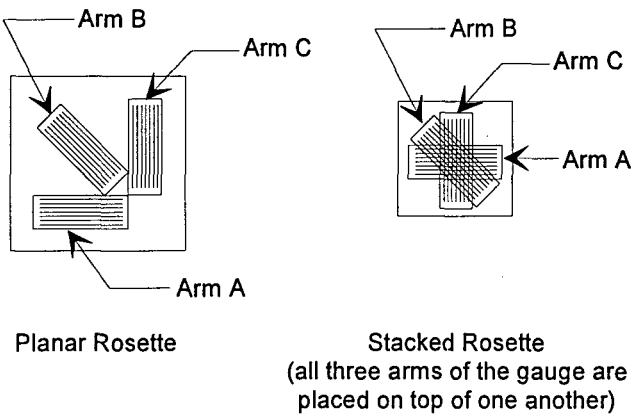

Figure 9: Planar versus stacked rosettes

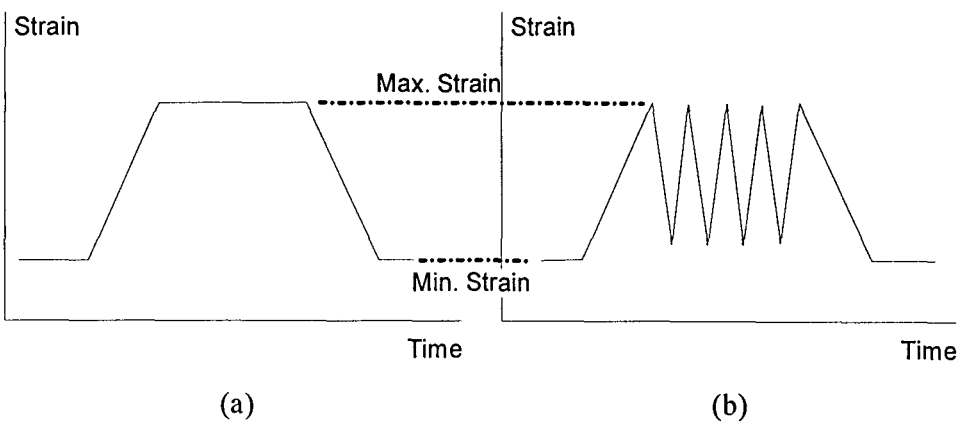

Figure 10: Fatigue damaging cycles can be overlooked if Max/Min strains, only, are examined. Both (a) and (b) above have the same Max/Min strains, but (a) consists of only one load cycle whereas (b) consists of several.

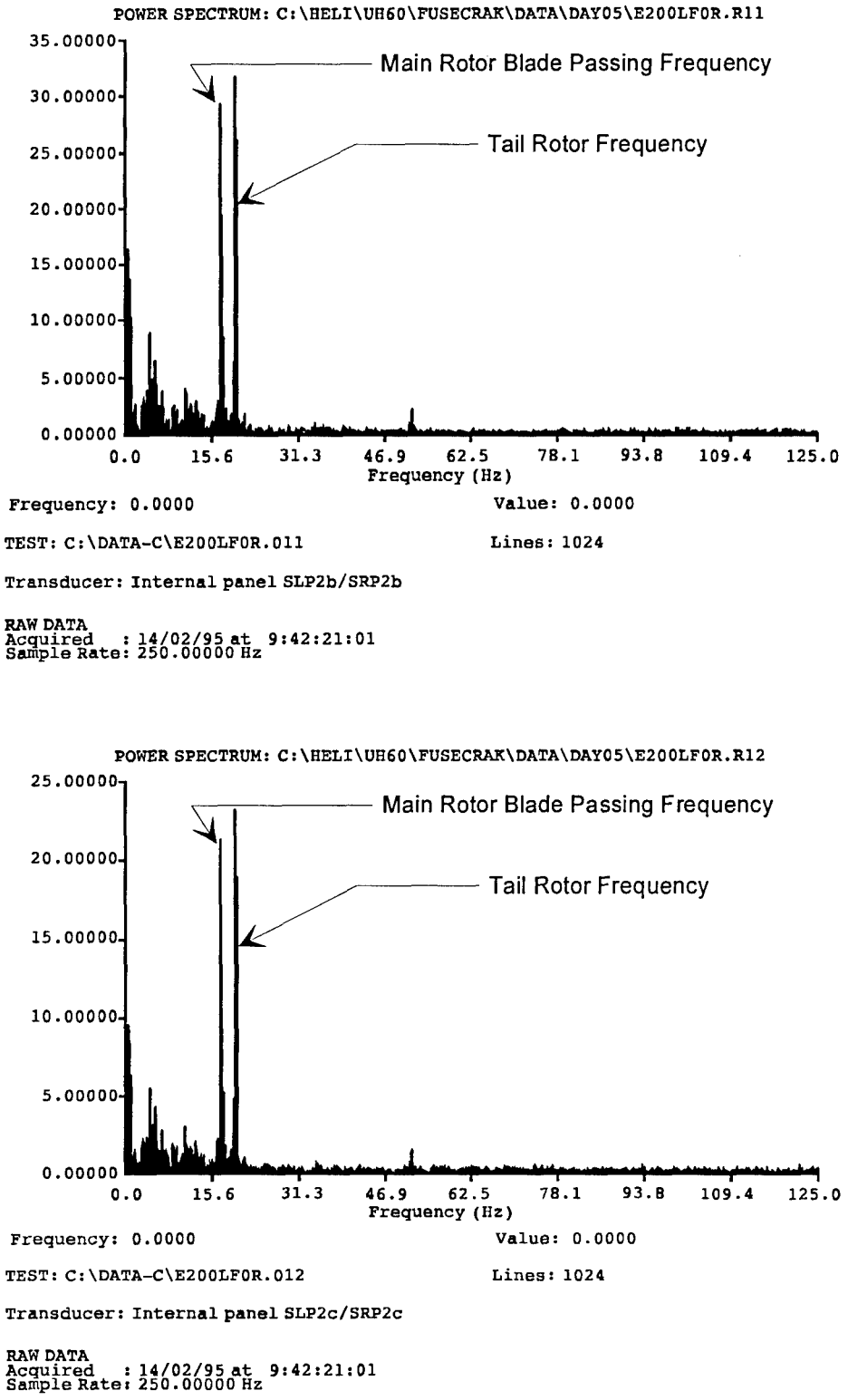

Figure 11: Frequency analysis of the strains measured by arms B (top) and C (bottom) of strain gauge SRP2. Aircraft configuration: ESSS (wings only, no tanks) at a gross weight of 20000 lb. Flight Condition: Hover.

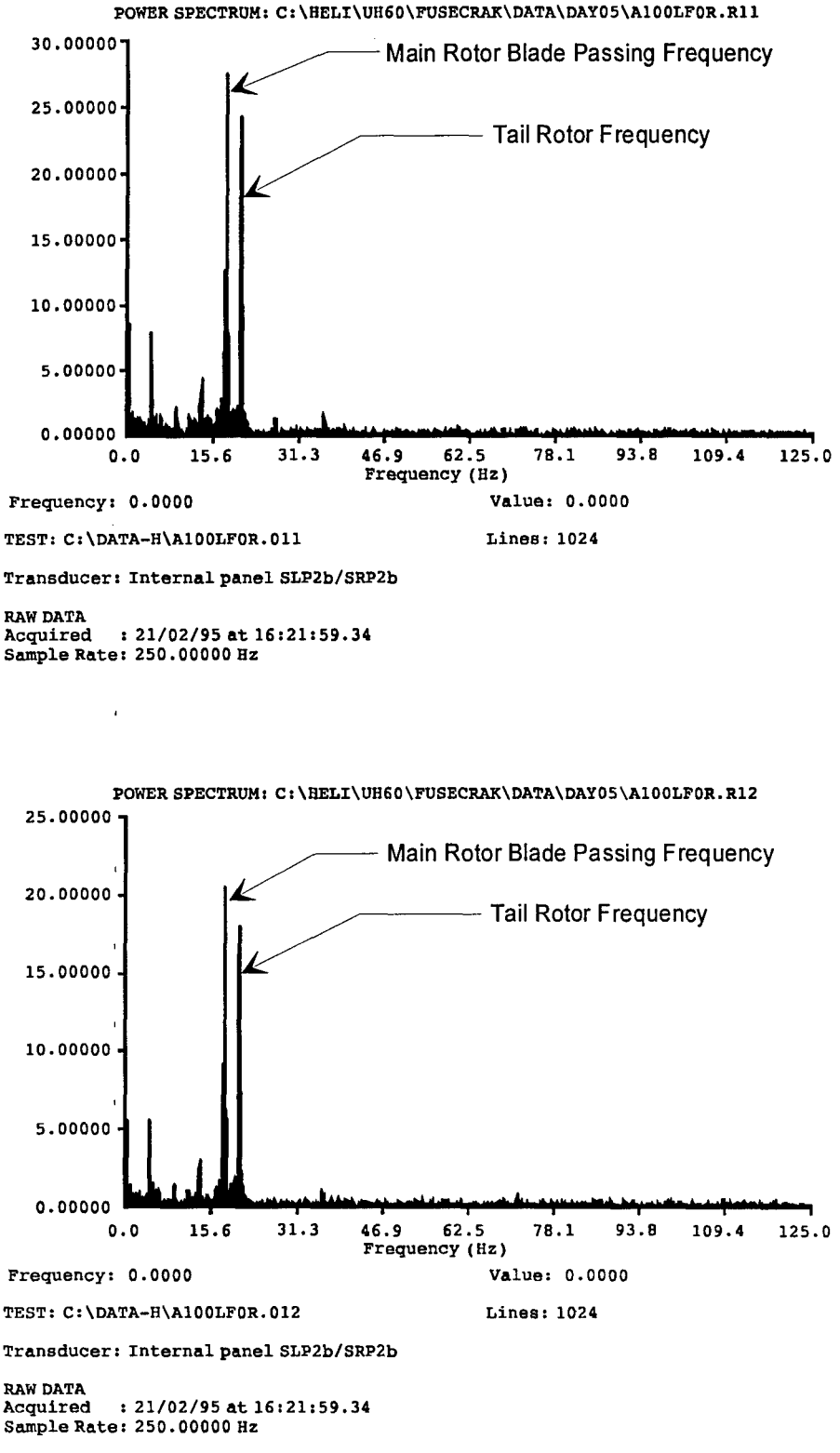

Figure 12: Frequency analysis of the strains measured by arms B (top) and C (bottom) of strain gauge SRP2. Aircraft configuration: ESSS (wings only, no tanks) at a gross weight of 16000 lb. Flight Condition: Autorotation at zero forward airspeed.

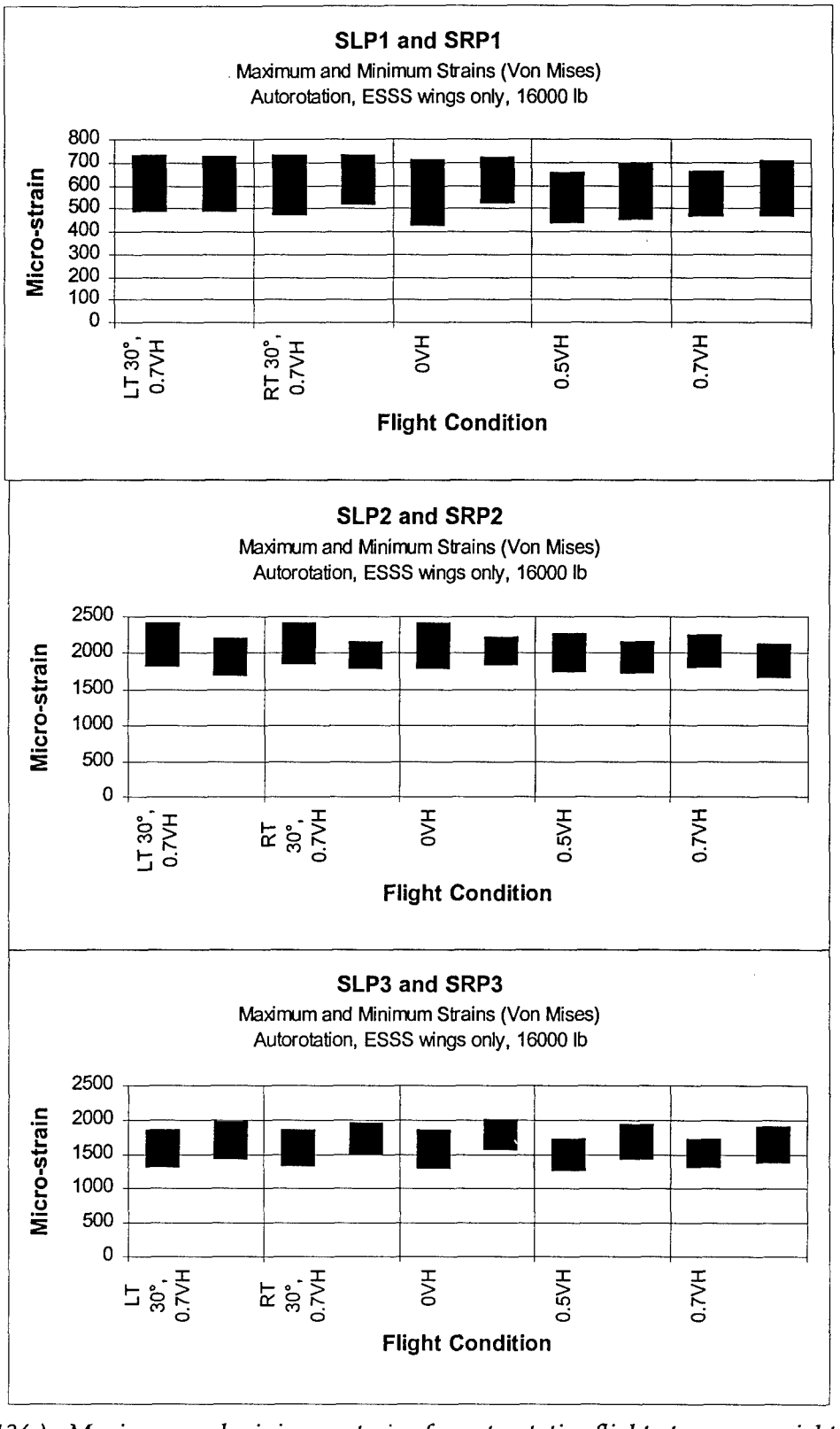

Figure 13(a): Maximum and minimum strains for autorotative flight at a gross weight of 16000 lb with only ESSS Wings mounted (no tanks).

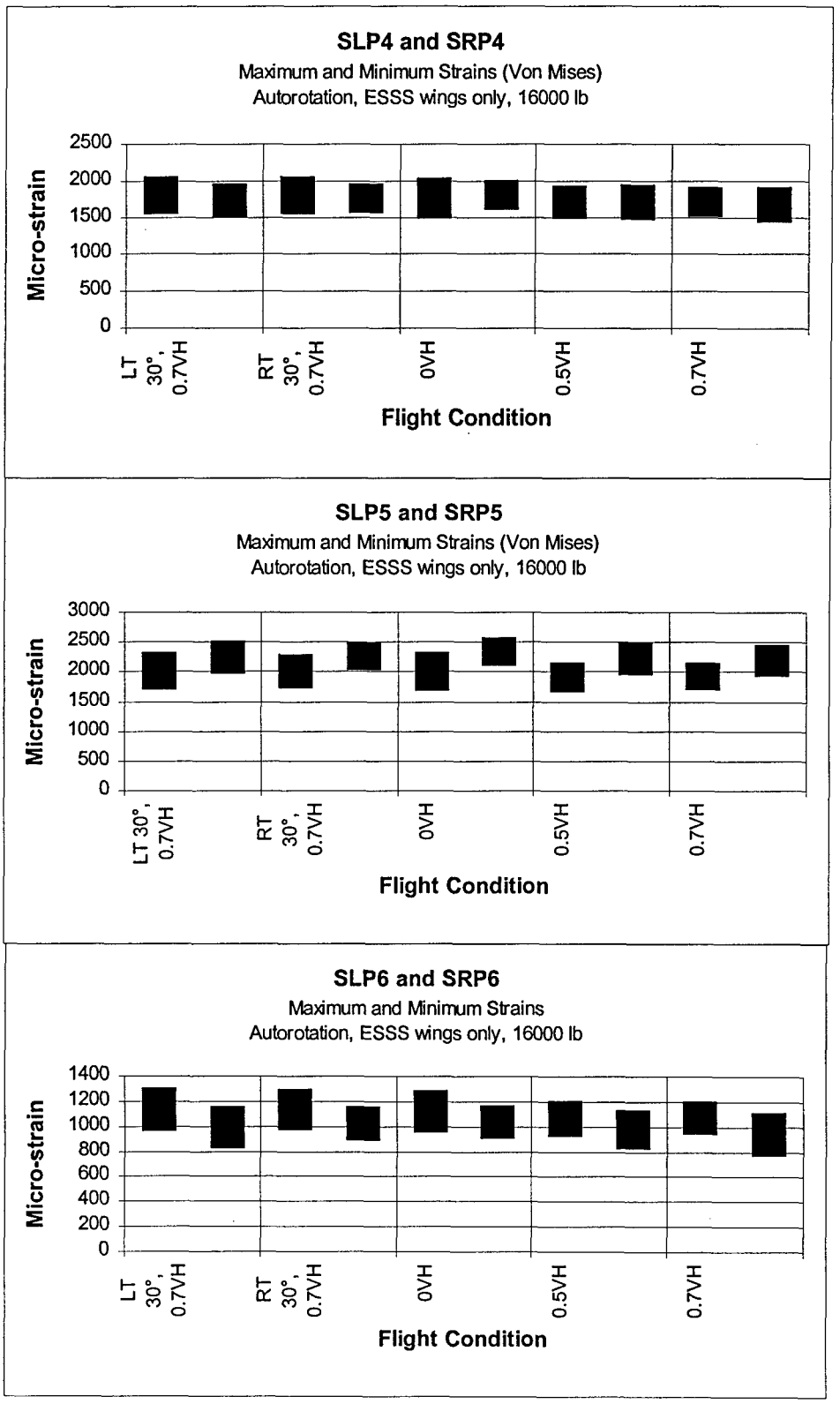

Figure 13(b): Maximum and minimum strains for autorotative flight at a gross weight of 16000 lb with only ESSS Wings mounted (no tanks).

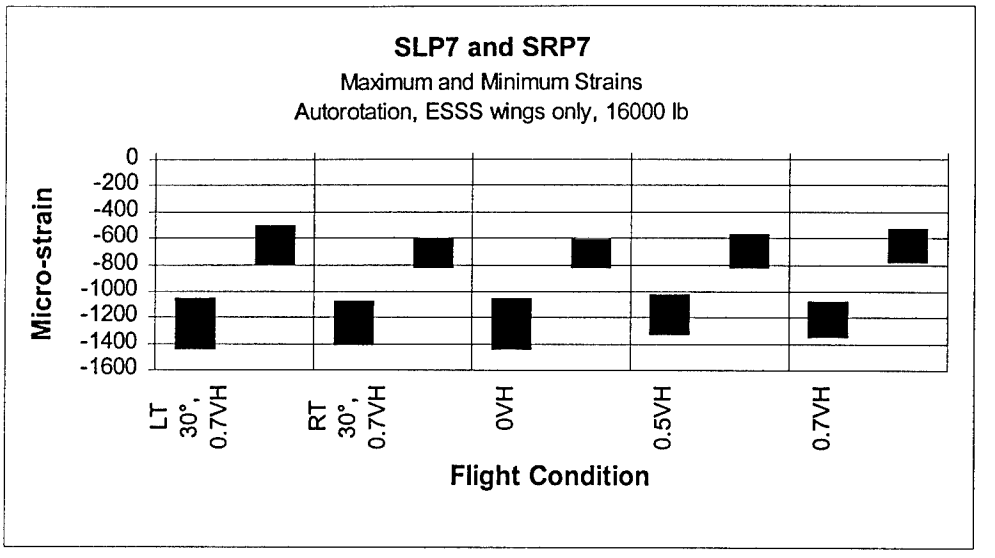

Figure 13(c): Maximum and minimum strains for autorotative flight at a gross weight of 16000 lb with only ESSS Wings mounted (no tanks).

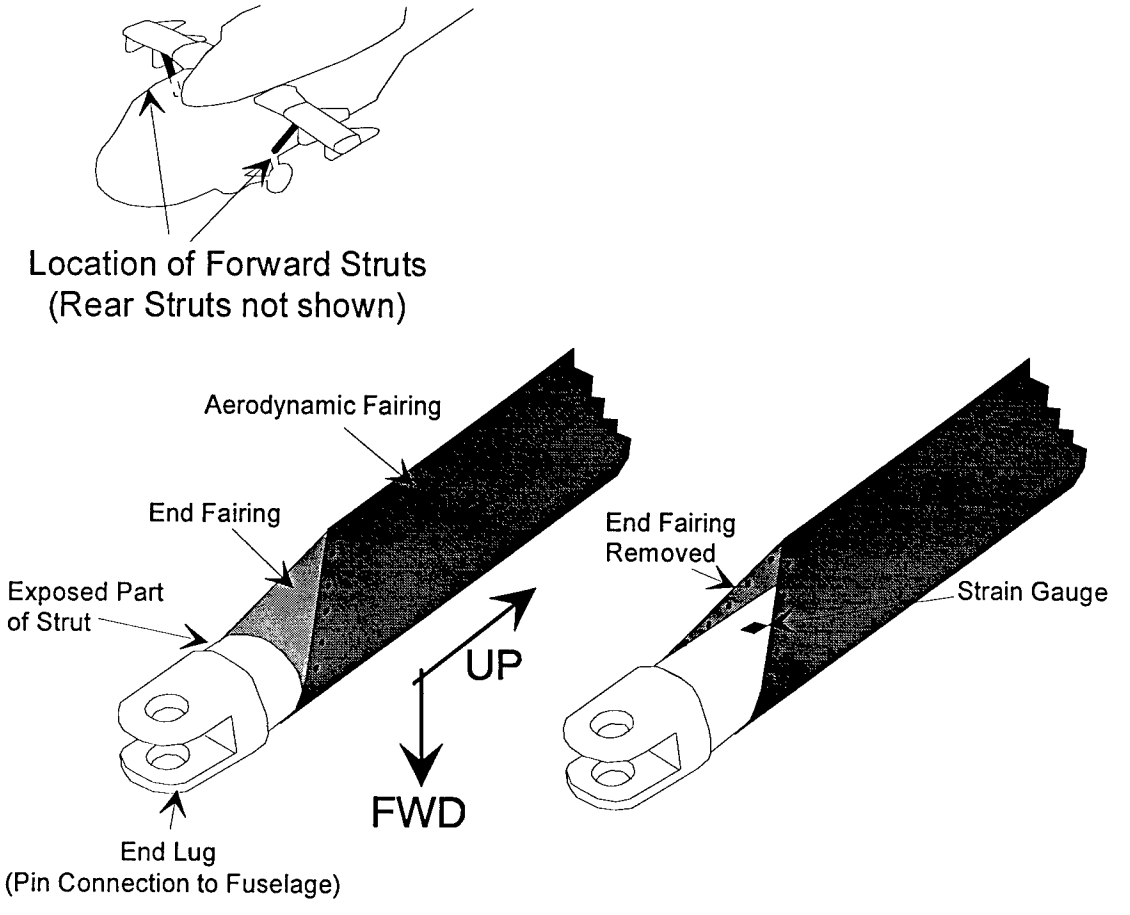

Figure 14: Strain gauge installation on ESSS struts.

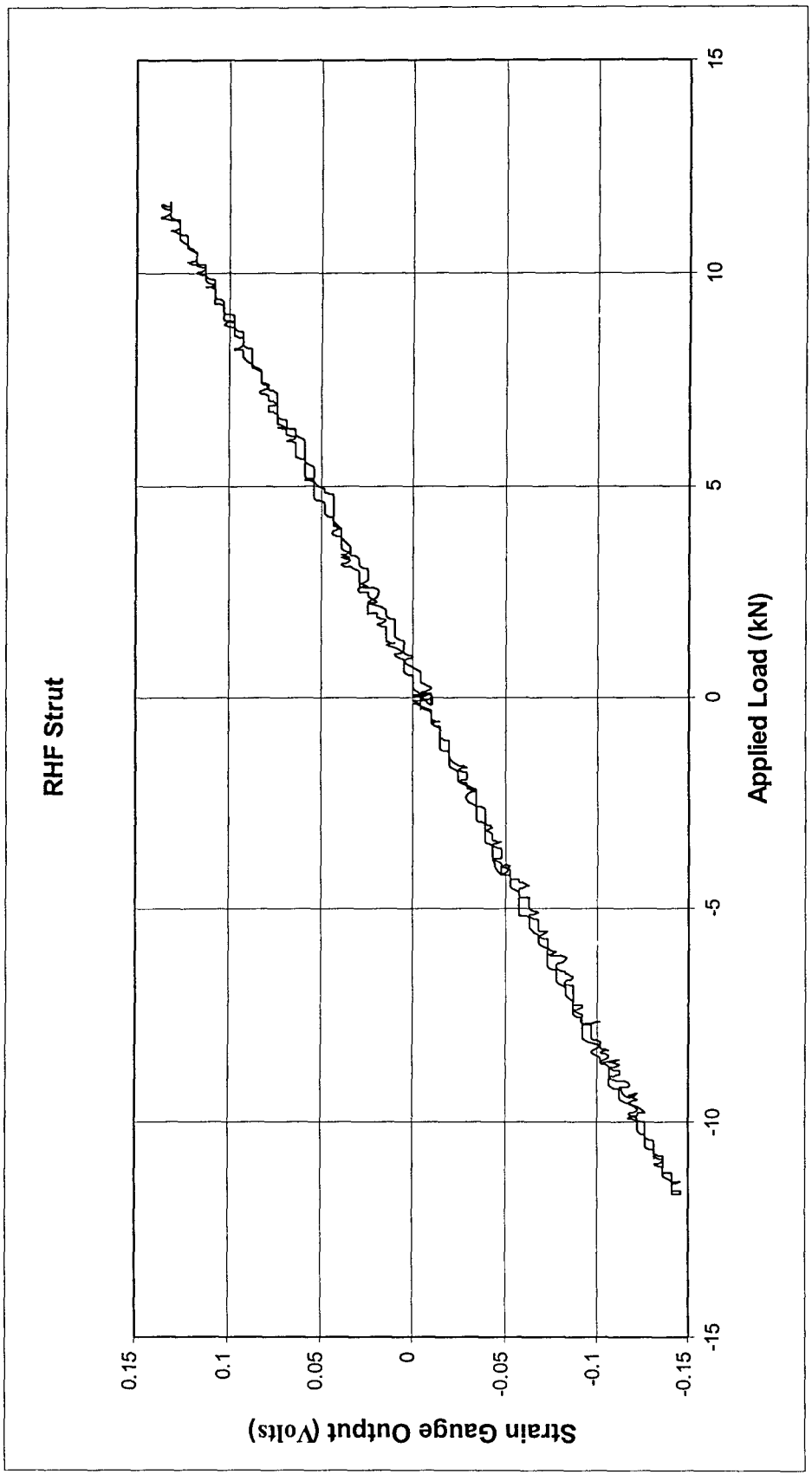

Figure 15: Strain gauge output curve for right-hand forward ESSS strut.

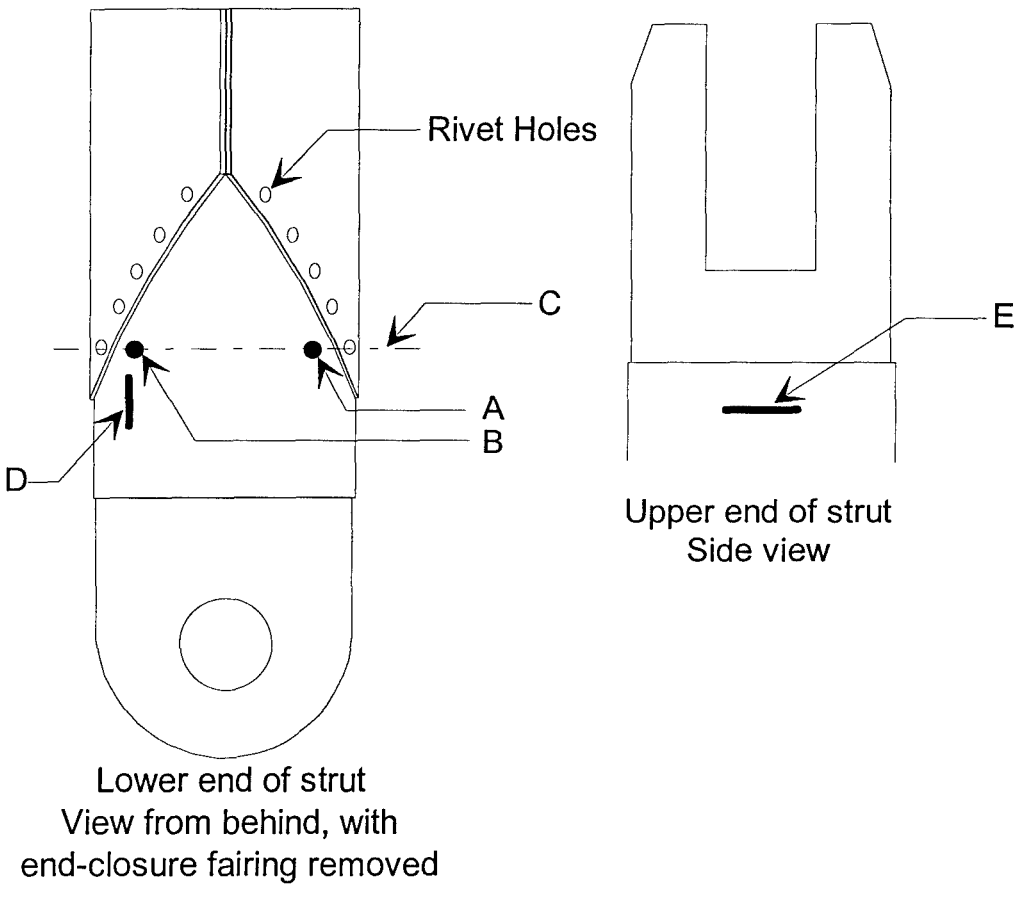

Figure 16: Strut damage.

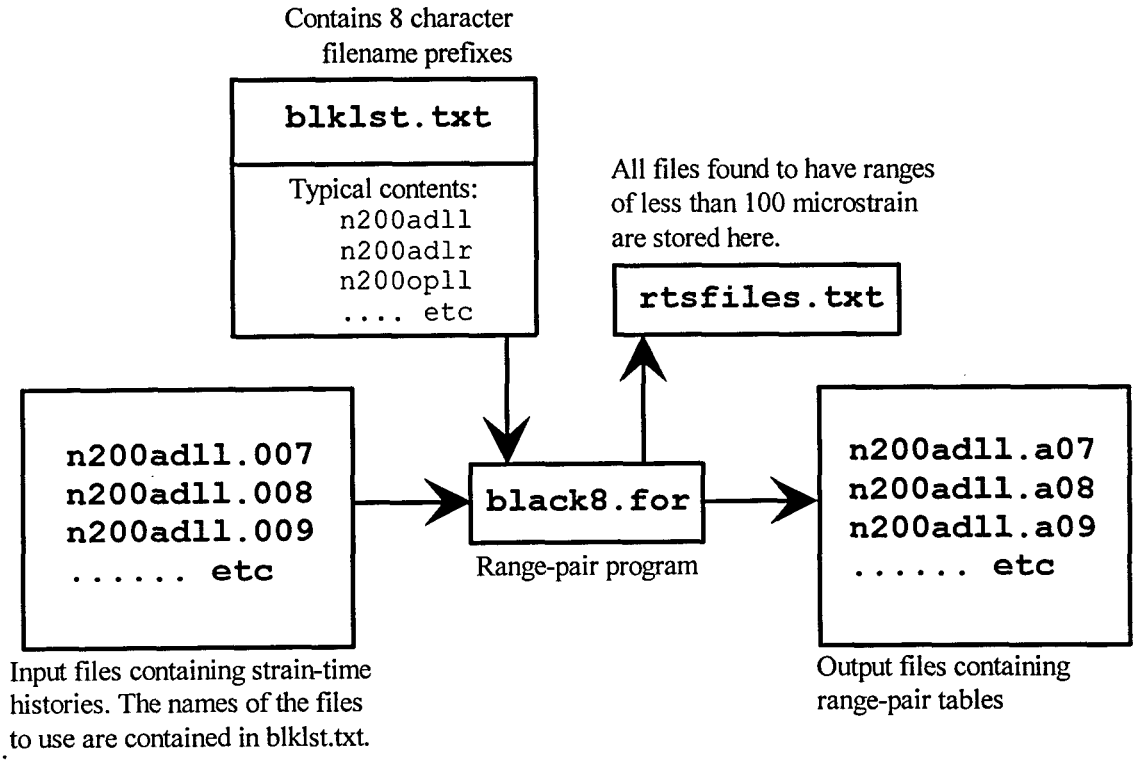

Figure 17: Interaction of peripheral files with "BLACK8.FOR" program.

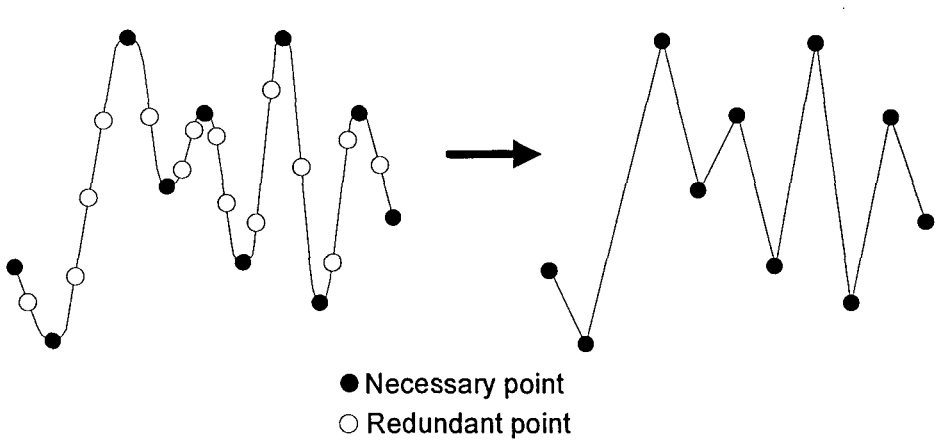

Figure 18: Removal of redundant data points.

(a)

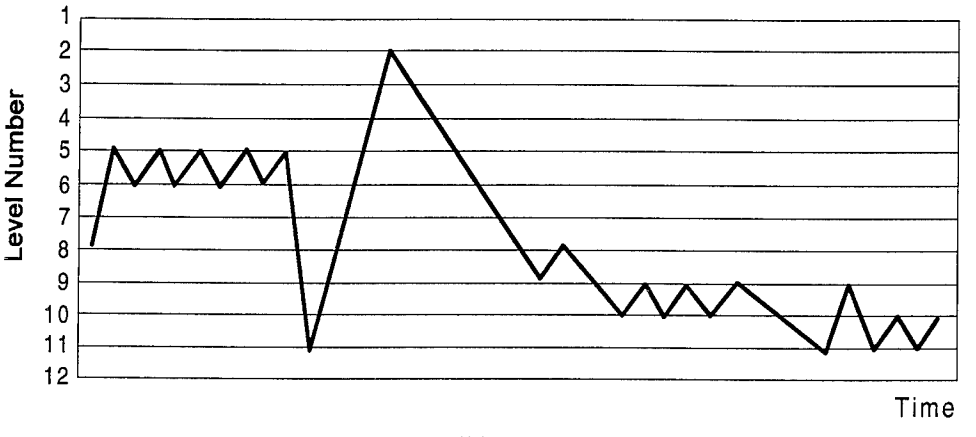

(b)

Figure 19: *Removal of degenerate data points from a load history.*

Figure 20: *Sample colour-map comparison.*

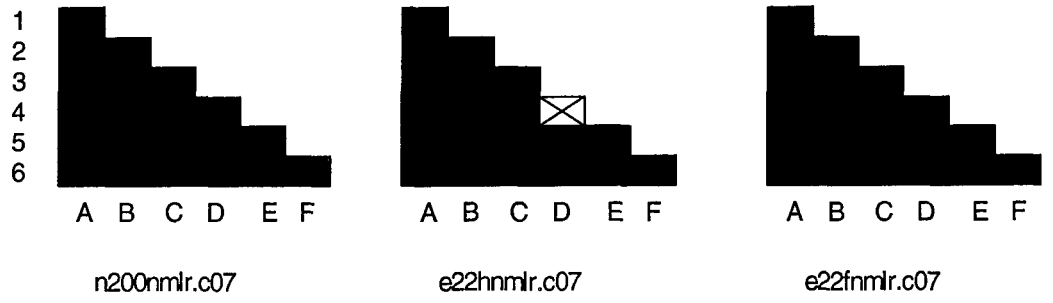

Figure 21: *Sample colour-map comparison showing increased number of high cycle count cells occurring in the 50%-full fuel tank case (middle).*

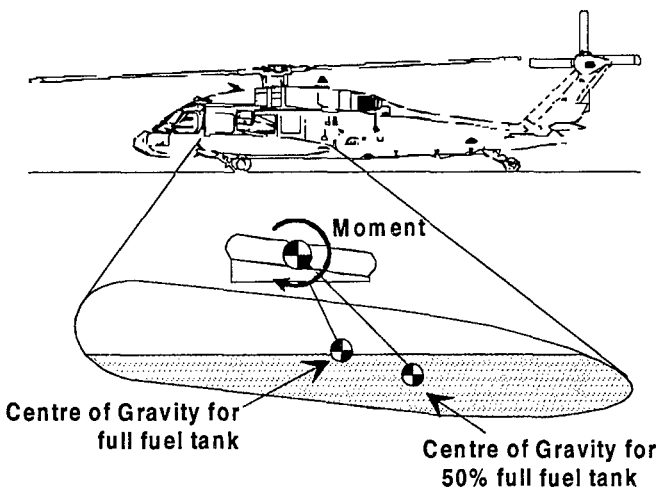

Figure 22: *ESSS side view showing the occurrence of a larger moment arm with the fuel tanks partially full.*

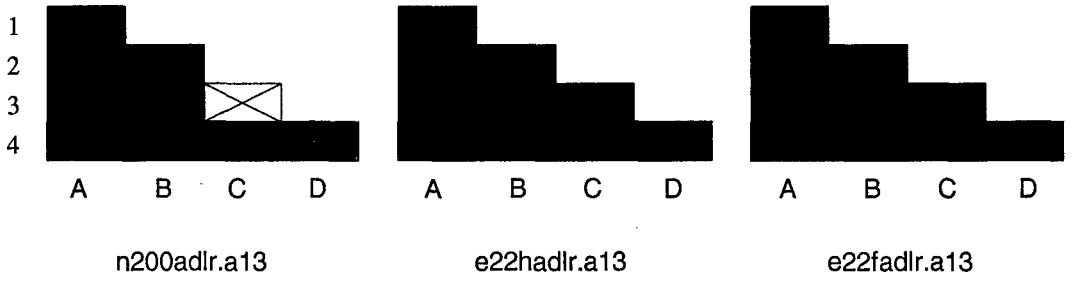

Figure 23: *Sample of colour-map comparisons illustrating some overall trends.*

The chart shows $D_{old} - D_{new}$ where D_{old} is the indicative panel fatigue damage from the old rigging method
D_{new} is the indicative panel fatigue damage from the new rigging method

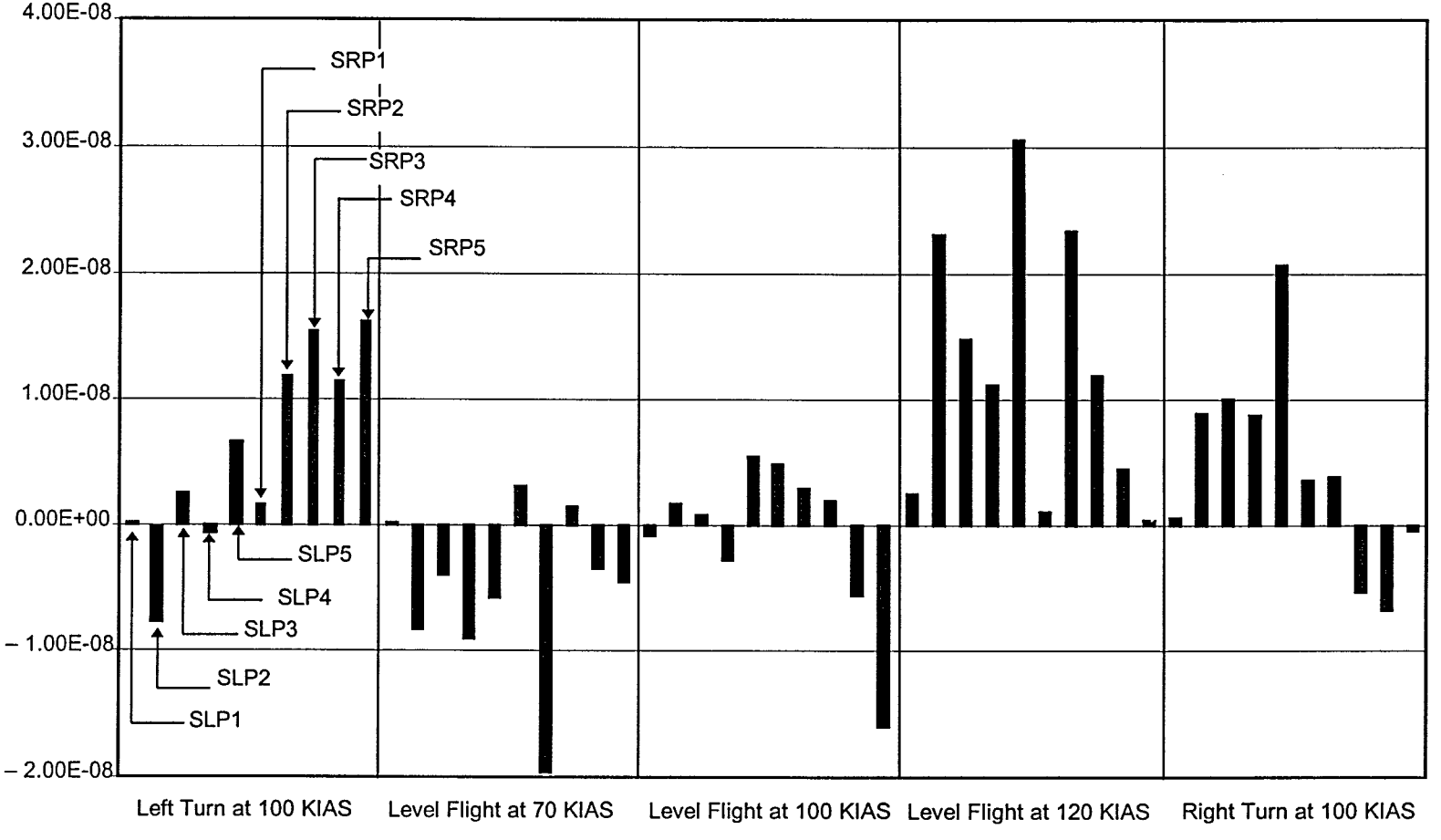

Figure 24: Comparison of indicative fatigue damage between the old and new rigging procedures.

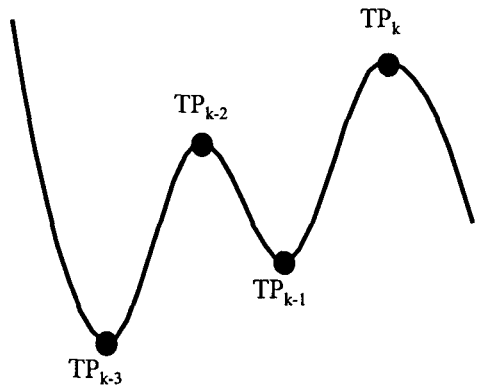

Figure 25: Four-point test.

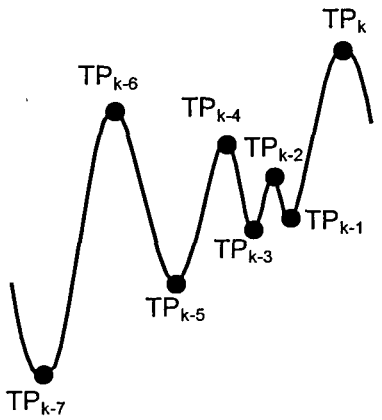

When the one-pass method reaches TP(k) with the contents of the turning point stack represented as shown:

- TP_k and TP_{k-3} will detect the range pair TP_{k-1}, TP_{k-2} which is then removed from the stack;
- TP_k and TP_{k-5} will then detect the range pair TP_{k-3}, TP_{k-4} which is also removed from the stack; and
- TP_k and TP_{k-7} will then detect the range pair TP_{k-5}, TP_{k-6}.

Figure 26: Repetitive pairing using one-pass method

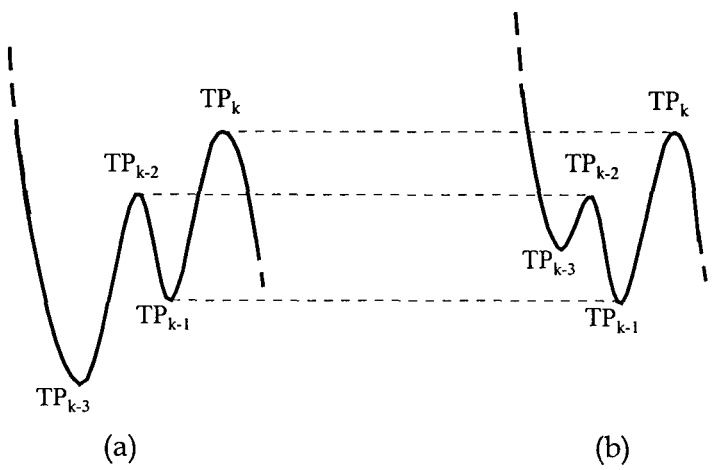

Figure 27: The three-point test.

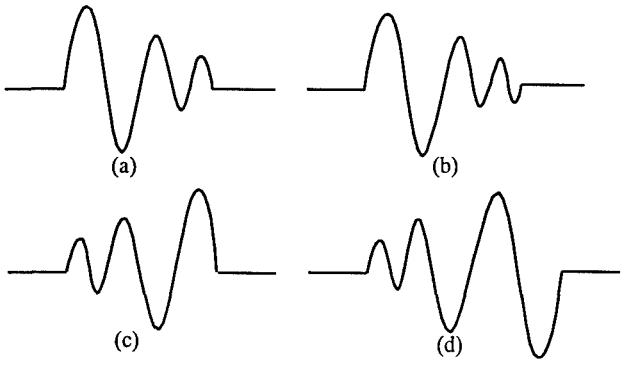

Figure 28: Possible sequences of unpaired data points from the three-point test.

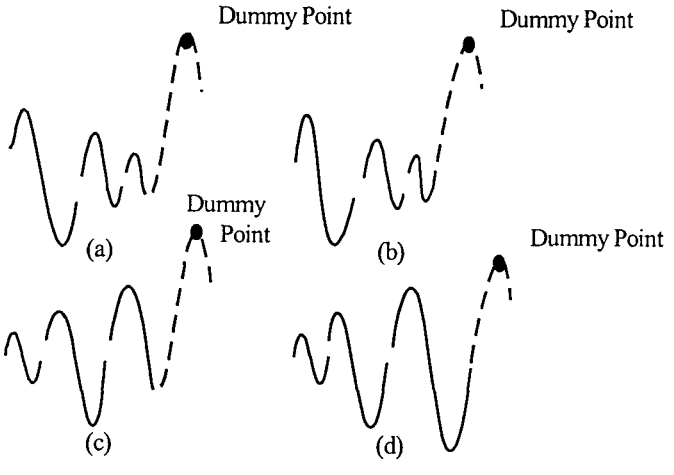

Figure 29: Pairing with 'dummy' turning points.

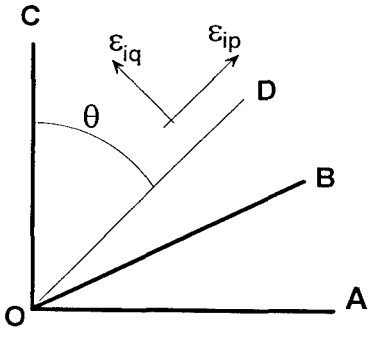

Figure 30: Orientation of the three arms (A, B, and C) of a rosette strain gauge relative to the directions of the principal strains.

S-70A-9 Black Hawk Helicopter: Internal Panel Cracking Investigation

D.C. Lombardo, C.G. Knight, L. Krake, S.A. Dutton and P.W. Smith

DSTO-TR-0457

DISTRIBUTION

AUSTRALIA

TASK SPONSOR: Director Technical Airworthiness -Logistics Systems Agency

DEFENCE ORGANISATION

Defence Science and Technology Organisation

Chief Defence Scientist
FAS Science Policy
AS Science Industry and External Relations
AS Science Corporate Management
} shared copy

Counsellor Defence Science, London (Doc Data Sheet only)
Counsellor Defence Science, Washington
Senior Defence Scientific Adviser/Scientific Adviser Policy and Command (shared copy)
Navy Scientific Adviser
Scientific Adviser - Army
Air Force Scientific Adviser
Director Trials

Aeronautical and Maritime Research Laboratory

Director
Chief, Airframes and Engines Division
Research Leader Structural Dynamics
Task Manager (K.F. Fraser)
Author(s): D.C. Lombardo
C.G. Knight
L. Krake
S.A. Dutton
P.W. Smith
R. Boykett
P.D. White

DSTO Library

Library Fishermens Bend
Library Maribyrnong
Main Library DSTOS (2 copies)
Library, MOD, Pyrmont (2 copies of Doc Data sheet)
Australian Archives

Defence Central

OIC TRS, Defence Central Library
Officer in Charge, Document Exchange Centre, 1 copy
U.S. Defence Technical Information Centre, 2 copies
Defence Intelligence Organisation
Library, Defence Signals Directorate (Doc Data Sheet only)

Air Force

Chief Engineer Army Aircraft Logistics Management Squadron
Director Army Aircraft Projects
Technical Liaison Officer U.S. Army ATCOM (St Louis)

Army

Director General Force Development (Land)
Commander Aviation Support Group (3 copies)

Navy

Director General Force Development (Sea)
Director Aviation Engineering
Chief Aeronautical Engineer, Naval Aircraft Logistics

UNITED STATES OF AMERICA

U.S. Army

F.H. Immen, Head Engineering Structures and Materials Division, U.S. Army ATCOM (St Louis, MO)
W. Elber, Director Vehicle Structures Directorate, NASA Langley Research Center (Hampton, VA)
E. Robeson, Aviation Applied Technology Directorate, U.S. Army ATCOM (Ft Eustis, VA)

U.S. Navy

G. Barndt, Structures Branch, Naval Air Systems Command (Washington DC)

Sikorsky

J.L. Harrell, Sikorsky Aircraft Australia Ltd

SPARES (10 copies)
TOTAL (58 copies)

DEFENCE SCIENCE AND TECHNOLOGY ORGANISATION
DOCUMENT CONTROL DATA

1. PRIVACY MARKING/CAVEAT (OF DOCUMENT)

2. TITLE

S-70A-9 Black Hawk Helicopter: Internal Panel Cracking Investigation

3. SECURITY CLASSIFICATION (FOR UNCLASSIFIED REPORTS THAT ARE LIMITED RELEASE USE (L) NEXT TO DOCUMENT CLASSIFICATION)

Document	(U)(L)
Title	(U)
Abstract	(U)

4. AUTHOR(S)

D.C. Lombardo, C.G. Knight, L. Krake, S.A. Dutton and P.W. Smith

5. CORPORATE AUTHOR

Aeronautical and Maritime Research Laboratory
PO Box 4331
Melbourne Vic 3001

6a. DSTO NUMBER	6b. AR NUMBER	6c. TYPE OF REPORT	7. DOCUMENT DATE
DSTO-TR-0457	AR-009-947	Technical Report	January 1997

8. FILE NUMBER	9. TASK NUMBER	10. TASK SPONSOR	11. NO. OF PAGES	12. NO. OF REFERENCES: 17
M1/9/285	AIR 96/081	DTA-LSA (RAAF)	119	

13. DOWNGRADING/DELIMITING INSTRUCTIONS

To be reviewed three years after date of publication

14. RELEASE AUTHORITY

Chief, Airframes and Engines Division

15. SECONDARY RELEASE STATEMENT OF THIS DOCUMENT

Australian Department of Defence and Defence Force Personnel and their equivalent in the US may have access to this document. Others inquiring should be referred to Chief, Airframes and Engines Division AMRL.

OVERSEAS ENQUIRIES OUTSIDE STATED LIMITATIONS SHOULD BE REFERRED THROUGH DOCUMENT EXCHANGE CENTRE, DIS NETWORK OFFICE, DEPT OF DEFENCE, CAMPBELL PARK OFFICES, CANBERRA ACT 2600

16. DELIBERATE ANNOUNCEMENT

Australian Department of Defence and Defence Force Personnel and their equivalent in the US

17. CASUAL ANNOUNCEMENT Yes

18. DEFTEST DESCRIPTORS

Aircraft Structures, Defence Projects (Australia), Black Hawk Helicopter, Fuselage Skin, Stress Fracture, Fatigue (Materials), Cracking

19. ABSTRACT

The Australian Army S-70A-9 Black Hawk fleet is experiencing numerous occurrences of cracking in an internal fuselage panel. The panel is not primary structure (i.e. it is not flight-critical), but it is essential. Cracking has occurred only on the right-hand side panel, and the standard repair scheme is inadequate. In October 1994, the Australian Army approached DSTO and the Royal Australian Air Force (RAAF) Aircraft Research and Development Unit (ARDU) for assistance in determining the cause of the cracking. To try to minimise the panel cracking, the Army had suspended use of the External Stores Support System (ESSS) which is used to carry external fuel tanks. Since this suspension was causing operational hardships, the Army wanted to know what was causing the cracking to determine whether less severe restrictions might be imposed until a proper repair could be devised for the panel.

In February 1995, DSTO and ARDU personnel conducted a flight investigation, at RAAF Base Edinburgh, South Australia, with Black Hawk A25-206. The data gathered were analysed and the results indicated that the ESSS was not responsible for the cracking. The panel strains are largely insensitive to the presence of the ESSS.

The cause of the cracking is a structural deficiency in the panel. Beads, pressed into the panel to provide stiffening, are creating a stress concentration factor of approximately 3.0 which couples with the large Ground-Air-Ground loading cycle to cause the cracking. Once initiated, the high frequency in-flight loading to which the panel is subjected causes the cracks to propagate rapidly.

There are no operational restrictions which the Army might apply to reduce the frequency or severity of the cracking. The only relief will come when a redesigned panel is installed.

DEPARTMENT OF DEFENCE
DEFENCE SCIENCE & TECHNOLOGY ORGANISATION
DSTO

SCIENCE CORPORATE MANAGEMENT BRANCH
DSTO SALISBURY RESEARCH LIBRARY-REPORTS DISTRIBUTION
PO BOX 1500 SALISBURY SA 5108

Reference: R9607/7/9 Pt4 Folio No.34
Contact: Natalie Mahlknecht
E-mail: Natalie.Mahlknecht@dsto.defence.gov.au

Telephone: (08) 8259 6255
Facsimile: (08) 8259 6803

17th May 2001

To All Copyholders
cc: To the Team Leader of Records & Archives

Notification of Downgrading/ Delimiting of DSTO Report

Please note that the Release Authority has authorised the downgrading/ delimiting of the report detailed here:

DSTO NUMBER	**DSTO-TR-0457**
AR NUMBER	**AR-009-947**
FILE NUMBER	**M1/9/285**
PREVIOUS Classification	**WAS:- LIMITED DOD**
REVISED Classification and Release Limitation	**UNCLASSIFIED** **Public Release**

Please amend your records and make changes to your copy of the report itself to reflect the new classification/ release limitation.

Mrs. Natalie Mahlknecht
Reports Distribution Officer
DSTO Research Library, Salisbury